Alma Mater Studiorum – Università di Bologna

DOTTORATO DI RICERCA IN

CHIMICA

Ciclo XXXIIII

Settore Concorsuale: 03/C2

Settore Scientifico Disciplinare: CHIM/04

Catalytic hydrogenation of vegetable oils derivatives

Presentata da: **Annalisa Sacchetti**

Coordinatore Dottorato

Prof. Domenica Tonelli

Supervisore:

Prof. Fabrizio Cavani

Correlatori:

Dott. Tommaso Tabanelli
Prof. Stefania Albonetti

Esame finale anno 2022

Keywords

Biomass

Heterogeneous catalysis

Hydrogenation

Batch reactor

Continuous flow reactor

Triglycerides

Fatty acids derivatives

Palladium catalysts

Metal supported catalysts

Abbreviations

Linoleic acid derivative	Poly-U
Oleic acid derivative	*Cis*-U1
Elaidic acid derivative	*Trans*-U1
Stearic acid derivative	S1
Internal Standard	IS
% weight/ weight	%w/w
Response Factor (*i*)	F_i
Fatty acid methyl esters	FAMEs
Iodine Value	IV
Nanoparticles	NPs
Thermogravimetric analysis	TGA
X-ray powder Diffraction	XRD
Temperature Programmed Reduction	TPR
Transmission Electron Microscopy	TEM
Scanning Electron Microscopy	SEM
Inductively coupled plasma atomic emission spectroscopy	ICP-AES
Gas Chromatography	GC
Gas Chromatography -Mass Spectroscopy	GC-MS
Contact time	τ
Yield (*i*)	Y_i
Conversion (*i*)	X_i
Room Temperature	R.T.

Abstract

Oils and fats, with their increase in production of 200% over the last thirty years, represent a realistic and adequate resource for chemicals and fuels production, and were the protagonist of this PhD project. Indeed, triglycerides can undergo many different reactions depending on the target product (e.g. Biodiesel, fuels, cosmetics, plasticizers, polymers and plastics) including hydrogenation. This reaction involves typically Ni-based catalyst or alternatively noble metals supported catalyst, at expense of harsher reaction conditions.

During this project the catalytic hydrogenation of a mixture of fatty acids derivatives was performed in two different reactors (discontinuous batch and continuous flow); the attention was pointed out on the type of the catalyst employed, involving an initial screening among different noble metals and support with subsequent in-depth optimization of the reaction parameters.

Interesting results were obtained in batch reactions with 0.3% wt Pd/C at 4 bar of H_2 and 90°C, ensuring full conversion of the starting material and complete selectivity towards the saturated fatty acid derivative. An insight of the kinetics of the reaction was performed, conducting the reaction for different time (0-6 hours). Also, fundamental parameters such as H_2 pressure, stirring rate, temperature, metal type and support were evaluated for determining the most advantageous conditions to guarantee complete starting material conversion and high yields of desired products. The same tests were then performed employing a continuous flow reactor, confirming the high activity of 0.3% wt Pd/C at low contact time of 0.2 min.

Despite stunning results were achieved with a single batch (discontinuous) or for low reaction time (1h in continuous), the catalyst performance started to worsen for multiple batch or longer time respectively. Investigations on the cause were executed, excluding immediately metal leaching thanks to ICP-AES analysis. Deactivation was attributable to absorption of reactants on the catalyst surface, which could lead to formation of oligomers. It was found that the deactivation rate, in the continuous reactor, was directly dependent on the hydrogen pressure, the contact time but even more importantly to the composition of the starting material: an increase of poly-unsaturated fatty acids derivatives affected negatively the catalyst stability, causing a faster decline of conversion and higher decrease in selectively. This was associated to a strong adsorption with consequent formation of oligomers, which occupied the active site, worsening the catalyst's performance.

The promising results obtained in the two reactors, especially in the continuous flow, open interesting prespective for further industrial applications.

Summary

1. Introduction – general aspects

1.1 Green chemistry

The definition and concept of Green Chemistry dates back to 1990s[1], defining Green Chemistry as "design of chemical products and processes to reduce or eliminate the use and generation of hazardous substances"[2].

In 1998, the fathers of Green Chemistry Paul Anastas and John Warner introduced the "Twelve principles of green Chemistry"[3], a guide for the design of new processes and products: they explicated the need to consider and evaluate some fundamental aspects of each reactant and product like their nature, the biodegradability, the toxicity, and all their environmental-related features. Also, they underlined the importance to shift towards more sustainable choices by reducing wastes, as much as the utilization of solvents and emissions[4] minimization.

Luckily, the concept of green chemistry found rapidly sharing among the scientific community: industries can put in action these principles for a more sustainable future, and their research, in collaboration with academic studies, is fundamental for the exploration of new green technologies and environmental friendly solutions[5,6,7,8].

Thereafter, the twelve principles are illustrated and shortly discussed[3]:

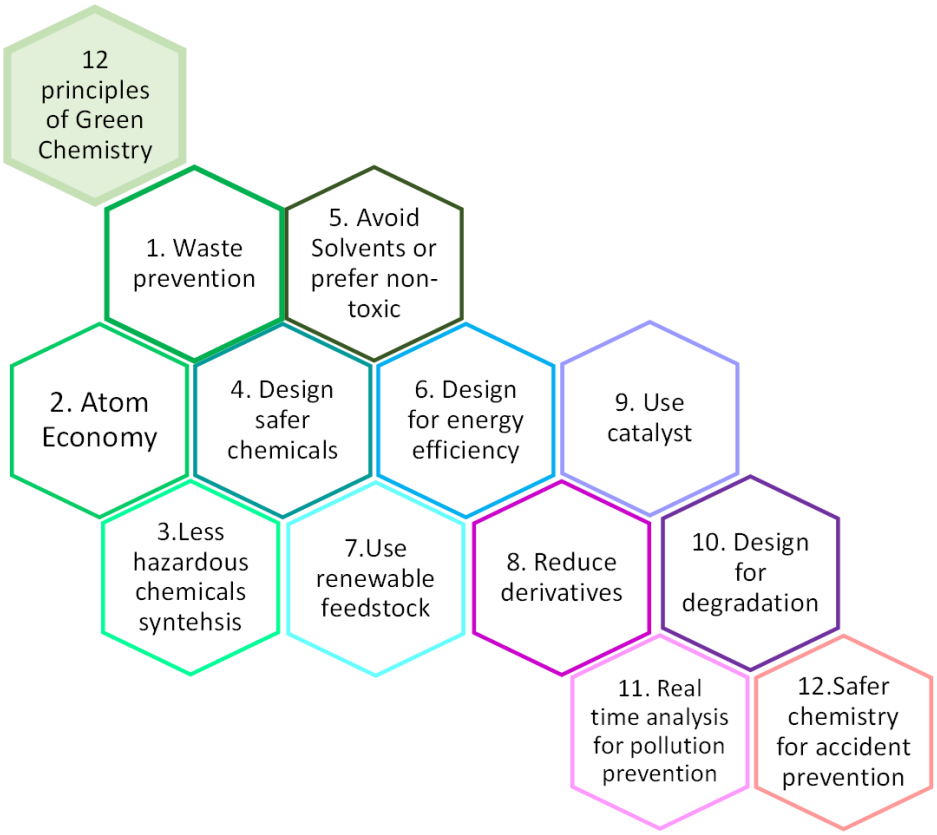

Figure 1. List of Twelve Principles of green Chemistry defined by Paul Anastas and John Warner. They were designed for lowering the environmental impact of a chemical process as much as possible acting, on the starting material, the reactants, eventual by-product formation and economicity of the process.

The application of these points is fundamental for improving an already existing process or for the development of a sustainable and environmentally friendly industrial production.

Waste prevention ensures the minimization of not reusable compounds, which require expensive and polluting disposals[9,10].

Also, the reduction of solvent is preferred, conducing the reaction in bulk[11]. If solvents cannot be completely avoid, non-toxic, bio-based or natural solvents (e.g water) are preferred over classical ones[12,13].

As the point 6 states, plants must be design in order to reduce energetic wastes and consumption: a more efficient utilization of energy will include heat recovery, avoiding the implementation of dedicated plant with hot vapour or cold fluids to heat or cool down inlet and outlet streams[14].

The choice of the starting material represents an important part of the overall process: prefer wastes or renewable starting material, like biomass[15]. Second or third generation biomass are even better over first generation ones, to avoid food competitors sources and dedicated cultures[16,17].

Catalysts are fundamental for preventing stoichiometric amount of reactants and to optimize the reaction conditions[18] (temperature, pressure, time of reaction). This is convenient in terms of energy production, consumption, safety and amount of reactants involved.

These points are the foundations for a more responsible and sustainable future and is important to apply as many principles as a process allows.

In this research project some aspects were the basis of the work, including:

- Utilization of renewable resources.
- Employment of an active catalyst for working in safer conditions and in a less energetically-demanding context.
- Avoid the utilization of toxic solvents.
- Atom Economy, related to the type of reaction involved[19].

More engineering-related aspects will be faced in a second moment, due to their major compatibility in industrial rather than lab scale.

1.2 Biomass

Fossil-based sources had provided major material for human and world development and progress.

However, nowadays we are at a point where it is not possible to count on classical fossil feedstock anymore, but it is time to find more sustainable alternatives[20].

There are two main reasons: the first is associated with the depletion of classical fossil feedstock due to its rapid consumption that had characterized the last decade's evolution.

The second is environmental-related, with the prospect of reducing the impact factor of a process aging both on the emissions[21] (including wastes produced) and on the sources employed for the production of goods[22].

For these two main reasons, the replacement of fossil-derived feedstock has been one of the main challenges and driving forces for modern chemical research.

Among all the possibilities, biomass have been subject of academic and industrial studies to make them valid substitutes for fine chemicals, energy and commodities production[23,24].

The term biomass refers to all the organic and bio-organic material derived from a photosynthesis process and represent the most abundant renewable carbon resource on Earth[25]. In other words, biomass is a combination of naturally derived materials, originating from crops, plants (shrubs, trees, algae) and wastes from anthropogenic activities, like residues from wood processing industry, shavings, sawdust[26,27]. Also, animal-derived wastes can strongly contribute as substitute to classical resources: for example, enormous amount of beef tallow are discarded from slaughterhouse; due to its uselessness in food industry it is employed for manufacturing soaps.

Considering all these possibilities, an extensive amount of biomass available is obtained, reaching 1.8 trillion tons; speaking in energetic terms, it corresponds to a potential production capacity of 33,000 EJ, which is more than 80 times the population's energy consumption per year[28]. Nowadays, biomasses are exploited only for 14% of their possibility, leaving high room for improvement. Also, their employment is not uniform across the Earth, considering that for instance the USA cover 3% of the energy demand using biomass, the central Europe the 3.5% while Finland and Sweden the 18% and 17% respectively[29].

Starting from oils and fat it is possible to obtain olefins via catalytic cracking; bio-based benzene, BTX, toluene can be obtained starting from lignocellulosic biomass via pyrolysis, dimerization and dehydrocyclization of bio-isobutanol. Also a Diels-Alder reaction between furanic compounds deriving from sugars can be executed[20,30]. Bio-polymers can be obtained using bio-based monomers (e.g: bioethylene) or other bio-derived precursors (e.g: azelaic acid and pelargonic acid derived from oxidative cleavage of oleic acid[31]). These are only few examples on the application of biomass as substitute of classical fossil sources.
Being a completely renewable energy resource, the net Carbon balance of CO_2in atmosphere is almost neutral, while fossil feedstock processing contribute increasing the total CO_2 registered[32,33,34].

In fact, the CO_2 balance after biomass processing is almost neutral, because the amount released in atmosphere is equal to the amount absorbed through photosynthesis process[6] (equation 1):

$$n CO_2 + n\ H_2O \rightarrow (CH_2O)_n + n O_2 \qquad (1)$$

On the contrary, the amount of CO_2 released by fossil sources accumulates in atmosphere, which is not in accordance with present objectives established by the European Commission, expecting to reach in 2050 the climate-neutrality[35]. This means to reach a target of net zero greenhouse gas emission[36].

Therefore, the replacement of chemicals with bio-derived alternatives is a key aspect, which characterized the industrial future. Issues related to the asset of the industrial plants and to economical competition with petroleum-based compounds must be faced, however, both the legislations and environmental concerns are driving towards more sustainable and eco-friendly alternatives.

With “The Joint European Biorefinery Vision for 2030” and “European Biorefinery Joint Strategic Research Roadmap” the European commission had established important points with the prospective to strongly include biomass and bio-refinery in the future industries[37]. In fact the main perspective is to significantly include before 2030 biomass as a consolidated realityfor the new technologies[38], fulfilling the following steps:

- Convert the 30% of overall chemical production into bio-based counterpart.

- Turn the 25% of Europe's transport energy with bio-fuels and make 30% of Europe heat and energy derive from biomass.
- Replace fibres and polymers with the corresponding bio-based counterpart such as viscose, bio-polymers, bio-plastics, nano-celluose and paper, which will remain 100% bio-based[20].

In terms of volume, the most abundant renewable raw material exploitable is cellulose being the 39% of the total, followed by lignin (30%) and other polysaccharides (like starch and hemicellulose). Finally, 5% of total renewable substances is composed of fats, terpenes, oils and protein[39], as shown below in Fig. 2.

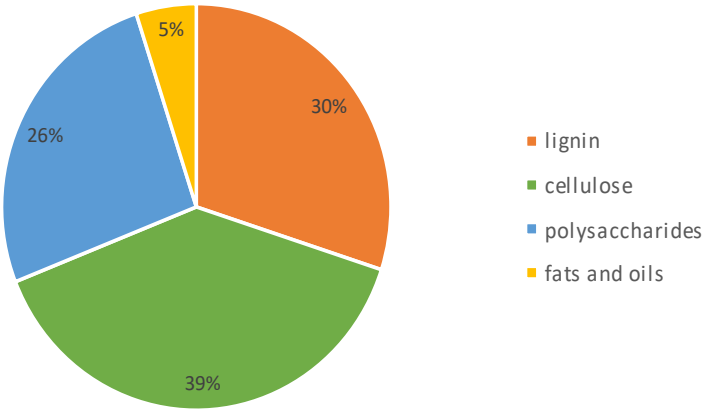

Figure 2. Distribution of raw material component expressed as % wt.

However, despite their minor amount, fats and oils are the major contributors in terms of bio-based energy and chemicals production. Their applications will be discussed later in Chapter 1.4.

1.2.1 Advantages and disadvantages of renewable raw material

Considering that the future industrial scenario requires a shift from consolidated fossil feedstock to renewable resources, a direct comparison between the two raw materials can be executed to visualize the benefits and drawbacks of each:

1) Renewable materials are constantly created in short time, unlike fossil feedstock, which requires long-term period to be generated. This aspect makes them suitable with green chemistry concept.
2) Almost no additional greenhouse effect is caused by burning and utilization of biomass and renewable source: as previously described, the amount of CO_2 emitted is equal to the amount required for the photosynthesis process, ensuring neutral addition of greenhouse gases free in atmosphere.
3) Bio-based products are often ecological and biodegradable, like for example lubricating oils based on natural oils and fat or bio-derived polymers[40]. However, this propriety is not always automatically assignable to all natural-derived products.
4) Renewable raw materials have a complex structure and are rich in oxygen and functionalization[41];This aspect can be directly exploit for chemical uses without any synthesis steps, typically necessary when using petroleum, as shown in Fig.3.

Talking about disadvantages that the utilization of renewable materials presents, they are mostly economical-related:

1) First, the extraction and transport of biomass is not always linear and easy as it is for petroleum and natural gas.
2) Biomass composition and typology are strongly dependent by environmental factors (geographical area, weather conditions, drought, etc.), as well as their availability can change from one year to another. Therefore, the biomass market is not constant, being subjected to many fluctuations.

Economic aspects of a process are important to consider since they are reflected on the price of the product: because of the low cost of petroleum and the chemicals related to it, the competition of bio-based products is still little in some markets (Table 1).

However, pushed by political regulations (e.g: introduction of biodiesel), subsidies and populations' ethical choices, this latter obstacle is being overcome.

Table 1. Price comparison between fossil and biomass derived basic chemicals. Table adapted from "Chemistry of Renewable" Chapter 1.4 [41].

Resource	Basic chemical	Amount (10^6 t /a)	Price (€/t)
Crude oil	Ethane	100	1000
	Propene	64	1000
	Methanol	25	150
	Benzene	23	900
	Toluene	7	250
Renewable resource	Cellulose	320	500
	Sucrose	169	200
	Starch	55	250
	Bioethanol	32	650
	D-Glucose	30	300
	Isomaltutose	0.07	2000
	D-Xylose	0.03	4500
	L-Sorbose	0.06	7500

1.3 Biorefinery

It has been demonstrated that biomass production is sufficient for industrial applications without compromising the food supply[42], therefore ethical problems related to the exploitation of edible sources in the chemical sector can be decline.

Biomass is processed in a so-called biorefinery, which is an integrated production plant for value-added products and energy.

Biorefineries can be divided based on the type of resource utilized:

- **Sugars-/starch- based biorefineries**: they produce mainly bio ethanol based on fermentation process for consequent production of bioethylene[43](Braskem[44]), especially in Brazil where the cost of sugar is very low; Polylactic acid is obtainable via polymerization from glucose-derived lactic acid[45] (NatureWorks[46]); 1,3-propanediol is obtained via fermentation of corn syrup (DuPont[47]) as well as succinic acid by fermentation of various sugars[48]. These are only few examples of the possibilities given by sugars and starch treatment.
- **Oil-/ fat- based biorefineries** are aimed to produced first and second generation biodiesel[49,50,51] and are related to the oleochemistry sector. Via catalytic cracking it is possible to obtain olefins from low value fats and oils[52]: with their long carbon chain, fatty acids are valid candidates for the formation of special chemicals and oily-derived monomers for bio-plastics (Novamont S.p.A[53]). Considering that nowadays the oil fractions are employed always more for industrials utilization rather than only for food purposes, modification on the crops are performed, for the obtainment of more dedicated and tailored oil composition, which would allow a better and complete exploit of the resource.
- **Wood-based biorefineries** cover a wide range of market such as bio-based chemicals[35,16,54] biofuels, electricity and heats;
- **Biowaste-based**, depending on the type of waste produced.

Asides from building up a dedicated plant for the biomass transformation, an alternative strategy has been developed which includes the adaptation of a pre-existing refinery plant, to meet the modifications that the utilization of biomass required.

1.3.1 Comparison between oil- and bio-refinery

In a biorefinery, biomass are processed for the obtainment of "green" platform molecules, unlike oil-refineries where hydrocarbons are obtained by fractional distillation of petroleum[55,41]. Oxygen, that characterized bio-derived platform molecules, must be removed together with molecular weight adjustment, before being employed for gasoline, jet fuel and diesel production[52,56]. On the contrary, oxygen is added to hydrocarbons derived from petroleum when chemicals are the main products of interests.

Figure 3 illustrates the two pathways from fossil based and bio based starting material to obtain chemicals and fuels:

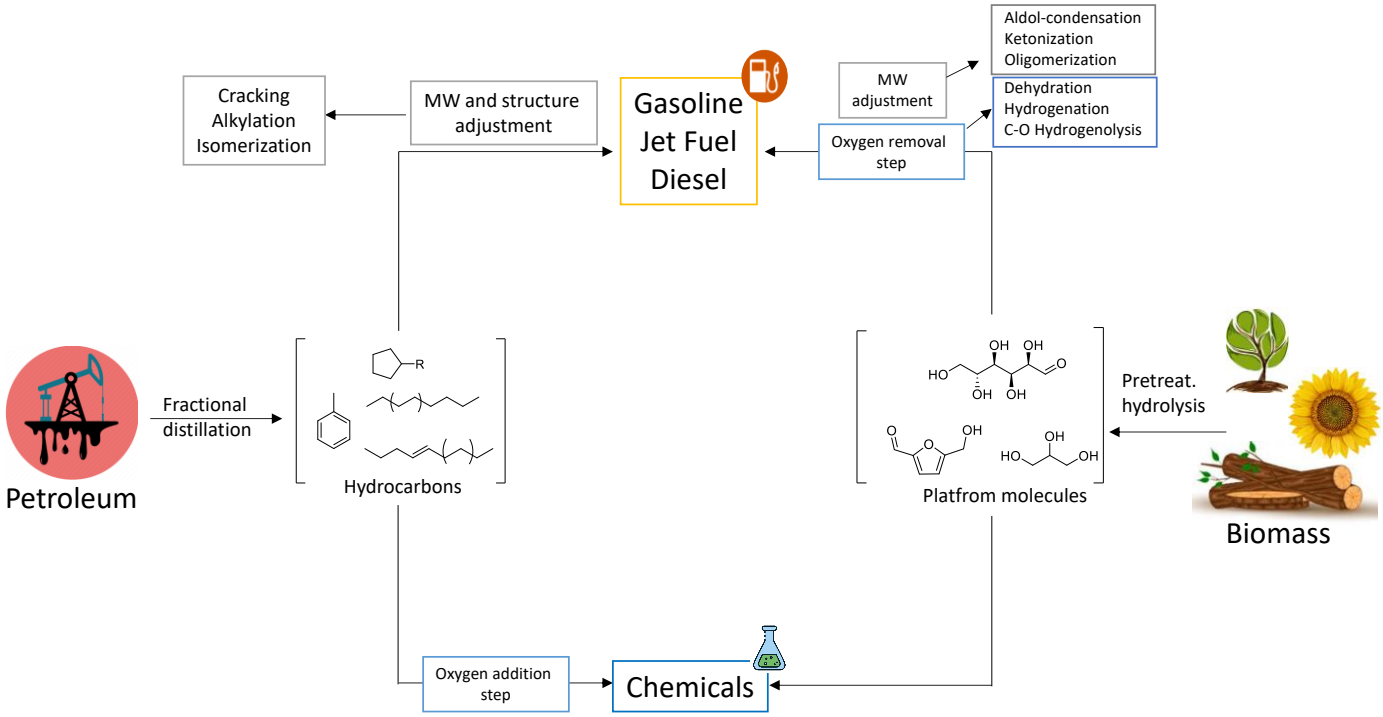

Figure 3: Flow scheme for the obtainment of the same products (chemicals or fuels) starting from fossil-based feedstock (petroleum) and renewable resources (biomass). Each starting material requires some adjustments and pre-treatments before being used. For example, the presence of oxygen is necessary when chemicals are the desired final product, while its removal from biomass platform molecules must be considered in case of fuels and gasoline production.

In fact, bio-derived platform molecules are rich in oxygen, but this does not represent a problem for their employment: the presence of multiple sites and functionalities makes them exploitable and adapt for many reactions and allows them to undergo multiple functionalization.

Table 2 below show the comparison between the composition of some biomass and petroleum. Evident differences are revealed for oxygen content, which accounts for up to 45% for biomass with only 1.5% for petroleum[57].

Table 2.Biomass and petroleum composition expressed as % w/w of Carbon (C), Oxygen (O), Hydrogen (H) and Sulphur (S).

	C (%)	O (%)	H (%)	S (%)
Wood biomass	49/57	32-45	5-10	<1
Herbaceous biomass	42-58	34-49	3-9	<1
Aquatic biomass	27-43	34-46	4-6	1-3
Animal and human waste biomass	57-61	21-25	7-8	1-2
Petroleum	83-85	0.5-1.5	10-14	0-6

The nature of the starting material can strongly vary from the season as much as from its origin: therefore the chemical plants must also be flexible and not peculiarly specialized to allow an universal adaptability to the starting material employed and optimal exploitation of the plant for the transformation of different types of biomass[58,59].

Talking about Europe there is a different distribution on the European land about the number of bio-refineries present and the type of starting material treated, including hemicellulose, lignin, oils/fats, starch, sugars etc.

From figure 4 it can be noticed that in northern Europe the majority of biomass is wood based; England, France and Spain are rich in sugar- or starch-based biorefinieries for bioethanol production, together with other bio-based chemicals.
Finally in Germany and in Italy the majority of biorefineries are oils and fats- based, including both the production of biodiesel but also their exploitation for the oleochemistry sector.

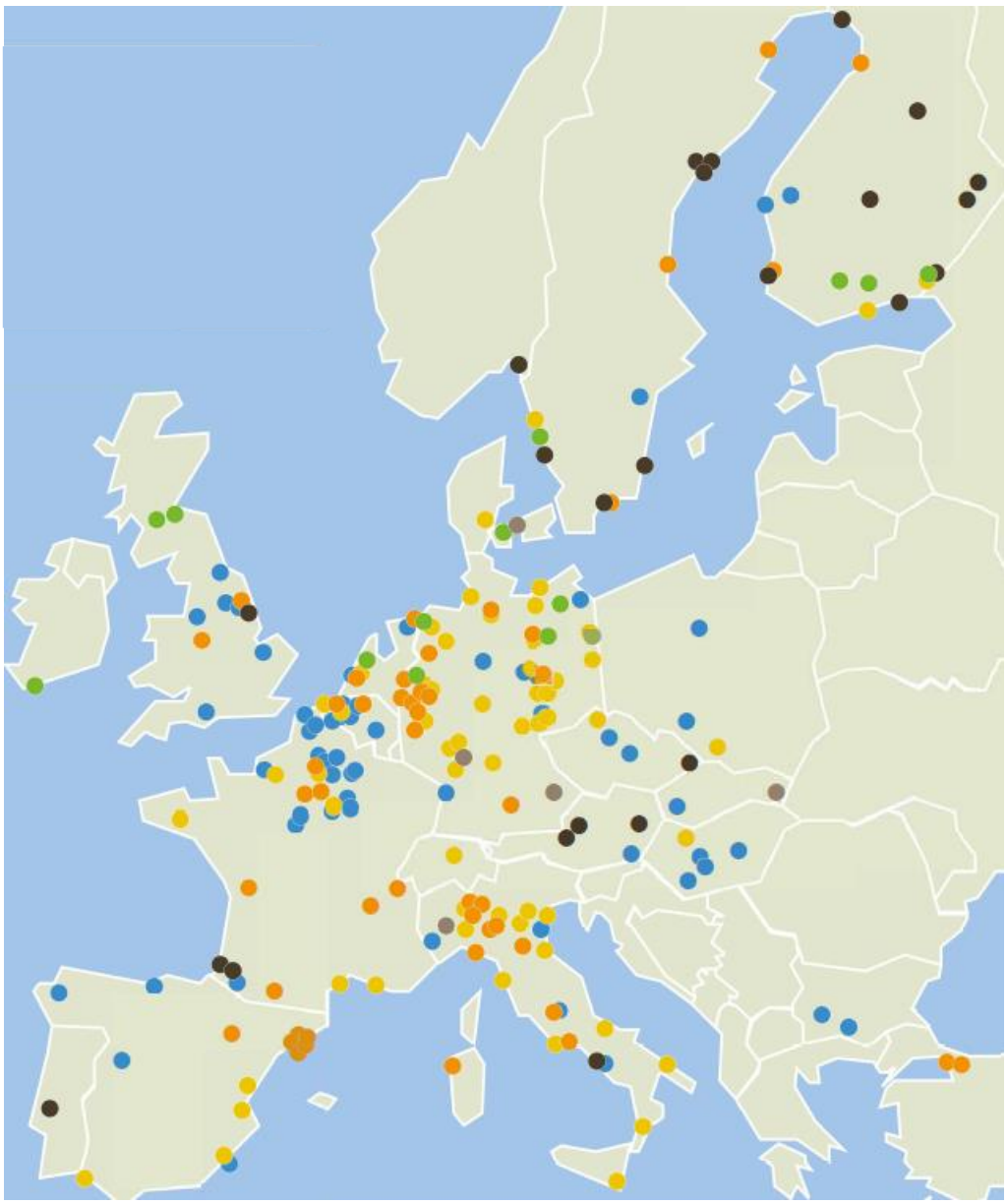

Figure 4. Distribution of different bio-refineries across Europe: ● biowaste-based; ● lignocellulosic; ● oil/fat-based-biodiesel; ● oil/fat-based oleochemistry; ● sugar/ starch- based; ● wood-based.

1.4 Oleochemistry

The oleochemistry is the direct connection between the availability of natural and renewable oils and fat and the possibility to substitutes fossil feedstock for chemicals and energy production at an industrial scale.

Independently from the biomass origin, the value-chain based on oleochemistry comprises the processing steps shown in figure 5:

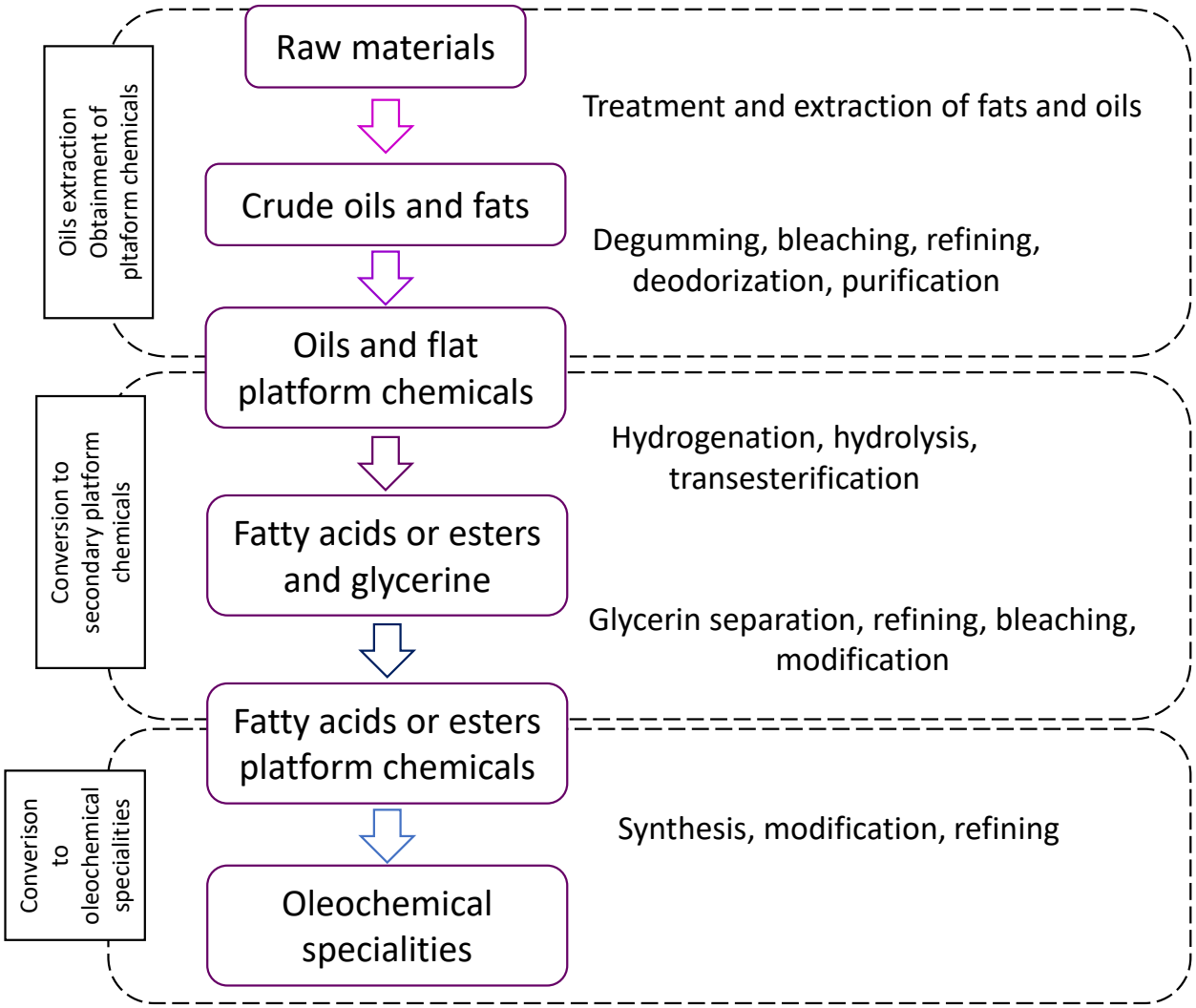

Figure 5. Oleochemistry value-chain for the treatment from zero of the renewable raw material to the obtainment of platform bio-derived molecules and final oleochemical specialities.

The oleochemistry deals with fats and oils, which differ mainly for the melting point, considering that their chemical structure is relatively the same: oils are liquid at room temperature, while fats have a solid consistency.

Oils and fats are triglycerides of fatty acids, which means that a molecule of glycerol is bonded to three carboxylic fatty acids, which can be different inside the same triglyceride. These latter can have zero, one or more double bonds, opening possibilities for the different isomers (*cis*, *trans*) and leading to differences in chemical proprieties and different specific sites that can undergo reaction, as evidenced in Fig. 6.

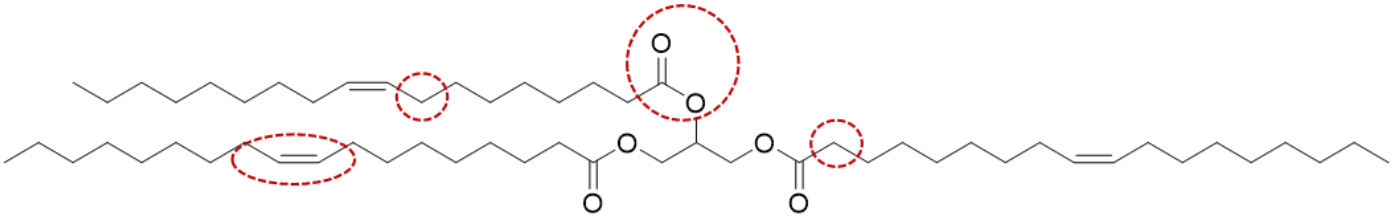

Figure 6. An example of triglyceride with reactive sites highlighted at different positions of the molecule.

The separation of glycerol and fatty acids can be performed following four different methods shown in Figure 7,8,9,10:

- Hydrolysis: adding three moles of water, one mole of glycerol is produced together with three moles of fatty acids. This method is called fat splitting and yields to 99% of separated fatty acids and diluted glycerol[41].

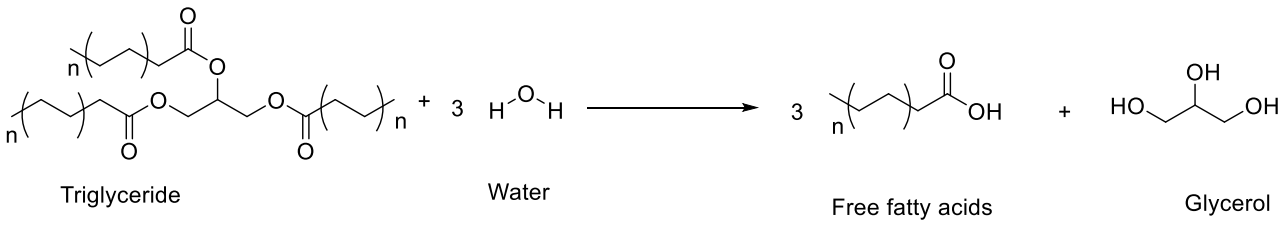

Figure 7. Water hydrolysis of a generic triglyceride into its fatty acids and glycerol

- Transesterification: this method involves the reaction of triglycerides with alcohol leading to the formation of fatty acids esters. Methanol is typically used with the formation of fatty acids methyl esters-FAMEs and concentrated glycerol.

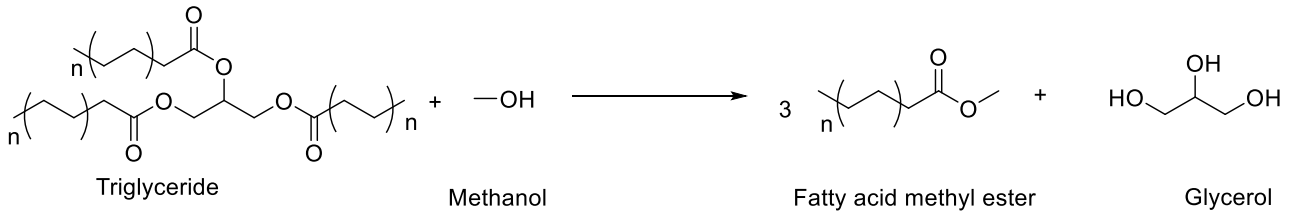

Figure 8. Transesterification of a generic triglyceride with an alcohol (in this case methanol) which lead to the formation of fatty acid esters (in this case fatty acids methyl esters) and glycerol.

- Saponification: reaction between NaOH and triglycerides to produce soaps accompanied by crude glycerol.

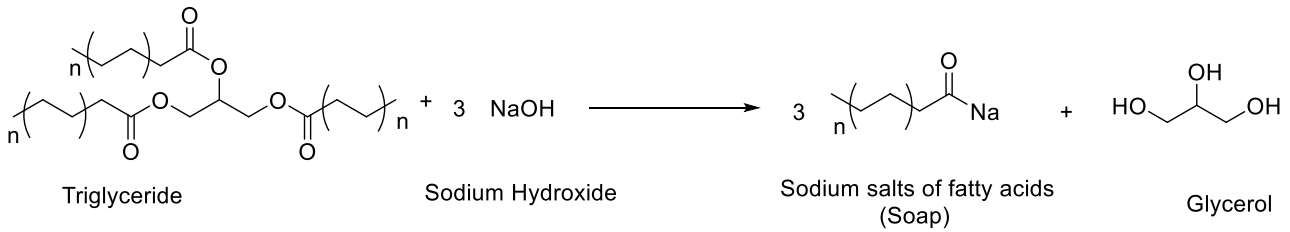

Figure 9. Saponification reaction between sodium hydroxide and a triglyceride.

- Hydrogenation of fats and oils into alcohols and glycerol, even if this latter method has not been fully developed yet.

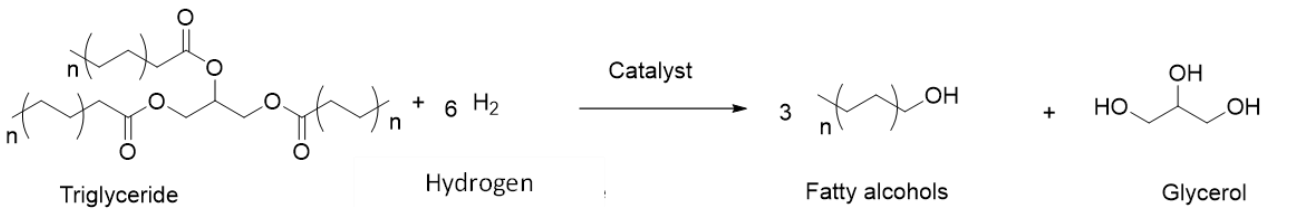

Figure 10. Direct catalytic hydrogenation of triglycerides to obtain glycerol and fatty acids.

1.4.1 Fatty acids

Fatty acids are the major raw material to produce bio-based chemicals and fuels. They are divided into saturated fatty acids (SFAs) and unsaturated (UFAs) which can have one or more double bonds along the carbon chain.

They are constituted of a non-polar carbon chain followed by a polar head, made of a carboxylic group (Fig 11).

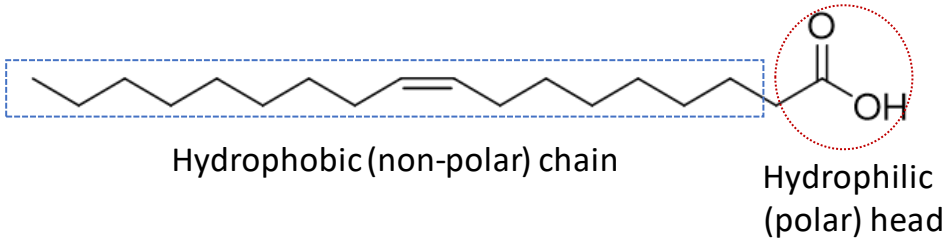

Figure 11. Representation of a fatty acid (in this case oleic acid) for observing thenon-polar aliphatic chain and the polar "head" formed by a carboxylic group. This is a surfactant-like configuration, making saturated fatty acids optimal bio-derived surfactant agents (e.g.: sodium-stearate, lithium-stearate, glycol-stearate etc.)

A typical vegetable oil is composed of 16-18 carbon atom fatty acids, with some minor components that account from 12 up to 22 carbon atoms. Vegetable fatty acids are commonly unsaturated, while an animal-derived present a higher degree of saturation[40].

The abbreviation for fatty acids description is composed of CX:Y where X represents the number of carbon atoms and Y the number of unsaturation present along the chain. If one or more unsaturation is present, the double bond position is indicated by Δ followed by the carbon number of the unsaturation. The letter *c/t* evidence the cis- or trans- isomer.

Tables 3 and 4 illustrate the most common fatty acids that can be found in nature.

Table 3. Common saturated fatty acids present in nature.

Abbreviation	IUPAC name	Common name	Occurrence
C 8:0	Octanoic acid	Caprylic acid	Butter, coconut oil
C 10: 0	Decanoic acid	Capric acid	Butter, coconut oil
C 12: 0	Dodecanoic acid	Lauric acid	Animal fat, coconut oil
C 14: 0	Tetradecanoic acid	Myristic acid	Animal fat, coconut oil
C 16: 0	Hexadecanoic acid	Palmitic acid	Animal fat, palm oil
C 18: 0	Octadecanoic acid	Stearic acid	Animal fat, palm oil
C 20: 0	Elicosanoic acid	Arachidic acid	Peanut, beet, cocoa oil
C 22: 0	Docosanoic acid	Behenic acid	Canola oil, peanut oil

Table 4. Unsaturated fatty acids present in nature, presenting up to three unsaturations

Abbreviation	IUPAC name	Common name	Occurrence
C 16:1 (Δ9/c)	*Cis*-hexadecenoic acid	Palmitoleic acid	Seed oil
C 18:1 (Δ6/c)	*Cis*-6-octadecenoic acid	Petroselinic acid	Parsley seed
C 18:1 (Δ9/c)	*Cis*-9-octadecenoic acid	Oleic acid	Palm oil, animal fats
C 18:1 (Δ9/t)	*Trans*-9-octadecenoic acid	Elaidic acid	Ruminant fats
C 18:2 (Δ9,12/*c.c*)	Octadecadienic acid	Linoleic acid	Sunflower oil
C 18:3 (Δ9,12,15/all *c*)	9,12,13-octadecatrienic acid	Linolenic acid	Hemp/linen oil
C 18:3 (Δ8,10,12/*t.t. c*)	8,10,12-octadecatrienic acid	Calendulic acid	Marigold
C 20:1 (Δ5, *c*)	*Cis*-5-eicosenoic acid	Eicosenoic acid	White marshbill
C 20:4 (Δ5,8,11,14/all *c*)	All *cis*- 5,8,11,14 eicosatetraenoic acid	Arachidoic acid	Liver, fish oil
C 22:1 (Δ13/c)	*Cis*-13-docosenoic acid	Erucic acid	Old canola
C 22:1 (Δ13/t)	*Trans*-13- docosenoic acid	Brassidic acid	Isomerization of erucic acid

Fatty acids are widely distributed in nature in lipids, oils, waxes, sterol, esters and other minor components but only oil-derived components are used at industrial scale due to their availability in large amount[60].

This has led to an increase in oil production of 211% since 1985[61,62] .

After the obtainment of fatty acids, they are purified to remove impurities such as minerals, gums, soaps and proteins, followed by distillation and/or crystallization for fatty acids separations[60].

The distribution of different fatty acids presents in a vegetable oil can strongly vary, as shown in figure 12:

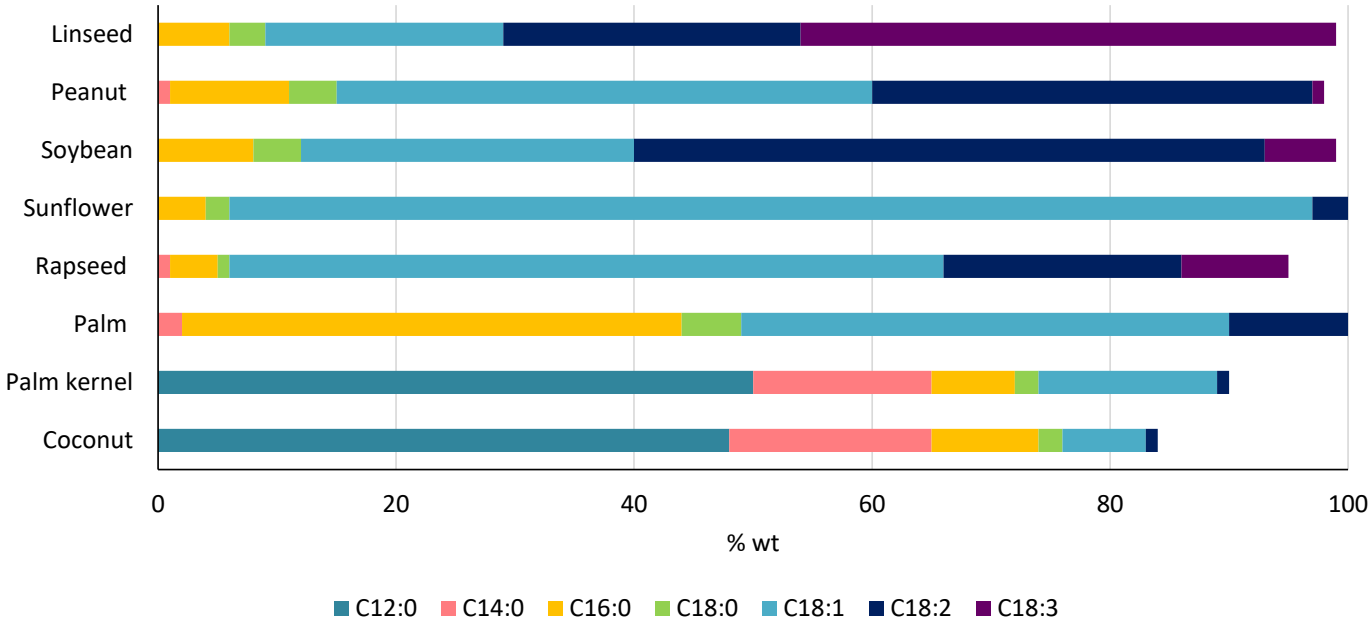

Figure 12. Overview of industrially important oils and their fatty acid composition (typical mean values expressed in % by weight).

Thanks to their chemical structure, fatty acids are useful tools for bio-plastic production, in cosmetic fields, for lubricants, oils and as starting platform molecules for further modifications. They can be transformed into fatty esters, like for instance the methyl esters of fatty acids (FAMEs) used for bio-diesel[63,64].

With NaOH treatment they are used for the production of soaps, as well as their metallic salts(with Mg, Ca, Zn) make them suitable for soaps and stabilizers in polymers industry[41,65].

The carboxylic group of the fatty acid can be modified for the production of biodegradable surfactants used in the health care sector, while the carbon chain can be subjected to modifications in concomitance of the double bond, for the obtainment of branched fatty acids[66,67].

Finally, carboxylic fatty acids allow undergoing a wide choice of classical reactions like hydrogenation (regarding both the double bond and the carboxylic moiety to obtain the alcohol), hydrolysis, oxidation, polymerization, etc.

These reactions are summarized in Figure 13:

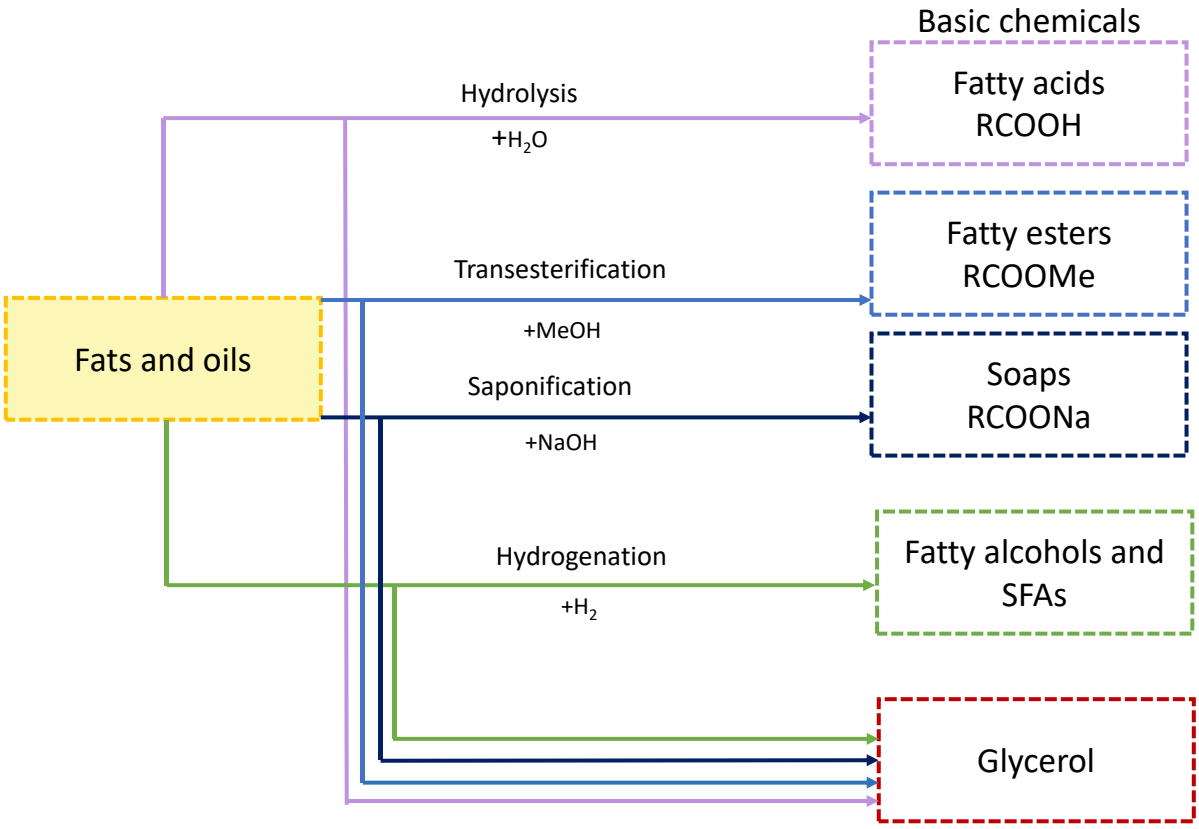

Figure 13. Product of basic oleochemicals from oils and fats, adapted from reference [39].

Therefore, fatty acids are strategic bio-derived molecules, which present high adaptability for many reactions and applications, ranging from biopolymers, to textile, personal care, pharmaceutics, feed, soaps, detergents and agricultural products, with a varied distribution on the market (Fig. 14).

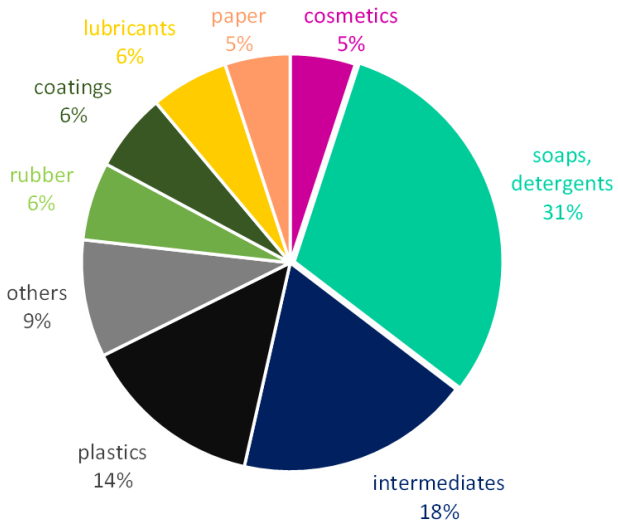

Figure 14. Market distribution of fatty acids derivatives in % weight [41]

1.4.1.1 Iodine Value

The IV is a way to classify the different fatty acids according to the number of unsaturations[68]. The calculation is based on the iodometric Wijs/Hanuŝ[69] method: an iodine solution is added to the unsaturated fatty acids with glacial acetic acid. Iodine reacts with the double bond and the amount of I^- unreacted is then allowed to react with potassium iodide, converting it to I_2. The amount of $I_2$is determined by back-titration with sodium thiosulfate standard solution ($Na_2S_2O_3$) and starch as indicator.

Therefore, the higher is the IV, the higher the amount of unsaturation in the molecule.

Table 5. Examples of Iodine Value for animal and vegetable fats. The highest the iodine value, the highest the number of unsaturation, which results in liquid consistency at room temperature.

Fat	Iodine value (gI/100g)
Beef tallow	42-48
Butter	25-42
Coconut oil	6-11
Palm oil	49-55
Sunflower oil	110-145
Soybean oil	120-139
Olive oil	75-94

1.4.2 Glycerol

In recent years, as a result of the boundless biodiesel production, the available amount of glycerol sharply increased. Triglycerides are broken into fatty acids and glycerol with four different processes as described in chapter 1.4.
Prior its utilization, glycerol needs to be purified with evaporation, distillation or refining as function of the purity required.

Glycerol has always been used for many applications (in cosmetics, as a sweetener, as plasticizer etc.) but the decline in its price opened new routes for its applications. Low price and large availability upset completely the process based on glycerol production[30,70,71], as shown in Fig. 15.

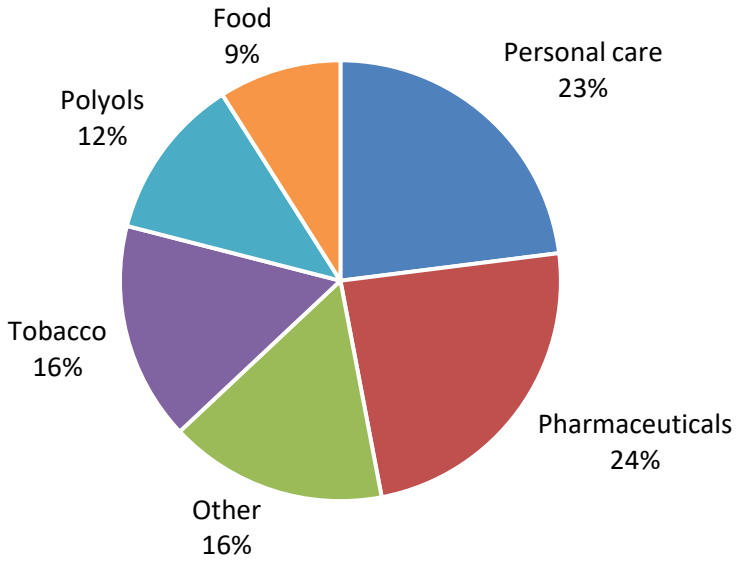

Figure 15. Glycerol- derived product distribution expressed in % wt.

A clear example is given by the fact that initially glycerol was produced starting from propene via epichlorohydrin route,employing first calcium hydroxide and later sodium hydroxide, while now epichlorohydrin is the target molecule starting from bio-based glycerol for the formation, by reaction with bisphenol A, of epoxy resins[72](Fig. 16 and 17).

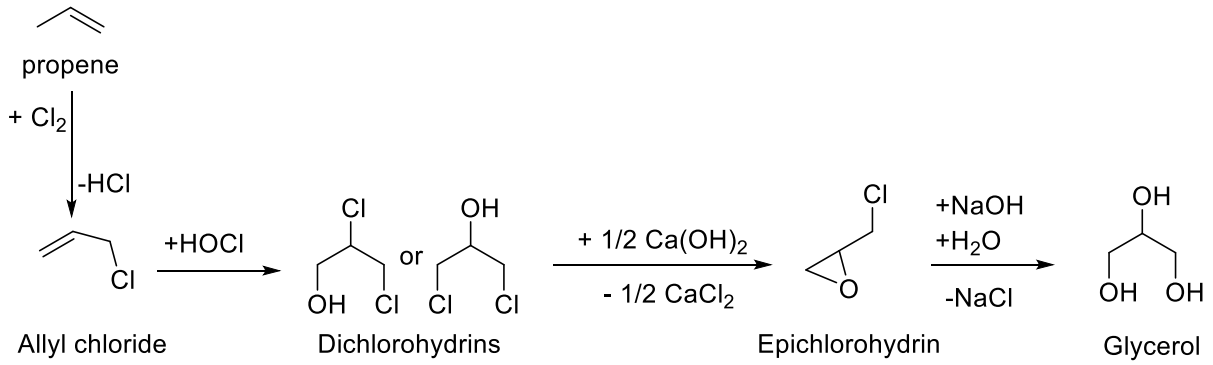

Figure 16. Glycerol production reaction starting from propene and passing through epichlorohydrin with the utilization of calcium and sodium hydroxide. This process was commonly used for producing glycerol before its over-production as a consequence of fatty acids utilization in chemical and fuels formation.

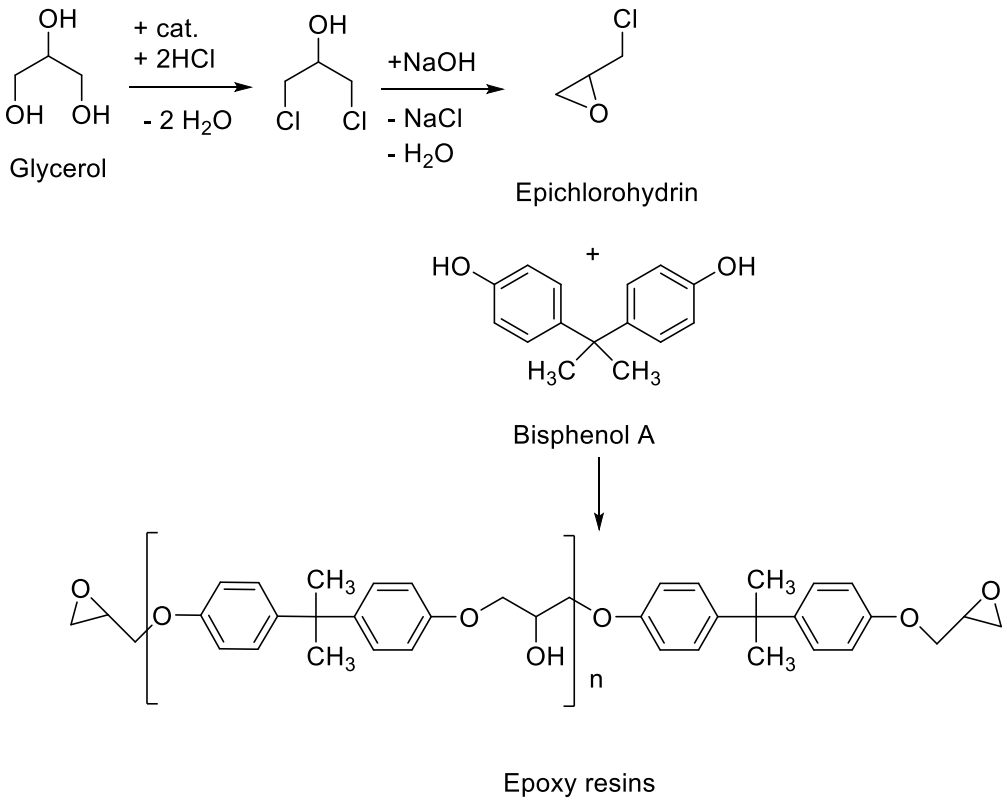

Figure 17. Today the same reaction of *Figure 16* is considered but in its opposite way: bio-derived glycerol is used to form epichlorohydrin. This latter forms bio-derived epoxy resins by reacting with Bisphenol A.

Glycerol became therefore an enormous resource due to its wide applications and possibilities: as additives (like glycerol tertiary butyl ether for diesel or glycerol ocatdienylether as emulsifier after hydrogenation[73]), as platform molecule for the formation of polymers

precursors (acrylic acid for polyacrylic acid and polyacrilates[74], epichlorohydrin for epoxy resins formation etc.). If submitted to decomposition glycerol produces syngas[75] ($CO+H_2$) , exploitable for many applications from Fischer-Tropsch process[76] to ammonia production.

In conclusion, it is important to underline the role of oleochemistry and oleochemical compounds in present industry, which represent a strong and feasible reality for future development.

Figure 18summarizes the possibilities that fatty acids opens and underlines that for each component of a triglyceride, multiple products can be obtained. Even more, the by-product glycerol covers an entire portion of the bio-derived chemicals market.

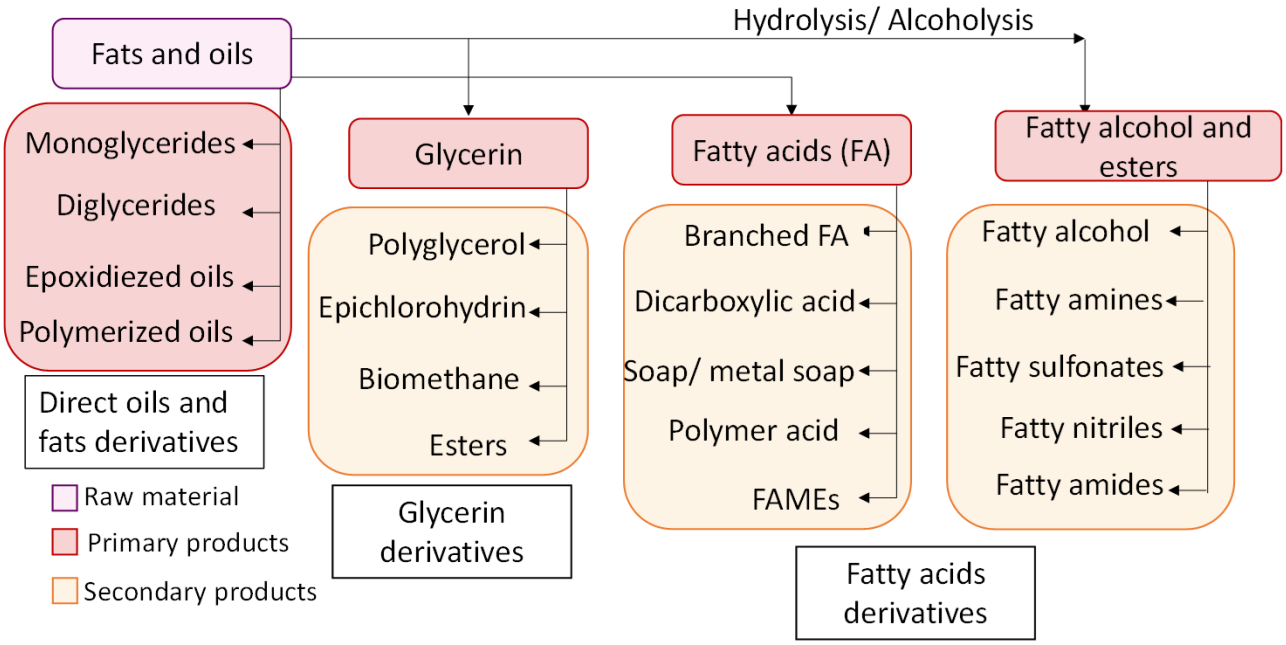

Figure 18. Schematic representation of the main products of oleochemistry and their origin. Figure adapted from reference [20]

2.Hydrogenation of fatty acids

As discussed earlier, fatty acids are suitable for many reactions and, among these, hydrogenations have been of great interest since the early development of utilization of vegetable and animal fats in industry.
Below, the mechanism of the reaction is described followed by a short historical overview about the development at the industrial scale of hydrogenation of fatty acids.

2.1Reaction mechanism

The metal catalysed hydrogenation occurs via Horiuti-Polany mechanism, that described the hydrogenation and isomerization of olefins on a solid catalyst[77].
Before the hydrogenation of an unsaturated molecule occurs, the hydrogen (H_2) diffuses from the gaseous atmosphere through the oil with final adsorption on the metal surface (H_2*). Subsequently, the hydrogen is divided into two H atoms still adsorbed on the catalyst surface (2H*), which are ready to interact with the unsaturated molecule.
The olefins (mono or poly unsaturated) are adsorbed on the catalyst surface through π bond with the double bond.
The formation of this latter is associated with the strength of adsorption of the double bonds on the active metal. The lower the electronic density of the metal, the higher is its ability to work as acceptors, leading to the strong adsorption of the double bond of fatty acids[78,79].

A first hydrogen atom is added with formation of half-hydrogenated fatty acid and subsequent σ-bond between the non-hydrogenated carbon and the metal; the initial *cis/trans* conformation is lost due to the possibility of the single bond C-C to rotate and to form geometric isomers in case of double bond restoration. This step is highly reversible, and lead to the possibility to multiple hydrogen exchanges.
After addition of the first H* there are two possibilities:

- Under hydrogen rich conditions, a second H* atom is added, and complete hydrogenation occurs, leading to the formation of the saturated molecule.
- Under hydrogen poor conditions the half-hydrogenated fatty acid can extract a second H atom from an adjacent C-H group, with possible shifting of the double bond along the carbon chain, depending on the -H abstracted. The free rotation of the half-hydrogenated intermediate and reversibility of the first step with further desorption results into *cis-trans* isomerization[80].

It is possible to summarize the hydrogenation of an unsaturated fatty acid into two steps with first reversible partial hydrogenation with formation of half-hydrogenated fatty acid, followed by complete hydrogenation with saturated fatty acid formation. The first step is an equilibrium and occurs very rapidly, while the second step requires more energy[81].
The mechanism of olefin hydrogenation is illustrated in Figure 19:

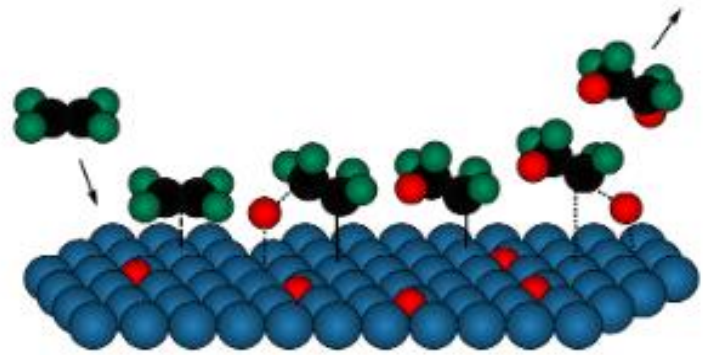

Figure 19. Profile of Horiuti-Polany mechanism: the black and green atoms form a generic unsaturated molecule; the blue atoms are the metal (Me), and red atoms are H* atoms. The double bond forms a π bond with Me on the catalyst's surface. The first H* bonds to the carbon atom with immediate formation of σ bond between the second C atom and the Me. Subsequently an additional H* is attached to the second C atom with final dissociation of the saturated product.

The interaction between the catalyst and the substrate must be calibrated, to allow the initial bonding through the double bond of the olefin and the final dissociation of products, as stated in the Sabatier principle: if the interaction is too weak, the substrate can't bind to the catalyst surface, while if it is too strong the dissociation of the product results impossible[82].

2.2History of hydrogenation of fatty acids

The first patent regarding hydrogenation of oils dates back to 1903 created by W. Normann (UK), which was the pioneer of fat hydrogenation (named *hardening*) employing finely dispersed Nickel catalyst[83].

Despite the success at lab scale, this process showed many issues for its scalability, but in 1910 the English Company Joseph Crosfield & Sons initiated the first large-scale industrial hydrogenation[84].

After that, the hydrogenation process went through many evolutionary steps, attracting many companies (Unilever, Lurgi, Procter Gamble) and pushing them to develop their techniques. At the end of 1900s major studies were performed not only regarding the purity of the final product to avoid metal contaminations but also to the presence of impurities on the starting material that could poison the catalyst.

The impurities, consisting of residues of animals or vegetable origins like phosphatides, carotenoids, sterols, and proteins, were typically removed by absorption with activated materials at 100-130°C under vacuum and filtered to ensure a determined purity of the starting material before hydrogenation.

Talking about food-related processes, hydrogenation of oils was mainly adopted for the obtainment of margarine, which was similar in butter about consistency but derived from sunflower or palm oil. Finely dispersed Nickel was employed as a catalyst for this process, which required high reaction temperature[20] (200-230°C).

Risks were associated to high temperature at which pressurized hydrogen must be handle and the ability of Nickel to form fat-soluble salts, which contaminated the final product. A filtration step, with correlated fire hazard issues because of the pyrophoric features of the metal, was planned, but it was not still enough to guarantee pure products, because some metal could cross the membrane[85].

Finally, it was demonstrated that in case of incomplete saturation of the double bonds and formation of the *trans*fatty acids, health-related issues overcome, being *trans*-FA responsible of many diseases including diabetes, cancer and coronary-related ones[86,87]. For these reasons *trans*-FA are subjected to strong regulations for human's consumption products[88,89].

Today, other precious metals such as Pd and Pt are used together with Ni, thanks to optimization of the recovery step, in order to avoid the contamination of the metal in the final product and to limit loss of the catalyst.

2.3 Uses of hydrogenated fatty acids

Beyond margarine production, catalytic hydrogenation has always been applied and studied for a century, with the prospective to render oils more stable to the oxidation process[79]. This would allow improving the shelf life of the product reducing the rancidity phenomena.
Also, it permits to modify the melting characteristics of the oils and to obtain products with a desired solid consistency.
However, hydrogenation of UFAs found important industrial applications related not only to the food industry but also in detergents and surfactants fields.
Carboxylic fatty acids have a bifunctional character with a polar head group and a nonpolar chain that confers solubility in organic solvents. For this reason, they can be ascribed as natural surfactants, as shown in figure 11 in Chapter 1.4.1.
The hydrogenated product of oleic acid, stearic acid, finds therefore many applications in the production of detergents and soaps[65,90], while its ester (glycol stearate and glycol distearate)is widely used for cosmetics and shampoo production.
Metallic salts of stearate (Zn, Ca, Cd) are used to soften PVC and textiles. Niche uses involve stearic acid as a negative pole for lead batteries.

2.4Catalysis- Hydrogenation aspects

Hydrogenation is a heterogeneously catalysed reaction that involves three phases[91]: the gaseous hydrogen, the solid catalyst and the liquid starting material represented, in our case, by the unsaturated fatty acids derivatives mixture to be converted into the saturated counterpart.

In a slurry system, from the moment when all three phases are in contact, the following steps occurs:

- Mixing and dispersion of the catalyst in the mixture by the mechanical stirrer. The mechanical mixing guarantees homogeneity of the hydrogen in the reaction mixture.
- Diffusion of the gas through the oil up to the catalyst surface: the two reactants diffuse through the microfilm formed on the catalyst surface, with the aim to reach the active sites[92].
- Adsorption of the unsaturated fatty acids on the catalyst surface.
- Hydrogenation of the reactant following the Horiuti-Polany mechanism (described above in chapter 2.1).
- Desorption of the products from the catalytic surface.
- Release of the heat due to the exothermicity of the reaction: for a unit drops in Iodine Value (IV) the heat released is 383 KJ/Kg.

Both reactants (H_2 and the starting oil) find diffusional resistance during their path to reach the solid catalyst.

For multi-phase reactions limitations about the transfer of the reactants occur at the interfaces between the gas and the liquid and the liquid and the solid.

Regarding H_2 (Figure 20), a first concentration gradient is present at the gas-liquid interface. Once the gas has become in the same phase as the oil (which is in this case the liquid phase), they both undergo a second concentration gradient, present at the liquid-solid interface.

This latter is more marked due to higher resistance at matter transport of the solid, therefore both $H_2$and oil concentration decrease sharply while reaching the internal active sites of the catalyst.

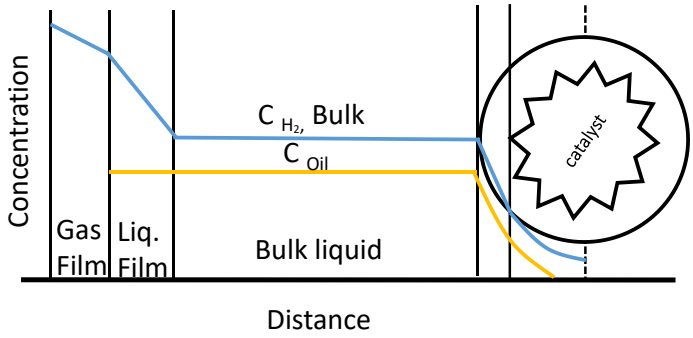

Figure 20. Schematic representation of diffusional limitations that the gas (H_2 in blue) encounter both in the liquid phase and in the solid catalyst before reaching the bulk of this latter. In yellow the diffusional limitation of the oil towards the solid catalyst is shown. The -y axis reports the concentration of each component and the x-axis the distance from the bulk of the catalyst.

For a given reaction is therefore possible that diffusional limitations of reactants through the liquid and solid film have control on the whole reaction rate, being in a so-called "diffusional regime". This is not the optimal condition because the availability of reactants on the catalyst surface is limited, leading to slower or incomplete reactions.

A preferable condition is the "kinetic regime": in this case, the reaction rate is not determined by the concentration of reactants that can effectively reach the active sites, but by the intrinsic kinetics of the reaction.

Increasing the agitation rate of a batch reactor is a possible way to avoid the diffusional regime and work in kinetic conditions.

2.4.1Nickel-based catalysts

As described before, Nickel was the first metal used for the hydrogenation of unsaturated fatty acids to obtain the saturated counterpart, thanks to its cheapness and high activity. Therefore, many studies were initially based on Nickel as metal, in form of supported nanoparticles or combined with other metals.
Sometimes the target molecule was the carboxylic acid completely saturated, others the saturated alcohol or the linear alkane.

Dating back to 1987, a process involved Ni-Raney for the hydrogenation of unsaturated carboxylic acid to stearic acid was patented by Ginzburg et al[93].
Ni-Raney is a high surface catalyst made of an alloy of nickel and aluminium: this latter is then removed by NaOH treatment which leads to the obtainment of a metallic sponge with a very high surface area, hence reactivity[94]. However, besides the toxicity of nickel, this catalyst is highly pyrophoric when exposed to air, increasing the danger of the reaction.

In 1996, the Okamura group studied the catalytic hydrogenation of linoleic acid with Ni supported on Al_2O_3 and SiO_2(5% wt) in a batch system at 423K and 300 torr of H_2using 0.1g of catalyst and 0.5 g of linoleic acid solution[95]. They studied the reaction mechanism adopting the Horiuty-Polany mechanism and evidencing that linoleic acid was adsorbed on the catalyst surface with one of the double bonds (Δ9 or Δ12) with first partial hydrogenation, which lead to a possible formation of the geometric isomers. Also, adjacent hydrogen could be subtracted from the absorbed carbon, leading to the formation of positional isomers. Complete addition of the second H atom to the half-hydrogenated bond led to the formation of oleic acid, which underwent the same process for the obtainment of the completely saturated acid. Also, they tested Cu/Al_2O_3 40% wt evidencing that, according to the metal used, the double bond present in Δ9 or Δ12 showed different hydrogenation behaviour. Despite the reduced activity, selectivity towards oleic acid was higher for Cu, while considering the whole process (selectivity towards stearic acid, linoleic acid conversion, metal loading) the most performing metal remained nickel.
Coming into more recent years, Ni-Nb-O composites catalysts were tested by Chung group in 2020, for the hydrogenation of stearic acid to n-alkene, exploitable in diesel production[96]. The results showed that catalyst $Ni_{0.5}Nb_{0.5}O_2$ effectively converted stearic acid to *n*-alkanes with nearly 100% conversion and >99% *n*-alkanes selectivity at mild conditions (513 K and 3.5 MPa

of H_2 pressure). They found that Nb species improved the dispersion of Ni species, which may supply more hydrogenation active sites.

Even more recent works, conduced by Igarashi in 2021,introduced TiO_2 as support for Ni for the reduction of *trans* fatty acid in soybean oil[97]. They used a semi-batch system, performing the reaction at 413Kwith 50 bar of hydrogen. They showed that Ni and Ni/TiO_2 had the same catalytic activity, evidencing that substrate conversion was not dependent on the support typology. Also, the supported metal presented a remarkable limited formation of the trans isomer. The formation of this latter was associated with the strength of adsorption of the double bonds on the active metal. The electronic effect given by TiO_2 to the metal Nickel favoured the adsorption of the double bond reducing the possibility to form the trans-fatty acid (TFA) and ensured complete hydrogenation.

Nickel/Palladium/Ruthenium – Graphene based nano catalysts were tested by Sarno group for hydrogenation of oils in a batch system (10 bar of H_2 at 100°C)[98]. In particular, they successfully controlled the *trans* isomer formation, reducing the full hydrogenation to stearic acid with Ruthenium and allowing multiple reuses of the catalyst thanks to the stability of graphene.

Considering the toxicity and its environmental consequences, replacements for Nickel were investigated, involving precious metal catalysts such as Pd, Pt or Ru.

2.4.2 Palladium-based catalysts

Noble metals are active for hydrogenation reactions and, according to what is found in literature, their activity and selectivity towards monocarboxylic fatty acids follows the order: Rh>Pd>Pt>Ru> Ni.
Similar trends is present for the tendency of trans fatty acids formation: Rh> Pd> Ru> Ni>Pt[99].
From an economic point of view, Ni is the cheapest metal, followed by Ru, Pt, Pd and finally Rh, as illustrated in table 6.

Table 6. Noble metal price expressed as EUR/ g according to the source [100]

Noble metal	Price (EUR/g)[100]
Pd	72.823
Pt	29.388
Ru	21.814
Ni	17.495
Rh	555.16

With the perspective of the application of a circular economy, the spent catalyst is not considered as a waste, but represents a source that can be efficiently separated and recycled, accompanied by null or low loss of activity. Therefore, the higher metal price compared to Ni can be amortized by its higher activity, less toxicity, and the possibility to be efficiently recycled and reutilized multiple times for the same reaction. If not, the separated catalyst can anyway undergo the regeneration process, remaining always inside the production process in line with the principles of a circular economy.

Palladium and Ruthenium supported on carbon were synthesized and tested by Mäki-Arvela for hydrogenation of linoleic acid to stearic acid, using n-decane as solvent[80]. The reaction was performed in a batch system, with 20 bar of H_2 and operating between 80-100°C.They found that initial hydrogenation rate was decreasing in the order 3% wt Pd/C >1% wt Pd/C > 5% wt Pd/C attributable to major hydrogen adsorption capacity, being for 1% wt Pd/C 2.5-fold of 5% wt Pd/C.

Considering the overall process,5% wt Pd/C was the most performing catalyst, reaching 90% of conversion in less than 2 hours, while 5% wtRu/C needed more than 4 hours. Also, deactivation was more prominent in the latter case occurring more rapidly for Ru catalyst.

Deactivation was correlated to the amount of monounsaturated fatty acids: the higher the amount of monoenic acid in the reaction products, the more extensive the deactivation. Even more, coke depositions were the major cause of loss in catalytic activity for prolonged reaction time.

Pd/SiO_2[101]and Pd/Al_2O_3[102]wereexploited in reactions with sunflower and soybean oil respectively. The aim was to evaluate the effect of the support for the conversion of linoleic acid to oleic acid, comparing silica with Ni-Raney and Alumina with Carbon. It was evidenced that the activity of carbon was 10 times major than alumina, working in a batch system at 165°C, with 3 bar of hydrogen after 100 minutes of reaction.
Regarding silica support the reaction was performed at 100°C and 5 bar of H_2 ; dimension of pores around 7-8 nm was the most favourable, and in combination with a metal loading of 0.8% wt, resulted in the fastest iodine value drop after 1 hour compared to Nickel.
Mesoporous Zr-SBA was evaluated by Thunyaratchatanon[103] as support for Pd, evidencing that the presence of Zr formed an electron-poor environment which improved adsorption of H_2 and molecules, boosting the catalytic activity. Increasing the Zr content, the adsorption of FAMEs was stronger and created steric hindrance for other FAMEs: in this way only a partial amount of FAMEs were hydrogenated, offering stability against oxidation and suitability for biodiesel application at the same time.
Bernas et al. examined kinetic aspects of hydrogenation of linoleic acidwith5% wt Pd/C powder catalyst[81]. They revealed that if the linoleic acid was adsorbed molecularly, the C=C formed a π complex with the surface which would lead, in presence of Brønsted acid sites, tothe formation of carbenium cation by protonation and lost of the double bond character. Subsequently an-H extraction from another C-C bond led to restoration of the double bond, shifted in position depending on the –H being extracted.

Bernas proposed three mechanisms, for hydrogenation of oils, being the first (mechanism I) more approximated and in line with Horiuty-Polany mechanism.

They revealed that if the linoleic acid was adsorbed molecularly, the C=C formed a π complex with the surface which would lead, in presence of Brønsted acid sites, to the formation of carbenium cation by protonation and loss of the double bond character. Subsequently, an -H extraction from another C-C bond led to the restoration of the double bond, shifted in position depending on the –H being extracted.

Bernas proposed three mechanisms, for hydrogenation of oils, being the first (mechanism I) more approximated and in line with Horiuty-Polany mechanism.
The addition of hydrogen to olefins is a surface reaction involving the addition of chemisorbed hydrogen to a chemisorbed olefin. The reaction rate presented a dependency on hydrogen pressure of 0.5 or 0 order: for low H_2 pressure (0.5-2 bar) the rate was of 0.5 order, while for higher pressure up to 20 bar the rate was of zero order. This can be explained by high amount of hydrogen and complete saturation of the active sites, which did not influence the rate of reaction. Mechanism II considered that H_2 reacted directly from the fluid phase, therefore the reaction rate was of first-order respect to H_2 pressure. Finally, Mechanism III included adsorption and desorption of hydrogen but also of organic molecules, the formation of geometric isomers, and double bond migration, offering therefore a completer and more complex scenario for the mechanism.
Among the three models, considering the complexity of Mechanism II and III, Mechanism I is usually adopted for catalytic studies on the hydrogenation of unsaturated fatty acids on metal-supported catalysts.

The mechanism for the reaction was a first partial saturation of linoleic acid, with the preferred formation of the cis isomer rather than the trans. Next, the full hydrogenation occurred leading to stearic acid.

2.5Deactivation

All catalysts deactivate with time: depending on the process the activity decay after few seconds or after several years. For example, in cracking processes catalyst mortality is in order of few seconds, while for ammonia synthesis the iron catalyst last 5-10 years[56].
Understanding the rate and the reason for deactivation is fundamental to design a robust catalyst in the operating conditions and to avoid rapid loss in its activity.
The mechanisms of catalyst deactivation are many, but it is possible to group them into three different categories

2.5.1Poisoning

Poisoning is the strong chemisorption of reactants, products, intermediates, or impurities, which occupy the active sites of the catalyst, rendering them unavailable for the reaction.
Poisonous substances have adsorption strength competitive with other molecules for the active sites of the catalyst[104,105].
Adsorbed poisons not only occupy three or four sites of the catalyst surface making it unavailable for the reaction but have a second effect: they can electrically modify the neighbour atoms, altering their ability to adsorb or desorb reactants and products. A third effect is the modification of the structure and geometry of the catalyst, which can be problematic especially for reactions that are sensitive to structure proprieties[106,107]
The first group of poisons includes group VA and VIA elements: N, P, As, Sb, S, O, Se and Te[108].
These elements poison the catalysts by interaction through their *s* and *p* orbitals and the importance of the poisoning effect can be changed by changing the number of bonding electrons. For example sulphur poisoning, which is one of the most common, depends on the degree of S oxidation state: the degree of poisoning efficiency is $H_2S>SO_2>SO_4^{2-}$according to an increase in oxidation state of S[109,110].Also, the poisoning effect increases with increase molecular size and electronegativity[109].

The second group includes heavy metals like Pb,Hg, Cd, Cu, which can form alloy and are therefore more complicated to remove.

The following table (Table 7) lists the most common poisons according to their chemical structure:

Table 7. Poison type according to chemical structure and orbitals interaction[56]

Chemical type	Example	Type of interaction with metal
Group VA and VIA	N, P, As, Sb, O, S, Se, Te	Through *s* and *p* orbitals
Group VII A	F, Cl, Br, I	Through *s* and *p* orbitals
Toxic heavy metals and ions	Hg, Pb, Sn, Zn, Cd, Cu, Fe	Occupy *d*-orbitals. Possible formation of alloy
Molecules with double bonds	CO, NO, HCN, benzene and unsaturated hydrocarbons	Chemisorption through the double bond and back bonding

Poison can also be divided in selective, non-selective, and anti-selective. Selective poisoning involves a strong and rapid reduction in catalytic activity, even at very low poison concentrations, due to their preferential adsorption on most active sites.

On the contrary, anti-selective poisoning occurs when sites of lesser activity are immediately blocked. Finally, non-selective poison occurs when the degree of poisoning is directly proportional to the concentration of the adsorbed poison.

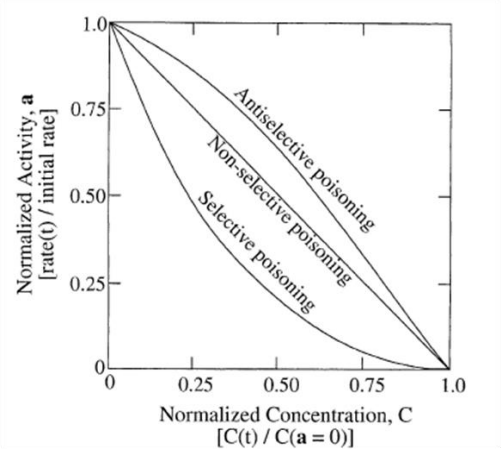

Figure 21. Type of poisoning as function of activity vs. normalized concentration

Fig 21 shows the activity versus poison concentration basedon the assumption of uniform poisoning and absence of pore diffusional resistance. However, these assumptions are difficult to meet at industrial scale, due to severe reaction conditions (T, P, etc.), which bring pore diffusional resistance. This means that a reaction occurs preferably in the outer shell of the catalyst, as much as the poison is adsorbed in the outer shell more easily. The trend of Figure 21 mimics what can happen also in the external part of the catalyst, being therefore an approximation.

For non-selective poisoning the decrease in activity is linear with poison concentration and the

rate is defined by the slope of the line.

Removal of chemisorbed poisonous molecules occurs via thermal treatments inducing degradation of the adsorbed species by heating or with chemicals that react with poisons and prevent their adsorption on active sites.

2.5.2 Fouling

Fouling of the catalyst is caused by the physical deposition of the molecules on the catalyst, blocking the pores and/or the active sites (Fig. 22).

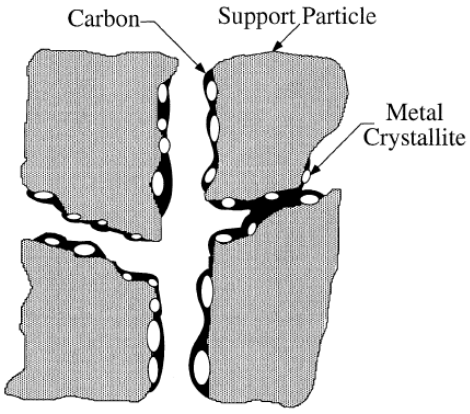

Figure 22. Magnification of particles fouled by carbon depositions.

The most common catalyst foulant is carbonaceous deposits (coke) which can vary from primarily carbon, defined soft coke with high H/C ratio such as graphite, to heavy molecules obtained via polymerization of hydrocarbons, classified as hard coke with a low H/C ratio. The reactions can be classified in coke-sensitive and coke-insensitive[111]. In the first case coke is deposited on the active sites, causing a drastic decline in catalytic activity. Typical examples of coke-sensitive reaction are hydrogenolysis and cracking. In the second case, the coke precursors formed on the active sites are rapidly removed by gasifying agents, like in catalytic reforming or Fischer-Tropsch process.

Carbon can deposit differently on the support, forming a mono- or multi-layer blocking the access of reactants to the metal surface; can encapsulate completely a metal particle, causing its complete deactivation; plug micro- or mesopores, making them impossible to access to reactants. Finally, in extreme cases, the presence of carbon filaments inside the pores can cause stress and fracture of the material, leading to the disintegration of the catalyst.

In reactions that involve hydrocarbons, the formation of coke is usually associated to the polymerization of olefins in presence of acid sites[112,113]. Dehydrogenation and cyclization of carbocation intermediates that are formed on the acid sites lead to the formation of aromatics, which subsequently form polynuclear aromatics and condense as coke[56].

Coke formation is favoured by increasing acid sites concentration while is discouraged by small pores size.

All carbonaceous deposits can be removed by gasification with the general reactions show in equations 2-5:

$$C + O_2 \rightarrow CO_2 \quad (2)$$

$$C + 2H_2 \rightarrow CH_4 \quad (3)$$

$$C + H_2O \rightarrow CO + H_2 \quad (4)$$

$$C + CO_2 \rightarrow 2\,CO \quad (5)$$

Reaction (2) is often the preferred route, however careful control of the temperature must be done, due to the exothermicity of the reaction. In an overheating condition, unwanted consequences on the crystallinity can occur, causing structure re-organization. An alternative to avoid high-temperature side effects is to combine reaction (2) with gasification by steam (reaction 4), which is endothermic[114]. In any case, removal of carbon coke with oxygen and high temperature must be conducted by stage and carefully controlled, in order to avoid structure reorganization[109].

Coke is not the only reason for catalyst fouling: high molecular weight molecules can deposit on the catalyst and can be removed by washing with chlorobenzene, liquefied propane, acids or alkali solutions[115,105].

A physical method like abrasion can be employed for removing deposited material: this method is useful when the foulant is weakly attached to the external surface.

The removal of foulants does not create unsolvable problems, due to the different possible alternatives for the proper elimination of adsorbed molecules. However, care must be taken to avoid the collapse of the structure or its reorganization, which could cause different catalytic activities.

2.5.3 Thermal degradation and sintering

During its life, the catalyst is continually exposed to heating cycles and thermal swings, which can cause a loss of surface area. Generally, the rearrangement of the structure occurs 0.3-0.5 times the melting point of the material and in a chemical environment, this phenomena can be accelerated[116]. Thermal deactivation of catalyst is caused by:

- Crystallite growth of active phase that cause loss of surface area.
- Collapse of the support.
- Chemically transformation of the phases, with probable shift from a catalytic active phase to a non-active.

The collapse of the support and loss of surface area is referred as "sintering", a phenomenon that takes place at temperatures higher than 500°C and increases exponentially with temperatures. Metals sinter faster in presence of vapor and oxygen, while slower with hydrogen.

In general, a catalyst that undergoes thermal degradation cannot be treated due to the irreversible character of sintering. Therefore, prevention is the best way to control sintering: MgO[117] and BaO[56] lower the sintering rate by reducing the mobility of the metal atoms, as well as the introduction of defects on the surface is a possibility to avoid this problem.

Gas reaction with solid catalysts can produce inactive phase due to parallel and undesired reactions that take place.

The table 8 shows some of the most known reactions that occur between the catalyst and a reactant, making it unavailable for participating to the reaction.

Table 8. Chemical reaction that can occur between the catalyst a reactant causing deactivation of the catalyst in a determinate process

Catalytic process	Gas/vapor composition	Catalyst (solid)	Deactivating chemical reaction	Ref.
Auto emission control	N_2, O_2, HCs, CO, NO	Pt-Rh/Al_2O_3	$2Rh_2O_3$+ γ-Al_2O_3→$RhAl_2O_4$+0.5 O_2	106,118
NH_3 synthesis and regeneration	N_2, H_2	Fe/K/ Al_2O_3	Fe→ FeO > 50 ppm O_2	56
Catalytic cracking	HCs, H_2, H_2O	LaY- zeolite	H_2O induces dealumination	54
CO oxidation	N_2, O, 400 ppm CO_2, 100-400 ppm SO_2	Pt/ Al_2O_3	Formation of $Al_2(SO_4)_3$ which blocks pores	54
Fisher-Tropsch	CO, H_2, H_2O, CO_2, HCs	Fe/K/Cu/SiO_3	Formation of Fe_3O_4	119
Fisher-Tropsch	CO, H_2, H_2O, HCs	Co/SiO_2	Formation of CoO*SiO_2 and collapse of SiO_2	120
Steam reforming	CH_4, H_2O, CO, H_2, CO_2	Ni/ Al_2O_3	Formation of $Ni_2Al_2O_4$	54

3. Aim of the work

The implementation of industrial process with bio-based and renewable starting material is a key aspect for the industry of the future, due to a depletion of classical fossil feedstock together with environmental issues.

Biomasses represent a present reality and can be widely employed in many chemical fields, depending on the fraction taken into consideration.

As part of the biomass, oils and fats have been subject of many studies and research since the early 1900s, thanks to their large availability and chemical structure, that makes them suitable for many functionalization and reactions.

With this premise, the principal objective of this PhD project was to find an active, selective and stable catalyst for the hydrogenation of a real mixture of fatty acids derivatives.

A complete description of the starting material is discussed in Chapter 4.4.

The catalyst had to satisfy different parameters regarding its toxicity, tolerance to water and air exposure and stability after different cycles of reaction in perspective of industrial applications.

After determining the optimal reaction parameters, a screening of different metal-supported catalysts was performed, evaluating the activity and selectivity in a discontinuous batch reactor and a continuous flow one.

Due to deactivation observed on the selected catalyst, big attention was pointed out on the main cause that could origin a decrease in performances of this latter: the in-deep study and understanding of the cause of deactivation gave the possibility to act on the source of the problem, guaranteeing optimal work conditions for the catalyst.

4. Experimental

4.1 Materials

The starting reaction mixture, described in Chapter4.4, was supplied by Novamont S.p.A and used as given for batch reactions, while a dilution was performed before its utilization with the continuous flow system.

Batch reactions were performed using the catalyst described in Table 9, in forms of powder or pellets (500 μm).

Table 9. List of catalyst used for reactions performed in the batch system divided by the type of metal.

Metal	Type of catalyst	Form	Supplier
Palladium	0.3% wt Pd/C	Powder	Johnson-Matthey
	1% wt Pd/C	Powder	Johnson-Matthey
	5% wt Pd/C	Powder	Sigma-Aldrich
	0.5% wt Pd/C	Pellets (500 μm)	Sigma-Aldrich
	1% wt Pd/Al_2O_3	Powder	Johnson-Matthey
	0.3% wt Pd/Al_2O_3	Powder	Johnson-Matthey
	1% wt Pd/ZrO_2	Powder	Home-made
Platinum	5 % wtPt/C	Powder	Sigma-Aldrich
Ruthenium	1% wt Ru/C	Powder	Home-made
	1% wt Ru/Al_2O_3	Powder	Home-made
Nickel	Ni-Raney ®	Viscous-Paste	Sigma-Aldrich

The catalysts provided by Novamont S.p.A and Sigma-Aldrich were used as received, without any pre-treatments. Regarding the homemade catalyst, the detailed synthesis proceduresare described in chapter 4.2.1.

For the continuous flow H-Cube Mini Plus® reactor, stainless steel cartridge CatCarts® (Fig. 23) were employed to hold the catalyst and were subsequently placed in the dedicated holding space. The CatCarts® employed during catalytic tests, described in Table 10, were 3 cm long with

Figure 23. H-cube Mini- Plus® CatCart® of 70 mm (top) and 30 mm (bottom) length.

an internal diameter of 4 mm.

Table 10. List of catalyst employed with the H-Cube Mini Plus® divided by supported metal. The cartridges that were not furnished by ThalesNano were created by filling empty cartridges with a precise amount of supported catalyst following the procedure described by the supplier. Catalysts were provided by Novamont or synthesized in laboratory.

Metal	Type of catalyst	Form	Supplier
Palladium	0.5% wt Pd/C	Pellets (500 µm)	Sigma-Aldrich
	1% wt Pd/C	Powder	Johnson-Matthey
	5% wt Pd/C	Powder	Sigma-Aldrich
	0.3% wt Pd/C	Powder	Johnson-Matthey
	1% wt Pd/Al_2O_3	Powder	Johnson-Matthey
	0.3% wt Pd/Al_2O_3	Powder	Johnson-Matthey
Platinum	5 % wtPt/C	Powder	Thales-Nano
Ruthenium	5% wt Ru/C	Powder	Thales-Nano
Nickel	Ni-Raney ®	Solid paste	Thales-Nano
Rhodium	Rh/C 5% wt	Powder	Thales-Nano

Standards compound for GC calibration were supplied by Novamont consisting of:

- saturated fatty acid derivative with a purity >98%.
- unsaturated fatty acid derivative with a purity of 87%.

All the reagents, furnished by Sigma-Aldrich and VWR, were pure grade and used as received: BF_3 10% in MeOH 1.3M, toluene, chloroform stabilized with ethyl alcohol >99%, 2,2 dimethoxypropane 98%, Methanol >99.9%, Toluene >99.8%, zirconium(IV) oxynitrate hydrate 99%, ammonium hydroxide solution 28–30% (NH_3 basis) , ruthenium(III) chloride hydrate 30-40%, Palladium chloride 99%, $Pd(NO_3)_2 \bullet 4NH_3$10% wt in H_2O, $RuCl_3 \bullet H_2O$ 99%, Carbon NORIT SX Ultra (powder). γ-Alumina received by Sigma-Aldrich was thermally treated at 700°C to fully obtained the γ phase before its utilization

4.2 Preparation of catalytic systems

In this section a complete description of the synthesis procedure adopted for the catalysts named as "home-made" in table 9 is reported.

4.2.1 Synthesis of *t*-ZrO_2

The synthesis of tetragonal zirconia was executed following the procedure proposed by Chuah[121]: a solution of $ZrO(NO_3)_2$ 0.3 M was added dropwise to a 5M NH_4OH solution under magnetic agitation at room temperature. The solution obtained was allowed to digest for 24 hours at 100°C under reflux system with a careful adjustment of the pH: concentrated NH_4OH was regularly dropped with the aid of an automatic pump which allowed draining of the solution for all the 24 hours for keeping the pH constant at 9.

After digestion, the solid was filtered and washed with abundant NH_4OH 5M. The solid was dried in the oven at 100°C overnight and lastly treated in static air at 500°C for 12 hours with a heating ramp of 5°C/min for the obtainment of tetragonal phase.

The final catalyst appeared as a white, grainy solid.

The time chosen for the digestion step can be varied according to the necessity: for longer digestion time (e.g: 48 hours) the active surface area increased at the expense of crystallinity. On the other hand, 20-24 hours of digestion bring to higher crystallinity but slightly lower surface area.

4.2.2. Synthesis of 1% wt Pd/ZrO_2

1% wt Pd/ZrO_2 was synthesized by incipient wetness impregnation technique (IWI). The mud point was found to be 0.85 mL of water for 1 g of ZrO_2, synthesized as described in Chapter 4.2.1. A precise amount of10% wt $Pd(NO_3)_2 \bullet 4NH_3$ in H_2O was mixed to a precise amount of water to reach the mud point. The liquid solution containing the Pd precursor was added drop wise to the zirconium oxide on a watch glass, being careful to spread the liquid as much as possible and waiting to the liquid to be completely adsorbed before proceeding with further addition.

The solid was dried overnight at 50°C before being treated at 400°C with N_2 flow for 2 hours followed by reduction in H_2/Ar 10% for 4 hours.

Prior reduction the solid appeared of orange colour while it turned grey/black after the treatment.

4.2.3 Synthesis of 1% wt Ru/C

1% wt Ru/C was prepared by IWI technique, prior obtainment of the mud point of the support Carbon (C NORIT SX ULTRA). Typically, a precise amount of ruthenium chloride hydrate ($RuCl_3$• H_2O) was dissolved into water in a beaker to prepare an impregnation stock black solution. The amount of the Ru precursor and water were selected as function of solubility of the ruthenium salt, the value of the mud point and the final % wt of Ru wanted (in this case 1% wt).

The required amount of Carbon was impregnated with the Ru following the procedure described above (Chapter 4.2.2).

The sample was then dried at 80°C for 3 hours and followed by reduction with TPR in H_2/Ar 10% at 400°C with a pre-treatment in N_2 at 120°C[122,123].

From the TPR profile (Fig. 24), it was possible to notice that the reduction started at 158°Cwith a first reduction peak at 176°C and successive peaks at 227°C and 289°C. The different reduction temperatures are synonym of the presence of nanoparticles with different dimension.

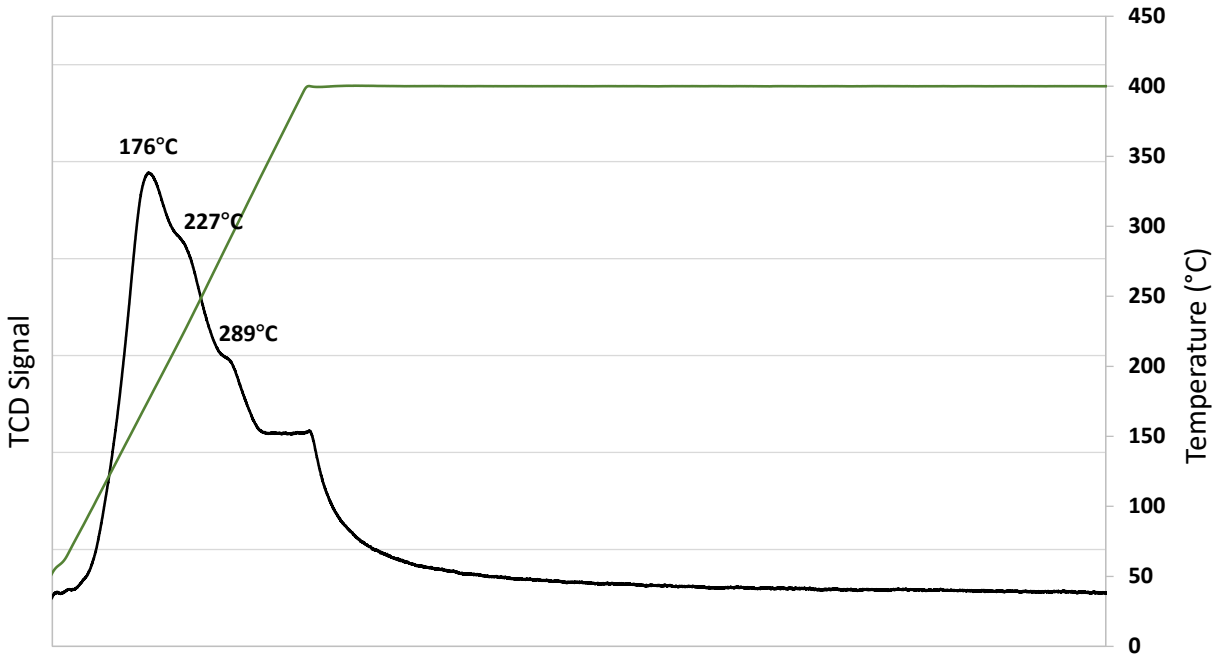

Figure 24. H_2-TPR profile of 1% wt Ru/C after calcination.

4.3 Characterization techniques

The characterization of catalysts is fundamental for understanding and exploring their proprieties; indeed, the surface area, the pore dimension, the crystalline structure and the acidity are only few parameters that can play a crucial role during a reaction.
Hereafter, the characterization techniques adopted for the catalyst employed are described.

4.3.1 Structural proprieties

4.3.1.1 Specific surface area

The specific surface area and total pore volume of the catalysts were measured by physisorption of liquid nitrogen at -196 °C using a *MICROMERITICS ASAP 2020* instrument.
The specific surface area measurement is done with the BET theory, which derives the name from their inventors Brunauer–Emmett–Teller.
This technique is based on physical adsorption of inert gas molecules (N_2) on a solid surface to calculate the overall surface area. Indeed, this latter (expressed as m^2/g) is directly correlated to the amount of the gas absorbed, by an extension of the Langmuir theory which is valid for a single layer of gas adsorbed on a solid surface.
The single-point approximation is based on only one measurement of the pressure of adsorption and the corresponding gas volume adsorbed; the formula used is here reported (Equation 6):

$$\frac{P}{V(P_S - P)} = \frac{c-1}{V_m \cdot c} \cdot \frac{P}{P_S} + \frac{1}{V_m \cdot c} \quad (6)$$

Where:

- P is the pressure.
- P_s is the surface gas of N_2.
- V is the absorbed gas volume
- Vm is the monolayer gas volume
- C is a constant directly related to surface and gas interactions

The value of "C" is much higher compared to other values, resulting in the simplified formula (Eq. 7):

$$\frac{P}{V(P_S - P)} = \frac{1}{V_m} \cdot \frac{P}{P_S} \quad (7)$$

In a typical analysis, 0.1 g of catalyst were loaded in the sample holder. The vacuum was created in the system heating up to 150°C in an oven, to desorb water or any other impurities present on the catalyst surface. Subsequently the sample holder was located in a proper container with liquid nitrogen at -196°C. The nitrogen was then flowed inside the catalyst and adsorbed both on the surface and on the pores of the catalyst.

The instrument measured the volume of the absorbed nitrogen over the system and, using the above simplified equation,gave the value of the specific surface area. Dividing the given value by the amount of catalyst initially loaded, the desired measure was obtained expressed in m^2/g.

4.3.1.2 X-Ray Diffraction (XRD)

X-ray diffraction allows the identification of the crystalline phases of a catalyst, together with the measure of the size, shape and internal stress of small crystalline regions. The information on the sample is given by the position, intensity, sharpness, and width of the diffraction lines.
The diffractogram obtained after the analysis is composed by different peaks, which gives immediately information about the crystallinity of the catalyst: the sharpest and narrow the peaks, the higher the crystallinity. On the other hand, a broad peak means lower crystallinity or amorphous phase.
Other information such as phase, preferred crystal orientation, sub-micrometre crystallite dimension and crystal defects can be extrapolated from the diffractogram.
The diffraction angle 2θ and the spacing between two planes (*h,k,l*) d are related by the Bragg's law (Eq. 8):

$$2d \cdot \sin\theta = n\,\lambda \qquad (8)$$

where:

- λ is the wavelength of the incident X-ray beam.
- n is the diffraction order.

XRD analysis were done in a vertical goniometric diffractometer (Bragg – Brentano geometry)

Philips PW 1050/81 with a PW 1710 chain counting. A nickel filter of 0.15418 nm was used to make monochromatic the Cu Kα radiation. The acquisition region was 5°< 2θ < 80°, with steps of 0.1° and count of intensity every 2 seconds. The range of analysis was 20°< 2θ < 80° with a scanning rate of 0,05°/s and time-per-step = 1 s.

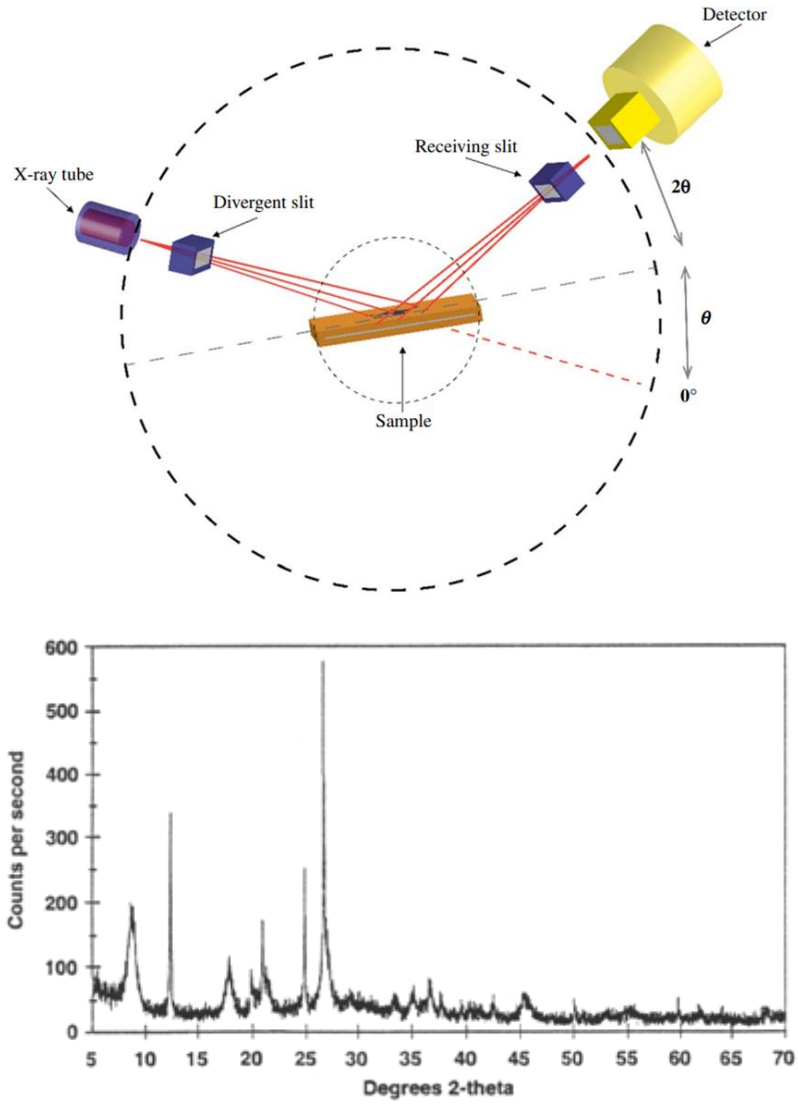

Figure 25. Scheme of the X-ray diffractometer set up with an example of a pattern obtained after the analysis.

PANalytical Company and the ―ICSD Database FIZ Karlsruhe‖ library were used for the comparison of the obtained diffractogram.

4.3.1.3 Transmission Electron Microscopy (TEM)

Characterization by transmission electron microscopy was carried out by a TEM/STEM FEI TECNAI F20 microscope with an EDS analyser. The powdered catalyst was suspended in ethanol for 20 minutes under ultrasounds, with following deposition on an gold grid with multi-foil carbon film and dried at 100°C before carrying out measurements.

The distribution of metallic particles was calculated by statistical distribution of at least 200 particles.

4.3.1.4 Scanning Electron Microscopy (SEM)

SEM/EDS analysis were performed using an EVO 50 Series Instrument (LEO ZEISS) equipped with an INCAEnergy 350 EDS micro-analysis system and an INCASmartMap for determining the variation of the elements in the sample.
The accelerating voltage was 25 kV, and the spectra were collected every 100 s with a beam current of 1.5 nA.

4.3.2 Composition

4.3.2.1Thermal gravimetric analysis (TGA)

Thermal gravimetric (or thermogravimetric) analysis allows the study of thermal decomposition, desorption of molecules present on the sample or phase transition due to a change on the sample's mass over time as a consequence of increased temperature.

TA SDT Q600 was used for the investigation of absorbed molecules on the catalyst surface by heating 10°C/min and flowing air or nitrogen, depending on the sample and the objective of the analysis.

As a matter of fact, catalytic materials based on carbonaceous supports are not suitable to undergo TGA with air if the individuation of organic absorbed molecules is the purpose. In fact, carbon can be treated in presence of air until 150°C without compromising the nature of the substrate. If higher temperatures are required, it is necessary to switch to inert gas (e.g.: N_2) which prevent not only the degradation of the carbon support but also of the heavy adsorbed organic molecules.

Other supports (e.g. Alumina, ZrO_2, TiO_2etc.) can stand air treatment at elevated temperature without any degradation issues.

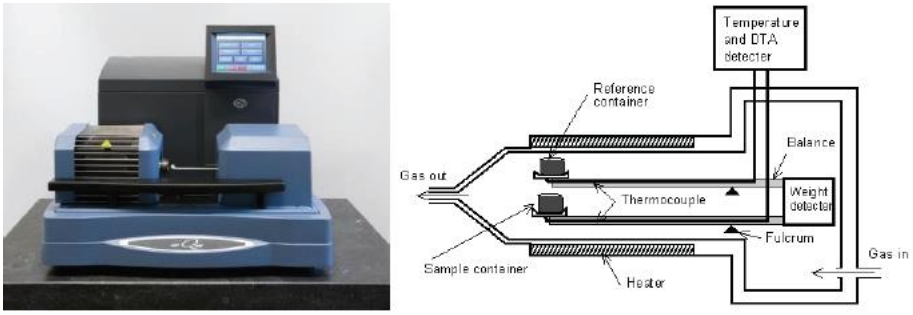

Figure 26. TA SDT 600 instrument used for thermogravimetric analysis (on the left) and TG analysis scheme (on the right)

4.3.2.2 Inductively coupled plasma atomic emission spectroscopy (ICP-AES)

Inductively coupled plasma atomic emission spectroscopy is an analytical technique used for the detection of chemical elements (Fig. 27).

The inductively coupled plasma, which is a high temperature source of ionised gas maintained by inductive coupling from cooled electrical coils at megahertz frequencies, produces excited atoms and ions that emit in the electromagnetic radiation at wavelength characteristic of a particular element.

The intensity of the emission of the light is proportional to the concentration of the elements.

The solution containing the sample is nebulized and introduced in the plasma flame, which creates an intense electromagnetic field: the sample is immediately converted into charged ions. The atoms lose their electrons, which are recombined in the plasma giving the characteristic wavelength of the element present.

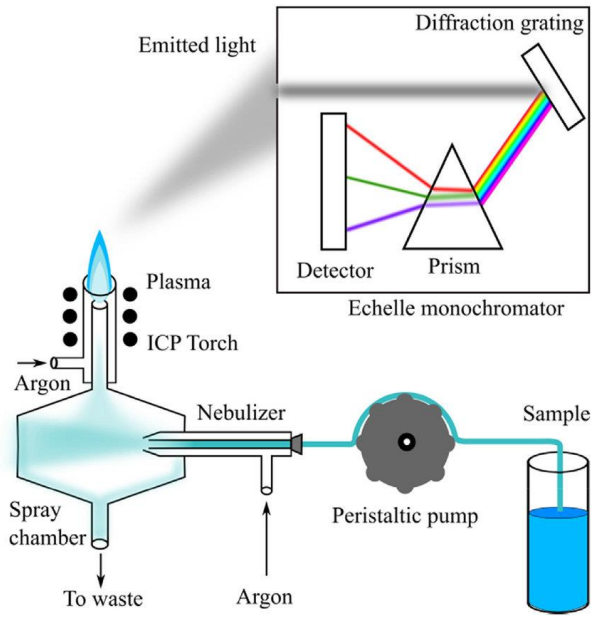

Figure 27. Inductively coupled plasma atomic emission spectroscopy (ICP-AES) in its different part: the sample passes through the nebulizer where is separated into charged ions. These latter emit radiation after encounter the plasma flame, which, after a passage into the monochromator, reach the detector and finally the computer.

Each element presents characteristics emission wavelengths, and according to the position of the resulting peak it is possible to identify the composition of an unknown sample.

4.3.3 Temperature programmed reduction analysis (TPR)

The reduction profiles were measured using a Micromeritics AutoChem II Chemisorption Analyzer, equipped with a Thermal Conductivity Detector (TCD). The analyses were carried out loading ≈ 100 mg of sample in a quartz reactor and using the following procedure for H_2-TPR experiments:

- Pre-treatment: the sample was pre-treated under He (30 mL/min) from room temperature (r.t.) to 450 ℃ (10 ℃/min) and hold at this temperature for 1 h.
- Reduction: after cooling to 35°C, the reduction analysis was performed using a 5% H_2/Ar(v/v) mixture (30 mL/min), increasing the temperature of the sample to450 ℃ (10 ℃/min) and keeping this temperature for 1 h.

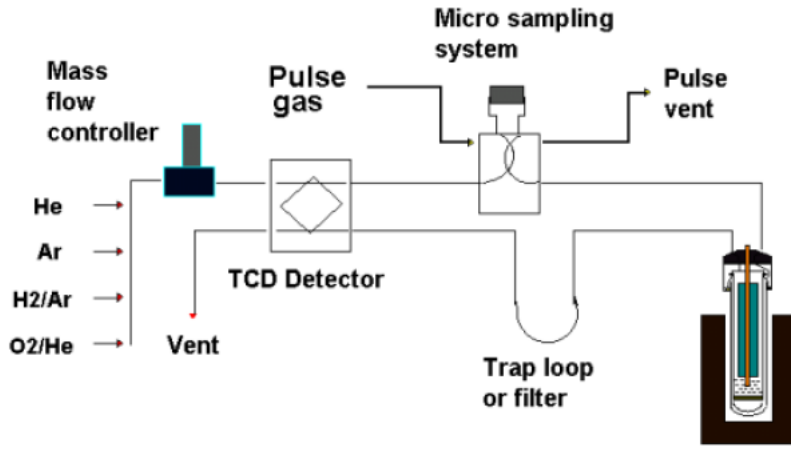

Figure 28. Temperature programmed reduction scheme

4.4 Starting material

The starting solution was supplied by Novamont S.p.A. and consisted of a complex mixture of water soluble carboxylic fatty acids derivatives (*d*-FA) shown in figure 29.
The acidic function was substituted by a metal cation (Li^+, Na^+, K^+ or Ca^+) in order to ensure complete solubility of the compounds in the mixture, especially for the saturated products formed during the reaction.

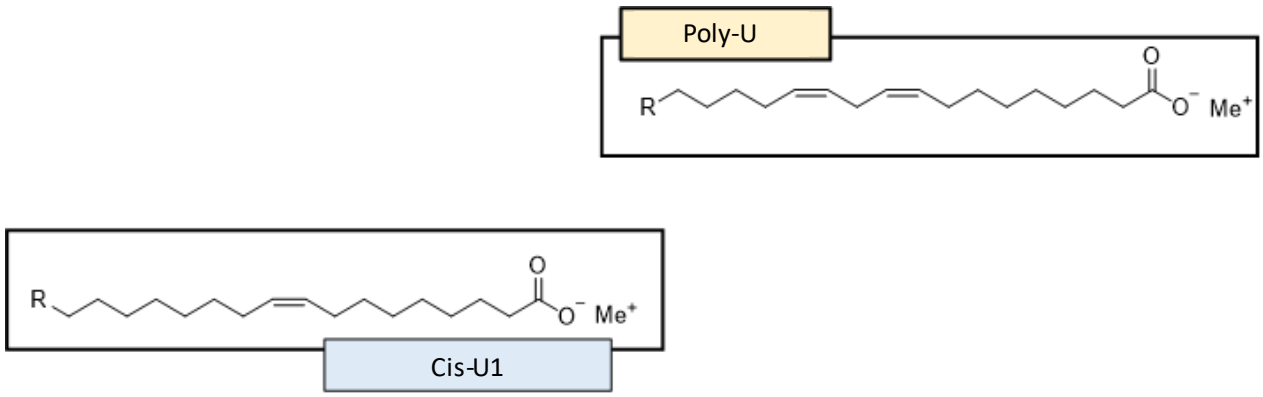

Figure 29. Representation of the main carboxylic fatty acids derivatives present in the starting material and taking part in the reaction. The "Me^+" represent a generic metal cation employed to guarantee complete solubility of the fatty acid derivatives in the mixture.

The solution had a pH equal to 12 with a medium concentration of acids of 30 g/L.
Except where otherwise specified, the composition of the typical reaction mixture was constant with a major amount of oleic acid derivatives Cis-U1. Table 11 evidence the % w/w of the two main components.

Table 11. Composition of a typical mixture composed of fatty acids derivatives used for reactions.

Carboxylic fatty acids derivatives	***% w/w***
Oleic acid derivative (*cis*-U1)	75 ± 2
Linoleic acid derivative (Poly-U)	7 ± 1
Others	15 ± 2

For batch reactions the solution was used as pure as described, while for continuous flow tests the solution was further diluted to obtain a final concentration of acid salts of 6 g/L.

This was proved to be necessary in order to avoid blockage inside the line of the instrument because of the viscosity of the solution and to prevent damages at the instrument caused by the alkaline pH.

After an introduction of the reactors used, the analytical procedure is reported, with a final description on the instruments used for the analysis and their operating conditions.

4.5 Batch reactor

Discontinuous reactions were performed in a batch system made of a stainless-steel 50 mL autoclave (Figure 30).The autoclave was placed in the proper heating mantel with mechanical stirring guaranteed by a magnetic stir bar and equipped with a reversible security valve (relief valve), which was set to 40 bar to ensure the safety of the reaction.

In a typical reaction 15 mL of pure solution (30 g/L) were introduced into the vessel with the appropriate magnetic stir bar and the desired amount of solid catalyst. The system was then sealed and purged with N_2 three times. H_2 was introduced, reaching the desired pressure, the autoclave was placed in the heating mantel, starting the stirring and the heating at the same time. The system was endowed of a thermocouple inserted in the heating mantel to control the temperature and the heat provided by the mantel and of an indicator thermocouple placed inside the reactor to reveal the exact internal temperature. "Time zero" of the reaction was taken when the set temperature was visualized on the second thermocouple display, hence reached by the internal mixture.

Figure 30. 50 mL stainless steel autoclave used to perform batch reactions. The autoclave was placed in a dedicated heating mantel, a manometer monitored pressure and temperature was controlled with two thermocouples.

After the desired reaction time, the system was quenched using an ice-bath, for rapidly stopping the reaction and avoid the formation of more products or by-products. When the system reached 30/35°C the outlet line was equipped with a septum, allowing the sampling and the GC-MS analyses of the gaseous phase. Then the autoclave was degassed, opened and the liquid phase with the catalyst were transferred into a falcon and centrifuged at 4500 rpm for 15 minutes in order to promote catalyst sedimentation. The liquid phase was removed and treated for GC analysis, the catalyst was dried overnight at 60°C and used for subsequent tests.

4.6 Continuous-flow reactor (H-Cube® Mini Plus)

A continuous flow system H-Cube® Mini Plus (Fig. 31) was employed for a different approach of the reaction involved: the study of the continuous-flow system allowed to take into account more aspects characteristic of this system useful for industrial applications and process intensification. The H-Cube® Mini Plus combines endogenous hydrogen generation from the electrolysis of water with a continuous flow-through system.

The instrument allowed working in the following range of operating conditions:

- Temperature: Room temperature- 100°C.
- Hydrogen pressure: 0-100 bar of H_2.
- Flow rate: 0.1-3 ml/min.

The starting material, which was diluted in order to avoid problems related to viscosity and basicity of the original solution, was pumped at a desired rate with a dedicated HPLC pump.

The catalyst was contained in a steel cartridge 30 mm in length and placed in a small oven, in order to work at the desired temperature. The total empty volume of the cartridge was 226 μL and around 50-70 mg of solid catalyst were introduced.

The cartridges were filled with catalyst and closed with the proper press, placing in order:

- Teflon o-ring.
- Steel disk.
- Teflon disk.
- Steel disk.
- Teflon o- ring with higher thickness.

The solution passed through a pressure controller and a mixer frit, where it started to be in contact with H_2 produced at fixed pressure. The liquid-gas mixture passed through the cartridge, which contained the solid catalyst; the post reaction solution flowed outside the reactor after passing through a back-pressure regulator valve and was collected for GC analysis.

The system was endowed of two internal devices:

- a special filter which was able to dry completely the H_2 produced in the electrolytic cell before entering the reactor.
- H_2 pressure was always kept 10 bar higher than the one set for the reaction, in order to guarantee a unidirectional stream of H_2 from the cell to the reactor. This system avoided contact between the solution and the cell.

Typical reaction conditions were: solution 6g/L, total flow:1.5 mL/min, T=90°C, P= 20 bar of H_2. Initially, lower pressure values were selected (e.g. 4 and 10 bar) for more comparable data with the batch system. However, because of an instrument limitation, the system was not stable enough in these conditions. Therefore, 20 bar was selected as the minimum operating pressure for the H-Cube® Mini Plus continuous flow tests.

Figure 31. H-Cue Mini Plus® used for continuous flow reactions. The starting material solution is pumped by an HPLC pump in the reactor where it is mixed with H_2 produced in situ by electrolysis of water. The reagents flow in the oven containing the cartridge filled with the selected catalyst. The oxygen produced is vented in the water container behind the instrument, while the post reaction solution, together with H_2 in excess, flow outside the instrument and are collected in a proper vial.

The contact time $\boldsymbol{\tau}$between the solution and the catalyst was calculated as:

$$\boldsymbol{\tau} = \frac{V_{Cat.}}{\dot{V}}$$

Equation 9. Formula used for the calculation of contact time during a continuous flow reaction

Where $V_{cat.}$ corresponds to the volume of the catalyst introduced in the cartridge and $\dot{V}$ to the volumetric flow rate (ml/min) of the liquid mixture pumped through the HPLC pump.

For the catalytic tests executed, τ was included between 0.1 and 0.2 minutes

The catalyst volume was calculated with the apparent density (ρ_{app}) of the solid: 1 g of solid catalyst was poured into a graduate test tube and occupied a certain volume. With the formula:

$$\rho_{app.} = \frac{m(g)}{V\ (mL)}$$

Equation 10. Formula used to calculate the apparent density of a solid catalyst.

It was possible to calculate the ρ_{app} of each catalyst and, based on the amount introduced in each cartridge, its volume.

4.7Recyclability tests

An important parameter for a catalyst is its lifetime, or more likely, the possibility of being reuse for multiple reactions.

Therefore, recyclability tests were performed in order to check the possibility to use the same catalyst for multiple reaction cycle without losing the targeted conversion and yields values.

Two different procedures were executed, differentiating between the discontinuous and continuous flow system.

4.7.1 Recyclability tests in batch reactor

As described in chapter 4.8 the solid catalyst was centrifuged with the post reaction solution, in order to obtain a complete separation of the two phases. The liquid upper phase underwent post-reaction analysis, while the "spent" catalyst was dried at 60°C overnight, to remove completely any water residues. The catalyst was re-introduced in the reactor vessel with a proper amount of fresh solution calculated for keeping the ratio catalyst: substrate constant as for the first cycle. The system was sealed, the internal air was evacuated introducing nitrogen and finally the relative pressure of H_2 was reached, always based on the amount of starting material used. The reaction parameters were set as the first cycle, and the same procedure described above was followed for the separation of the post reaction solution and the catalyst, for reutilizing the catalyst for a new cycle.

4.7.2 Recyclability tests in continuous flow reactor

Long-time on-stream reactions were conducted to evaluate the stability of the catalyst after several hours of reactions (3 or 5 hours) without any modification or thermal treatment on it. The liquid phase was collected every 30 minutes, which corresponded to the minimum volume analysable, and data were plotted on a graph for checking the trend of activity of the catalyst. As for the batch reaction, the liquid mixture underwent the classical procedure described in 5.3.5 and 5.3.6 and analysed by GC.

4.8 Post reaction treatment

In order to ensure the solubility of fatty acid derivatives in solution, their metallic form was obtained, with the substitution of the –OH group with a $-O^{-}Me^{+}$ and subsequent alkaline pH. Therefore, after the reactions, a standard procedure of precipitation of the acids was followed before the derivatization step. This latter was crucial to obtain volatile derivatives of the fatty acids, which because of their low volatility were not suitable to be analysed without proper modification (see chapter 4.9*Derivatization*).
Specifically: 15 mL of solution (30 g/L) were heated at 50°C and mixed with a magnetic stirrer. Mineral acid was added dropwise, until pH=2 was reached. A substantial difference was observed in the nature of the solution: after adding the acid a white flaky suspension was observed, becoming solid after stirring for 30 minutes with a constant temperature of 50°C. The system was cooled down and the solid obtained was filtered and washed with water until neutral pH was reached.
The white solid obtained was dried overnight at 50°C and underwent to derivatization procedure.

4.9 Derivatization

The mixture of fatty acids derivatives was analysed by gas-chromatography as previously described. However, in order to be analysed, fatty acids must be converted into their corresponding methyl esters (fatty acid methyl esters-FAMEs) thanks to the possibility to esterified the carboxylic functionality with an alcohol in presence of a suitable acidic catalyst.
The obtainment of a mixture of methyl ester shows several obvious advantages for the analysis compared to their parent acids. First, the possibility to create hydrogen bonds within different acids molecules as well as with the column's stationary phase is reduced. This leads to an increase of the volatility of the sample with consequent easier vaporization in the GC inlet ,preventing adsorption issues and blockage of the products inside the column. Also, in combination with the use of a proper GC column, methyl ester derivatives present a considerable ease for *cis/trans* isomers separation.
The initial step of derivatization (Fig. 32) involves a protonation of the acidic group to give a oxonium ion, which undergoes exchange reaction with the alcohol releasing water. The intermediate obtained is subsequently transformed into the final ester by losing a proton.

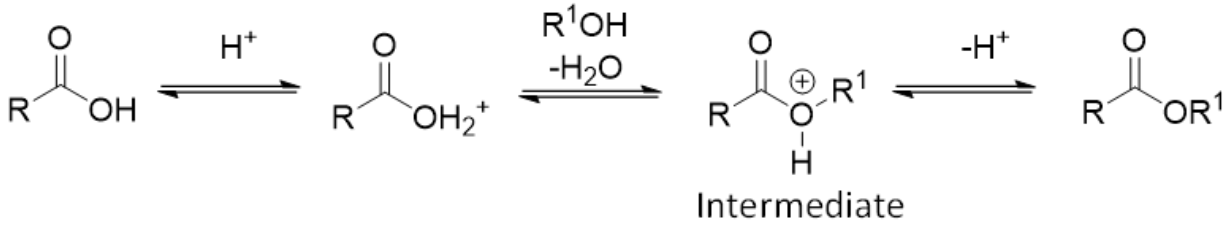

Figure 32. Acid-catalysed derivatization reaction of a generic fatty acid with alcohol (R^1OH).

All the steps involved in this reaction are reversible and for ensuring complete esterification large excess of alcohol was adopted.
Water that is formed during the reaction can reacts with the newly formed ester, leading hydrolysis of this latter with fatty acid restoration, as shown in Fig. 33.

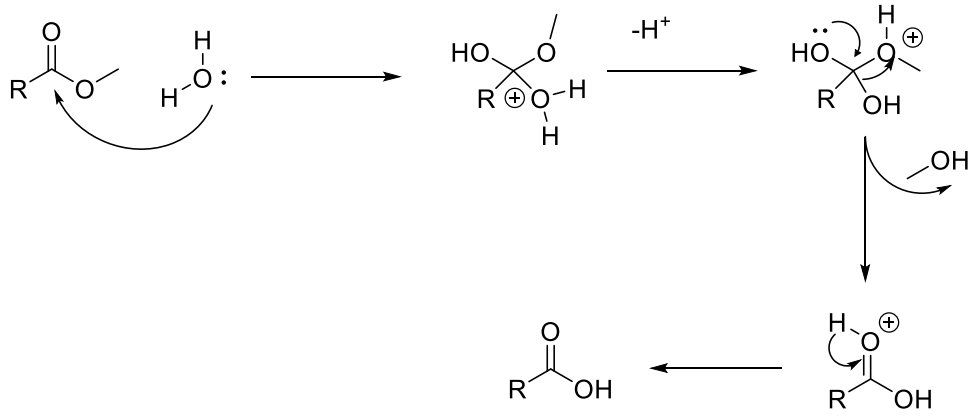

Figure 33. Competitive reaction for esterification of fatty acids: acid catalysed hydrolysis of fatty acid methyl esters with water leading to restoration of the free fatty acids.

Therefore 2,2-dimethoxypropane was used as scavenger to react with water and ensuring complete esterification.

The mechanism of the reaction between 2,2-dimethoxypropane and water is shown in Fig. 34:

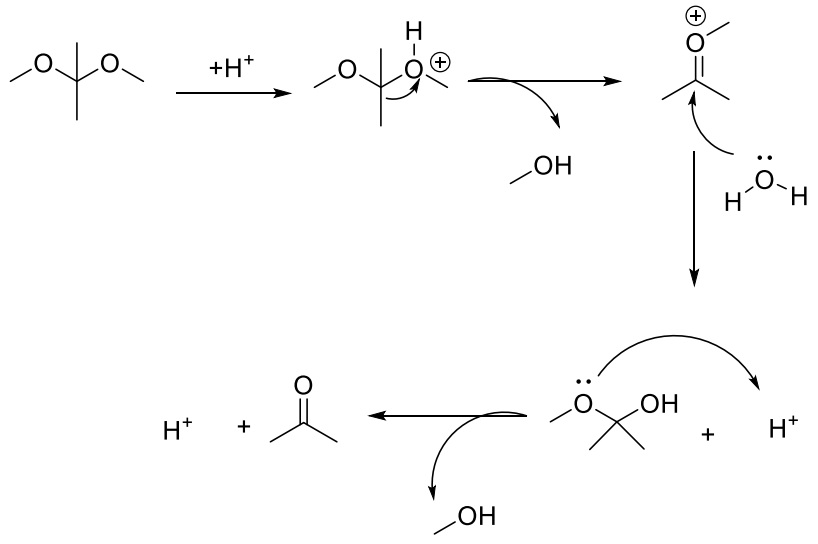

Figure 34. Acid catalysed reaction of 2,2-dimetoxypropane acting as water scavenger to prevent hydrolysis of fatty acids methyl esters. The reaction yields to two molecules of methanol and one of acetone.

Boron trifluoride in methanol (BF_3 in MeOH) acts as acid catalyst: when coordinated with methanol, shows strong Lewis acid character becoming therefore a powerful and useful catalyst for methylation purpose[124].
An internal standard was added to the post-reaction mixture before the derivatization procedure, in order to guarantee its complete esterification. The choice of the internal standard fell on brassylic acid: with its thirteen carbon atoms and similarity with the target molecules it represented the most optimal choice for the analysis.

The typical derivatization protocol used for both the qualitative and quantitative evaluation of the mixture composition was:

1. Weigh approximately 0.06 g of the solid mixture (m_{sample}).
2. Addition of 450 μL of internal STD solution (0.34% wt of brassylic acid in methanol, obtained by dissolution of 0.063 g of brassylic acid in 10 mL of MeOH).
3. Addition of 2,8 mL BF_3 in methanol (10% wt) and 150 μL of 2.2-dimethoxypropane.
4. Heating the solution at 80°C for 1h.

A solvent separation was performed with chloroform and water to allow the extraction of the methylates; a small amount of anhydrous Na_2SO_4 was then added to the organic phase, for a complete removal of water and the resulting derivatives products were injected and analysed via GC and, whenever needed, GC-MS.

4.10 Gas chromatography analysis (GC)

FAMEs were analysed and quantified using a Shimadzu GC-2025AF model equipped with auto-injector AOC-20i.

The column employed was a capillary Agilent J&W DB-23 that is specifically designed for the efficient partition of FAMEs and of *cis/trans* isomers. The column showed highly polar characteristics, with an internal stationary phase made of 50% cyanopropyl-methylpolysiloxane with total length of 60 m, internal diameter (ID) of 0,250 mm and active layer thickness of 0,25 μm.

The injector temperature was kept at 250°C (523 K) with a split ratio of 40:1. Helium was used as carrier gas with a flow of 3.8 mL/min in column. The syringe automatically injected 1 μL of sample.

The optimized ramp temperature was 50°C for 5 minutes, increased until 180°C with a heat of 15°C/min, increased again until 240°C at 20°C/min and kept at 240°C for 15 minutes.

Each compound was calibrated using the reference standard compound described in Chapter 4.1.

Consequently, calibration lines were obtained in order to establish for each component a response factor (***F*****$_i$**), essential for the quantification of each compound during catalytic tests.

F**$_i$** was calculated as follow:

$$Fi = \frac{n_i(g)}{n_{STD}\ (g)} x \frac{A_{\ STD}}{A_{\ i}}$$

Equation 11. Formula used to calculate the response factor of each component *i*after GC calibration

where:

- ***i*** represents the specie subject of calibration.
- ***STD*** the internal standard made by dissolution of 0,34% of brassylic acid in 10 mL of MeOH.
- ***n*** corresponds to the exact number of moles for the compound *i*or the internal STD.
- ***A*** is the effective area value obtained after chromatograph integration.

4.11 Gas chromatography – Mass Spectrometer (GC-MS) analysis

Gas chromatography coupled with mass spectrometer was occasionally employed to confirm the presence of the products obtained and to recognize unknown compounds.

The GC-MS used was an *Agilent Technologies 6890N* GC coupled with a mass spectrometer *Agilent Technologies5973* inert system with electron impact ionization filament (EI) and quadrupole mass analysers-photomultiplier. The capillary column was an Agilent J&W HP-5MS (5% phenyl-95% methyl siloxane), 30 m x (ID) 0.250 mm x 1,05 μm. Helium was used as carrier gas with a flow of 1 mL/min, the injector was maintained at 250°C with split mode of 40:1. Total flow was 23.9 mL/min and the injection volume was 0.5 μL.

The ramp temperature was maintained as the one for GC analysis.

However, it must be considered that, due to the completely different nature of the columns, the exit orders of compounds were reversed.

4.12Expression of results

After proper calibration of the main compounds at GC as described in chapter 4.10, the relative response factor was calculated.

After each reaction the %w$_i$of each compound present in the final mixture was calculated:

$$\%w_{i=} \frac{\frac{\frac{AREA_i}{AREA_{STD}}}{F_i} \cdot n_{STD}}{m_{sample}}$$

Equation 12. Formula used to calculate the % weight of every mixture component before or after the reaction.

Where:

- n_{STD} is value of moles of internal standard introduced.
- m_{sample} is the weight of the sample used for the derivatization step.
- Area$_i$ and Area$_{STD}$ are the Area values obtained by GC integration of the sample *i* and the Internal standard respectively.
-F*i*s the response factor of the component *i* obtained after GC calibration (as expressed in Equation 11).

Conversion of oleic acid derivative ($X_{cis\text{-}U1}$) was calculated considering the moles effectively present at the begin of the reaction (n^0_{cis-U1}), calculated referring to the exact composition of the starting material, with the formula:

$$n^0_{Cis-U1} = \frac{m_{TOTAL}(g) \cdot (\frac{\%w_{cis-U1}}{100})}{MW\ (\frac{g}{mol})}$$

Equation 13: Formula used to calculate the moles of *cis*-U1 at time zero of the reaction

The exact amount of *cis*-U1 was obtained multiplying the total mass of starting material weighted for its %w in the starting mixture. Then, dividing by the molecular weight, the exact number of moles was obtained.

From here, *cis*-U1 Conversion ($X_{cis\text{-}U1}$) was calculated with the formula:

$$X_{\ cis-U1} = \frac{n^0_{cis-U1} - n_{cis-U1}}{n^0_{cis-U1}} \cdot 100$$

Equation 14: Expression to calculate the conversion of *cis*-U1 using the moles obtained after GC quantification

Or using directly the %w of *cis*-U1 before and after the reaction:

$$X_{cis-\mathrm{U1}} = \frac{\%w^{0}_{cis-\mathrm{U1}} - \%w_{cis-\mathrm{U1}}}{\%w^{0}_{cis-\mathrm{U1}}} \cdot 100$$

Equation 15. Expression to calculate the conversion of *cis*-U1using the %w calculated with ***Equation 12***

Yields of product (Y_i)were calculated dividing the number of moles of the moles of the product *i*by the total moles of starting material:

$$Yi = \frac{n_i}{n^{0}_{cis-\mathrm{U1}}} \cdot 100$$

Equation 16. Expression used to calculate the Yield of every product based on the moles calculated by GC.

For each catalytic test a graph reports the conversion of *cis*-U1 and Yields of the main products, referred to the initial moles of *cis*-U1as described in equations 14 and 16.

5. Results and discussion

5.1 Catalysts' characterization

5.1.1 XRD. t-ZrO_2

Tetragonal-$ZrO_2$was synthesized as a candidate for different supports screening. After the synthesis, described in Chapter 4.2.2, the catalyst structure was analysed by means of XRD. The diffractogram shown in Fig.35 evidenced sharp crystalline peaks at 2θ = 30.370°, 35.322°, 50.563°, 60.338° and 75.017°, typical of the tetragonal phase. No evidence for the presence of monoclinic phase was found, thank to the optimized synthesis procedure.

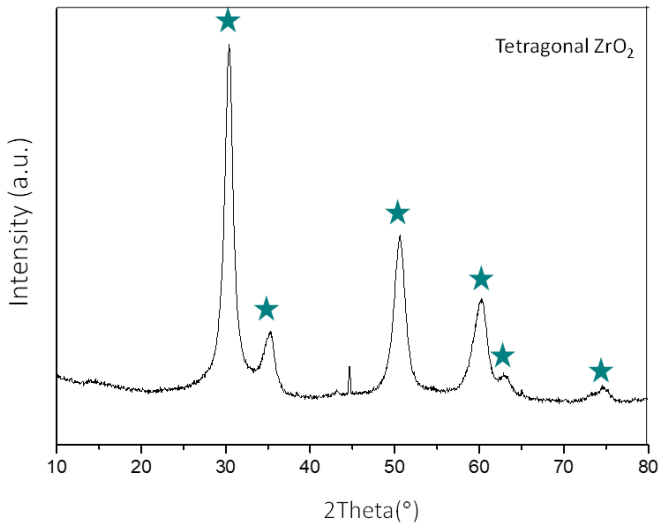

Figure 35. XRD diffractogram of tetragonal ZrO_2- rif. Code 00-050-1089.

5.1.2 XRD of1% wtPd / ZrO_2

Palladium supported on ZrO_2 was synthesized according to the IWI procedure previously described, with a Pd content of 1% wt.

The catalyst was analysed by means of XRD: the reflections at 2θ = 39.037°, 47.112°, 68.098°, 80.211° are typical of Pd phases (111), (200), (220), (311) respectively.

These peaks appeared to be very small due to the low amount of Pd present and because of the high dispersion of metal nanoparticles on the support.

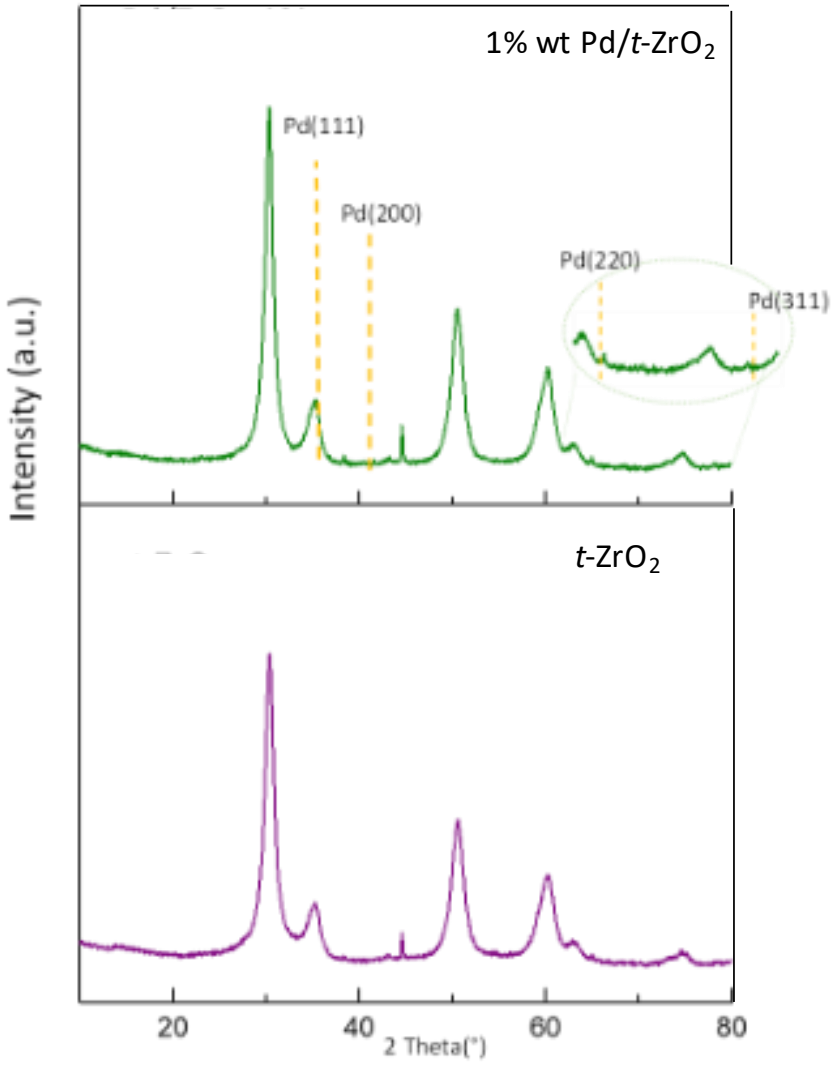

Figure 36. XRD diffractogram of palladium supported on tetragonal ZrO_2in 1% wt.

5.1.3 XRD Pd /C

5% wt Pd/C, 1% wt Pd/C and 0.3% wt Pd/C were analysed by means of XRD, presenting broad peaks attributable to the carbonaceous material, along with weak reflections attributable to Pd at 2θ = 40.001°, 79.811°. The weak peaks that characterized the metal confirmed the uniformity of palladium nanoparticles distribution.

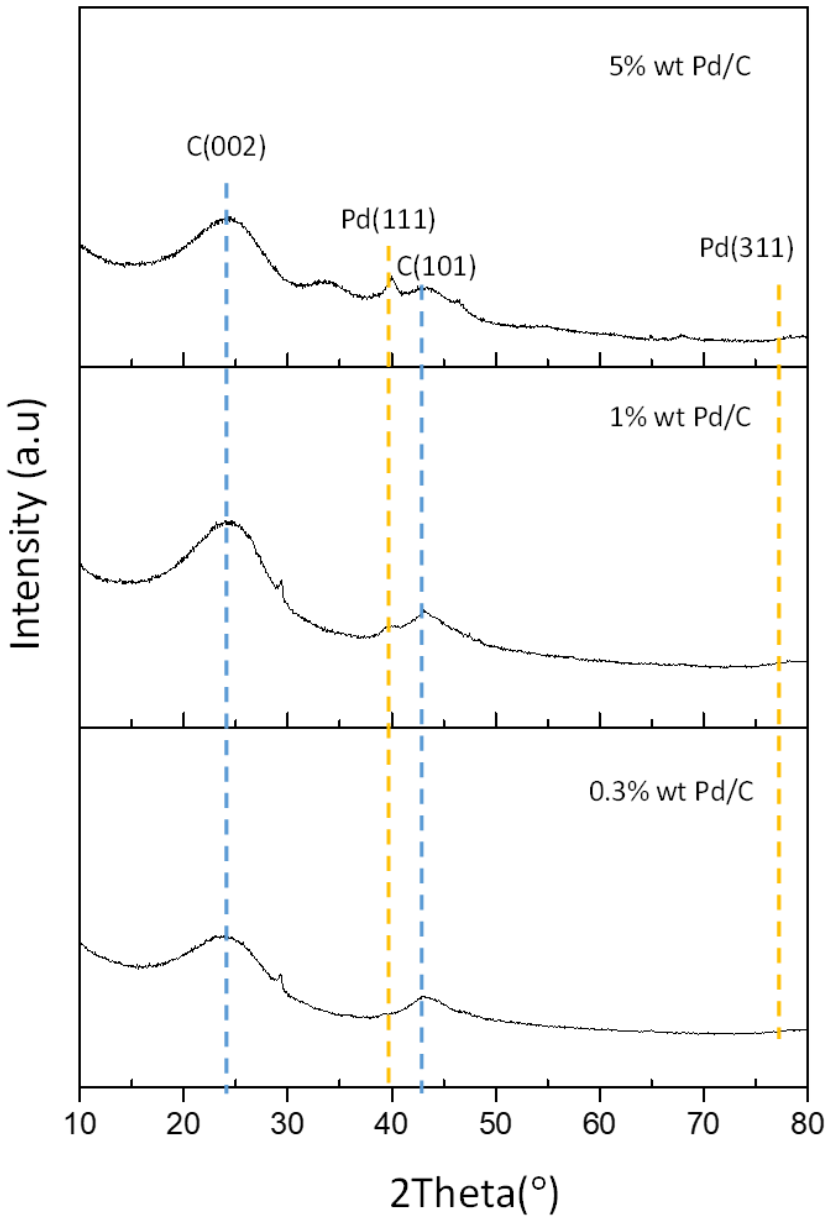

Figure 37. XRD diffractogram of Pd/C at 1% wt (top) and 0.3 % wt (bottom).

5.1.4 XRD 1% wt Pd/ Al_2O_3

1% wt Pd/$Al_2O_3$was characterized by means of XRD evidencing peaks typical of the alumina support at 2θ = 19.898°, 37.685°, 45.707 °, 67.013°, corresponding to (111), (311), (400) and (440) crystallographic planes.

The presence of a small peak at 2θ = 39.893 ° highlights the presence of palladium (111) in small amount and uniformly distributed, as shown by the absence of further characteristic reflections. Finally, small peaks typical of palladium oxide were shown at 2θ = 34.476° and 61.349°, probably due to air exposure of the catalyst.

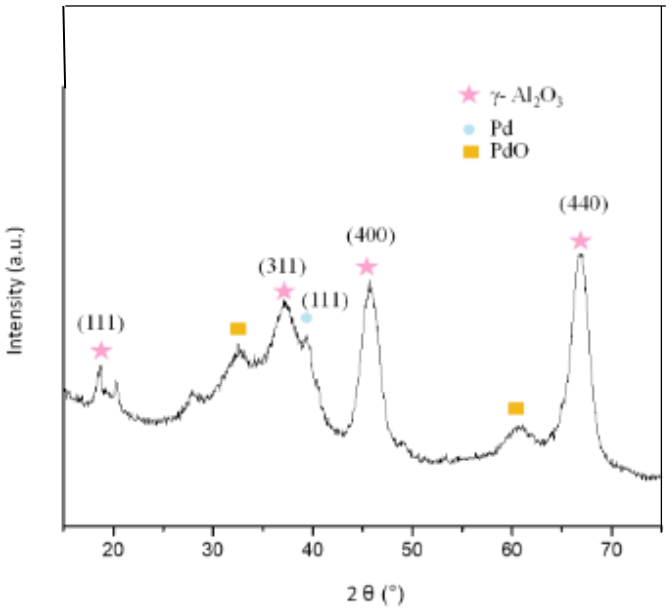

Figure 38. XRD diffractogram of1% wt. Pd/Al_2O_3

5.1.5 XRD. 1% wt Ru /C

1% wt Ru/C was characterized by XRD, evidencing the typical broad peaks for the active carbon support. Two small reflections at 2θ = 36.105° and 57.957° evidenced the presence of the phase (100) and (102) respectively. Their low intensity accompanied by the absence of further Ru characteristics reflections, evidencing nanoparticles well dispersed on the support.

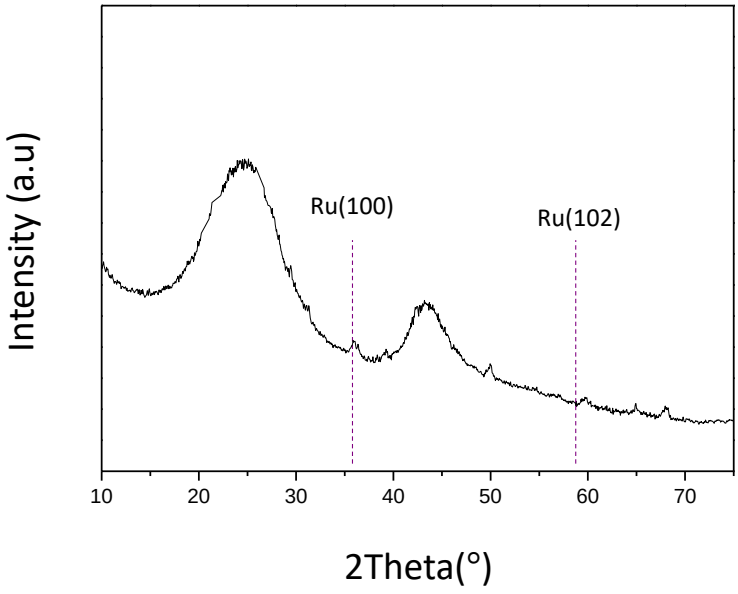

Figure 39. XRD diffractogram of 1% wt Ru/C

5.1.6 Active Surface area

Catalysts were analyzed by means of BET in order to measure the active surface area. All the samples were treated as explained in Chapter 4.3.1.1.

The differences in surface area evidenced in Table 12 are attributable both to the size of metal nanoparticles and the type of support: active carbon shows a very high surface area thanks to the presence of internal micropores; lower values are expected for alumina and zirconia.

Table 12. Active surface area of the catalysts employed measured by BET analysis. The measures were affected by an error equivalent to the 10% of the final value.

Catalyst	Surface area (m^2/g)
Pd/C 0.3% wt	987 ± 98
Pd/C 1% wt	888 ± 89
Pd/C 5% wt	650 ± 65
ZrO_2	198 ± 20
Pd/ZrO_2 1% wt	120 ± 12
Al_2O_3	268 ± 27
Pd/Al_2O_3 1% wt	201 ± 20
Pt/C 5% wt	582 ± 59
Ru/C 1% wt	841 ± 84

5.2 Reaction pathway

The reaction pathway from the unsaturated fatty acids derivatives to the saturated molecules presents a first step of hydrogenation from the poly-unsaturated to the mono-unsaturated compounds. The latter are then converted into the saturated molecules in two possible ways: via direct hydrogenation of the *cis*-U1 or after isomerization with formation of the *trans*-isomer (*trans*-U1), as described in Fig. 40[80].

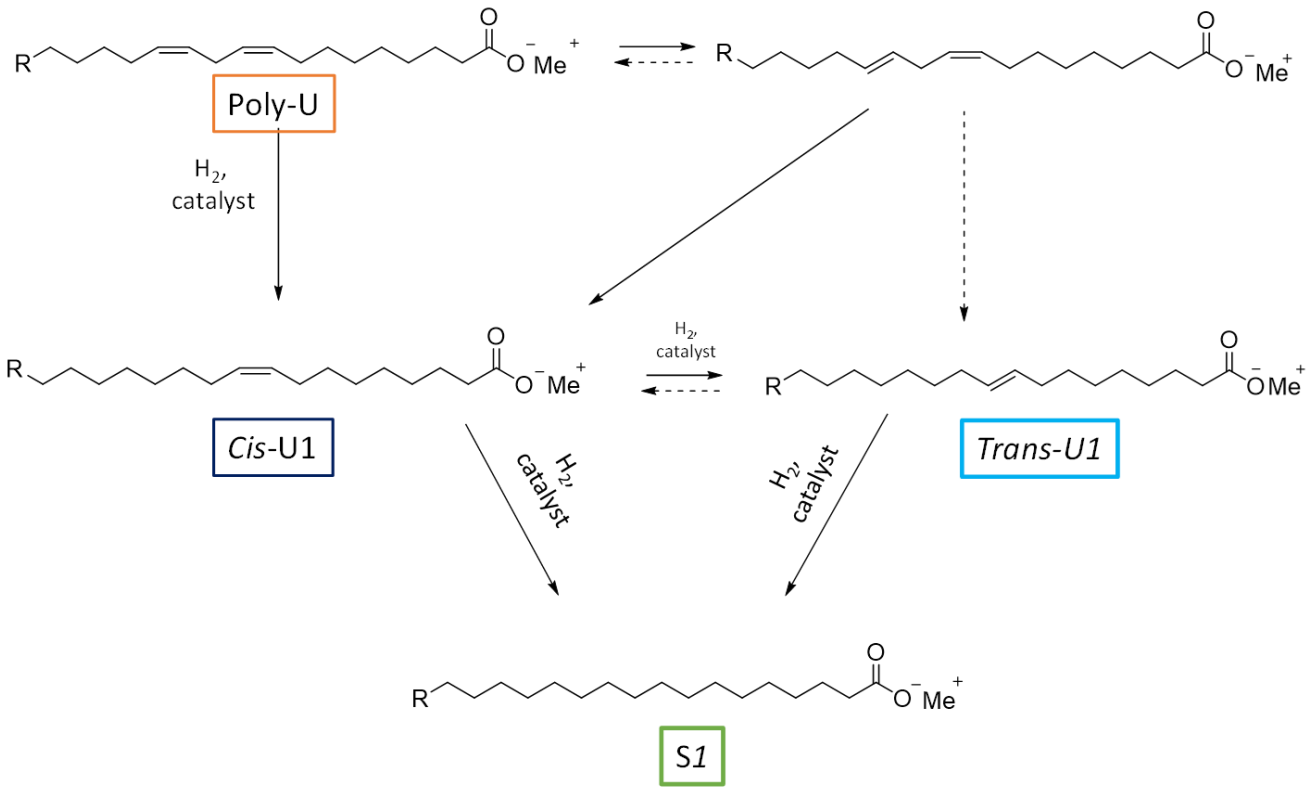

Figure40. Reaction pathway forthe catalytic hydrogenation of fatty acids derivatives. The linoleic acid derivative undergoes a first hydrogenation step of one of the double bonds with subsequent formation of the *cis*-monounsaturated fatty acid derivative. This latter can both undergo isomerisation to form the more stable trans-U1 or hydrogenation to form S1. The *trans* isomer is itself submitted to hydrogenation reaction to yield S1.

During the catalytic tests it was possible to notice the immediate consumption of the poly-unsaturated linoleate in most of the cases and the corresponding formation of the *trans*-isomers. More details about the reaction pathway are reported in the following chapters.

5.3Batch reactions

All batch reactions were performed as described in the chapter 4.5, considering the "time zero" of the reaction when the reaction mixture reached the set temperature. It is important to notice that we always observed a non-nil conversion at the zero time, since a non-negligible conversion of the reactant already occurred during the heating step.
Before each reaction, a leak test was performed by pressurizing the system at 20 bar of $H_2$to ensure the reliability of the sealed system.

Considering that in literature is found that the stainless steel reactor contributed to hydrogenation of 2-butyne-1,4-diol to 1,4-butanediol[125],a blank test with the starting material, hydrogen but without any catalyst was previously performed. The reaction was performed with 15 mL of the supplied starting material, at 90°C, with 4 bar of hydrogen, with a stirring rate equal to 750 rpm for 1 hour.

No variation of the initial reactants' concentration was observed, indicating the absence of non-catalytic reactions or *cis/trans* isomerisation.

The same result was obtained performing a second blank test with a Pd/C catalyst but in inert atmosphere, operating for 1 hour at 90°C and 750 rpm.

These tests proved that both the catalyst and the hydrogen are fundamental for the occurrence of the reaction and thermal effect on the isomerisation process is null.

5.3.1 Influence of the catalyst shape

Mass diffusional resistance at the gas-liquid and liquid-solid interface must be considered when dealing with three phase reactions (see chapter 2.4) considering the influence of the catalyst shape. Indeed, solid catalysts are found in two main different forms: powder and pellets, with a different range of dimension and shape. Pellets are obtained by compacting the powder into tablets and by subsequently crushing the tablet over sieves to obtain the desired particle size. Catalysts in form of pellets provide higher bulk density and surface area per unit volume than powder and are expected to preserve their mechanical integrity; a pressure drop is observed in case of pellet crushing into powder with alteration of flow distribution and possible heat accumulation. The catalyst in the form of powder represents the most cost-effective choice, showing higher surface area available and lower internal diffusional drawbacks.
For an initial screening the two forms of catalysts were tested: 5% wt Pd/C in the form of powder and 0.5% wt Pd/C in the form of pellets of 500 μm size (35 mesh)**,** while keeping the Pd/Substrate ratio constant.Indeed, 0.0045 g were used for the 5% wt Pd/C in the powder form and 0.045 g for the 0.5% wt Pd/C.The reactions were performed for 1 hour, with 4 bar of hydrogen, at 90°C and setting the stirring rate at 750 rpm.

As shown inFigure41, the pellet-shaped catalysts turned out to be almost inactive: only a slight conversion of *cis*-U1 with yield to the *trans*-U1 of 5% were achieved. Yields ≤ 1% wt was observed for the saturated S1. On the other hand, the powder form showed promising results: 90% *cis*-U1 conversion was obtained with yields to the -*trans* isomer and the saturated product of 21% and 72% respectively. Also, complete conversion of the di-unsaturated fatty acid derivative (poly-U) was observed, unlike pellets where the same reactant composition (Table 13) was detected after 1 hour of reaction.

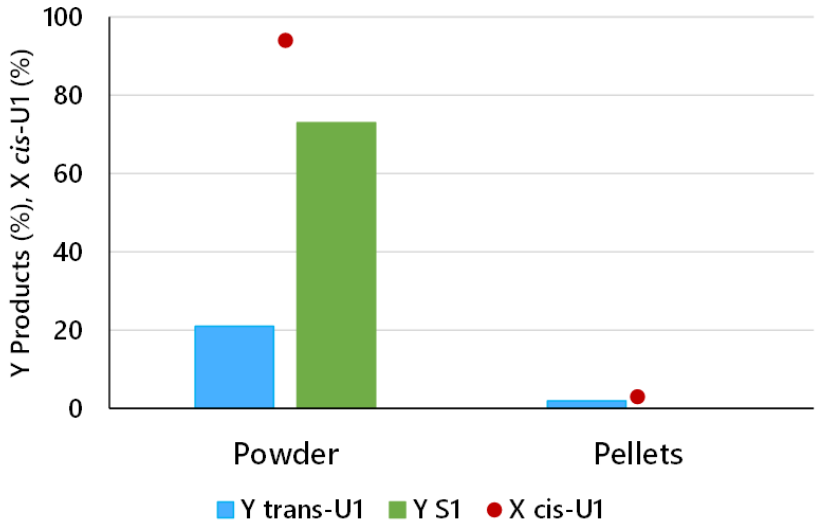

Figure 41. Conversion and yields of S1 and *trans*-U1 as function of catalyst shape. Reaction conditions: batch reactor, T=90°C, P=4 bar, stirring rate750 rpm, 1 hour, 15 mL of solution 30 g/L, 0.5% wt of catalyst.

Table 13 shows the distribution of the products after reaction, evidencing what stated before:

Table 13.Acids derivatives distribution after reaction of *Figure 41.*

Fatty acid derivative	***% w/w pellets***	***%w/w powder***
Oleic acid derivative (cis-U1)	75 ± 2	6 ± 1
Elaidic acid derivative (trans-U1)	3 ±1	19 ± 2
Stearic acid derivative (S1)	2 ± 1	56 ± 2
Linoleic acid derivative (poly-U)	7 ± 1	0
Others	15 ± 2	15 ± 2

Therefore, thanks to the higher activity and selectivity towards the stearic acid derivative (S1), the powder form was chosen as the most suitable shape for the hydrogenation. Moreover, considering that the catalyst was not stored under nitrogen and no reduction pre-treatments were carried out before the reaction, we could observe that the hydrogen pressure employed for the reaction and the low temperature used were enough to *in-situ* reduce and activate the Pd nanoparticles.

5.3.2 Influence of stirring rate- determination of the kinetic regime

Another important aspect related to the diffusional resistance was evaluated: the boundary limit between the diffusional and kinetic regimes.

In the first case, the rate of the reaction is determined by the slow diffusion of the reagents through the gas-liquid and liquid-solid interface. This condition is not preferred, and diffusional resistance must be kept as low as possible. The kinetic regime is obtained when the determining step of the reaction is the occurrence of the reaction, hence no limitation in the transfer of reagents is present.

A simple way to check if the reaction is under kinetic or diffusional regime is to perform the same reaction in a batch system (e.g. autoclave) while maintaining all the main parameters (type of catalyst, temperature, H_2pressure, ratio between reactants and catalyst) constant but changing the stirring rate.

In the case of diffusional regime, an increase in conversion is expected when increasing the stirring rate, thanks to higher turbulence in the system with better mixing and contact of the phases. Conversely, if no changes in conversion are found after an increase of the stirring rate, the system is working under kinetic conditions. However, an excessive stirring rate can be counterproductive, because would cause vortex formation with sticking of the catalyst in the reactors wall and reduced contact of the catalyst particles with the reagents.

Considering the above statements, tests were carried outby comparing the trend of the reaction while changing the stirring rate at 100, 500, 750 and 1000 rpm, for 1 hour reaction time using 5% wt Pd/C in the form of powder.

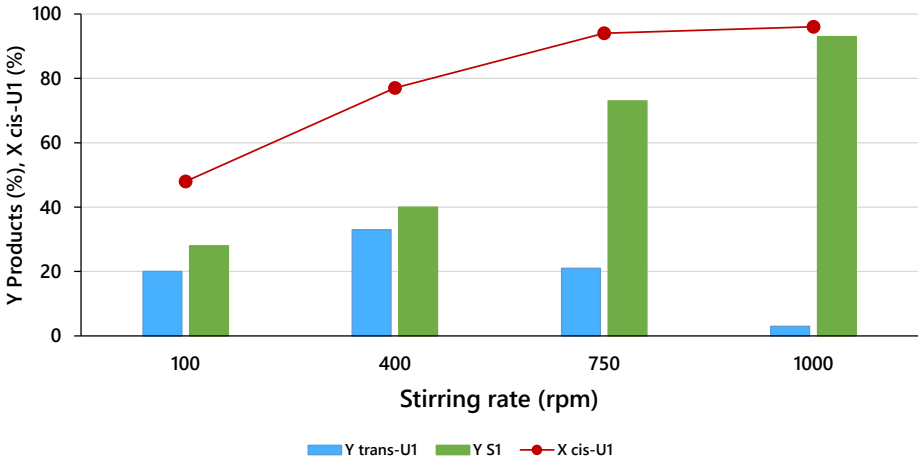

Figure 42. Conversion and yields of S1 and *trans*-U1 as function of stirring rate. Reaction conditions: batch reactor, T=90°C, P=4 bar, stirring rate: 100, 400, 750 and 1000 rpm, 1 hour, 15 mL of solution 30 g/L, 0.5% wt of catalyst.

From Figure 42it can be noticed that, by increasing the stirring rate from 100 to 750 rpm, the conversion rapidly increased, shifting from 47% to 93%. The system was therefore working under diffusional regime, where the diffusion of the reactants through the liquid and the solid was the limiting step of the reaction. By increasing the stirring rate at 1000 rpm a slight increase in conversion ($X_{Cis\text{-}U}$= 95%) was still observed, but a much higher selectivity to the saturated product appeared, being up to 90%, meaning that still the system was under diffusive control. However, we noticed that performing reaction at the higher stirring rate, led to an excessive whirl of the mixture with deposit of the catalyst on the reactor walls. We finally decided to carry out the reaction at 750 rpm.

Table 14 compiles the fatty acid derivatives content after reaction.

Table 14. Acids derivatives distribution after reaction of *Figure 42.*

Fatty acid derivative	% w/w 100 rpm	%w/w 400 rpm	% w/w 750 rpm	%w/w 1000 rpm
Cis-U1	36±2	17 ±1	6 ±1	3 ±1
Trans-U1	16 ±1	25 ±2	17 ±1	5 ±1
S1	22 ±1	47 ±2	50 ±2	81 ±2
Poly-U	0	0	0	0
Others	16±2	12±2	15±2	11 ±1

5.3.3 Influence of H_2 pressure and reaction time

The steps involved in hydrogen activation include first the dissolution of the gas in the liquid media, then the diffusion onto the catalyst surface. The rate of dissolution is proportional to the difference between H_2 solubility at the working temperature and pressure, and its concentration[126].

After having reached the active catalyst, H_2 is adsorbed on the surface where the dissociation into two H* atoms occurs, as illustrated in figure 17. The symbol * indicates that the molecule is adsorbed on the surface of the catalyst:

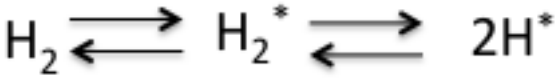

Equation 17. Schematic representation of H_2 adsorption and dissociation on the catalyst surface: Firstly, hydrogen is adsorbed on the catalyst surface with subsequent split into two adsorbed atoms.

The concentration of H* is proportional to the square root of H_2^* and for H_2 pressure below 110 bar the concentration of H* can be assumed to be proportional to the square root of hydrogen concentration ($\sqrt{H_2}$). This means that higher hydrogen pressures can increase hydrogen solubility in the oil[126,127]. Also, the rate of geometrical isomerisation between monounsaturated groups is half order with respect to hydrogen concentration, while the rate of hydrogenation of the double bond is first order in hydrogen[128].

The mechanism involved for hydrogenations is the one described by Horiuti-Polanyas stated in chapter 2.1, where the hydrogen concentration plays a central role for the completeness of the reaction.

Indeed, concentration was increased by pressurising the system at 4 bar and 10 bar of H_2. The reaction was conducted at different times (0, 1, 3 and 6 hours) with the aim of studying the differences of products distribution over time and the effect of H_2pressure simultaneously (Fig. 43).

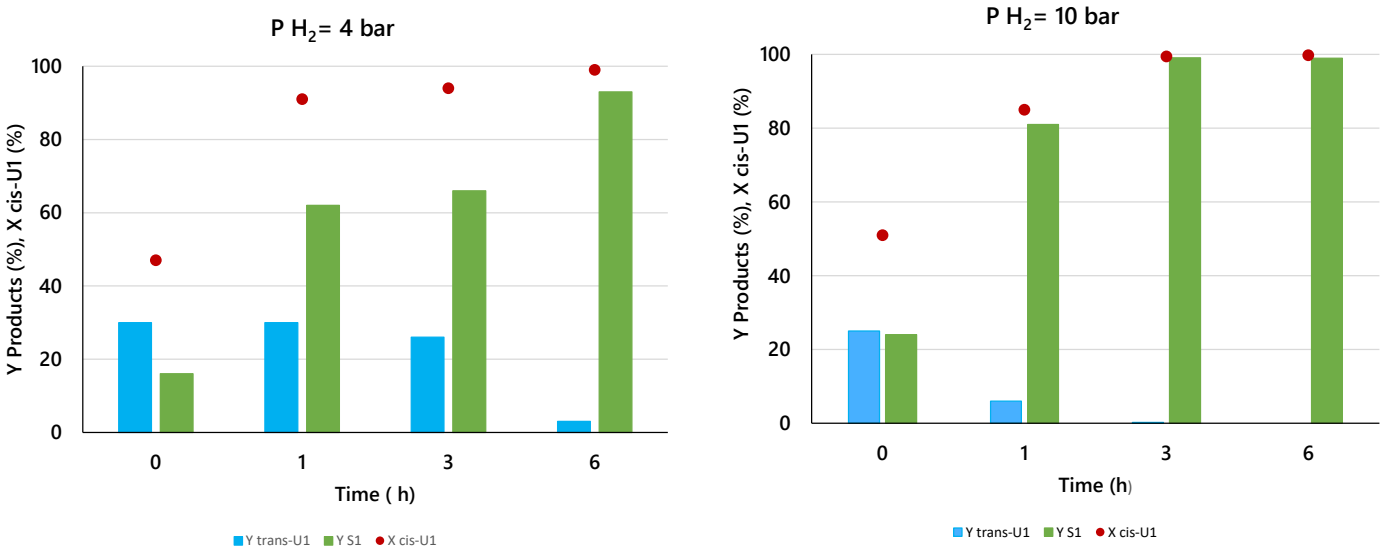

Figure 43. Conversion and yields of Stearic acid derivative (S1) and elaidic acid derivative (*trans*-U1*)* as function of pressure with5% wt Pd/C. Reaction conditions: batch reactor, T=90°C, P H_2=4 bar (left) and 10 bar (right), stirring rate: 750rpm, 15 mL of solution 30 g/L, 0.5% wt of catalyst.

Batch reactions were performed at 0 min, 30 min, 1 h, 3h and 6h in this way having an insight on the reaction kinetics.

Regarding the conversion of oleic acid derivative (*cis*-U1), it is possible to notice that no relevant differences between the two pressures were observed: conversion shifted from ≈50% at 0 h reaction time to ≈80% after 1 h and was complete in 3 hours both at lower and higher hydrogen pressure.

However, the products distribution was more influenced by hydrogen concentration: for the reactions conducted at 4 bar there was still an important presence of the elaidic acid derivatives (*trans*-U1) after 3 h reaction time, which decreased after 6 h (yield from 25% to 5%). For pressure equal to 10 bar, a tiny amount of the *trans*-isomer was detected after 3 h reaction time and no trace of it were found after 6 h.

From these results we could conclude that:

- For both systems a rapid and immediate consumption of starting material *cis*-U1 was observed in 1 hour of reaction. From here we could conclude that when dealing with H_2pressurelower than 10 bar, the consumption of *cis*-U1 was not directly associable to the pressure present in the reaction system. In fact, an increase of H_2 did not sensibly accelerated the conversion of the starting material to the trans-isomer or to the saturated compound;
- *Cis*-U1 was converted for yielding both the *trans*- isomer and the saturated compound S1.

- The products distribution of elaidic derivatives *trans*-U1 and stearic derivatives S1 was more pressure dependent. As stated before, in conditions where H_2 was largely in excess the full hydrogenation was favoured thanks to higher availability of H*. Therefore, minor amount of the *trans*-compound was detected and direct formation of S1 from *cis*-U1 occurred (Fig. 44). On the other hand, lower H_2pressure slowed down the full hydrogenation, allowing major formation of the *trans* isomer[91].

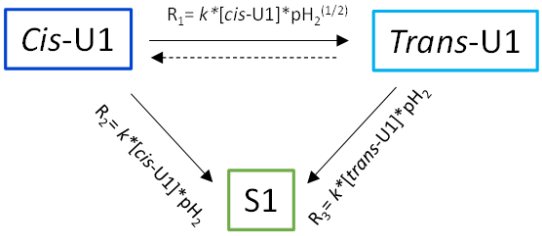

Figure 44. Schematic representation of isomerisation and hydrogenation reaction

To conclude, the effect of hydrogen pressure over conversion and products distribution was investigated; at low pressure (lower than 10 bar), the latter did not significantly affect the substrate conversion but had an influence on the rate of transformation of the *-trans* isomer to the hydrogenated product.

In both cases the linoleic derivative (Poly-U) was immediately consumed leading to the formation of the monounsaturated derivative, as can be noticed by products distribution showed in Table 15.

Table 15. Product distribution of the mixture after reaction described in Fig. 43

	4 bar				***10 bar***			
Fatty acid derivative	**% w/w 0h**	**%w/w 1h**	**% w/w 3h**	**% w/w 6h**	**% w/w 0h**	**%w/w 1h**	**% w/w 3h**	**% w/w 6h**
Cis-U1	36 ± 2	10 ± 1	4± 1	0	36 ± 2	11 ± 1	1± 1	0
Trans-U1	26 ±1	17 ± 2	22± 1	2± 1	20 ±1	7 ± 2	10± 1	6± 1
S1	31 ± 2	50 ± 2	55± 2	85± 2	23 ± 2	63 ± 2	77± 2	85± 2
Poly-U	0	0	0	0	0	0	0	0
Others	10 ± 2	17 ± 2	14± 1	13± 1	12 ± 2	13 ± 2	14± 1	10± 1

5.3.4 Influence of metal loading

Palladium was initially tested as the catalytic species because of its known activity in hydrogenation reactions. Catalysts with metal loading lower than 5% wt were initially examined, employing 4 bar of H_2 at 90°C, 750 rpm, with a 30 g/L solution of the starting material. The usual0.5% wt of catalyst was loaded and the reaction was performed for 30 minutes.

The powder-catalysts with lower metal loading rather than 5% employed were:

- 1% wt Pd/C.
- 0.3% wt Pd/C.

The results, were compared with the 5% wt Pd/C, previously used as the reference catalyst for setting the reaction parameters.

Surprising results (Fig. 45) were obtained with the 0.3 % wt Pd/C catalyst: almost complete conversion was reached after 30 minutes of reaction time and total selectivity toS1was obtained.

Conversely, with the 5% wt Pd/C catalyst, after 30 minutes conversion was 54% only, much lower if compared to 97% obtained with 0.3 % wt Pd/C and 1% wt Pd/C.

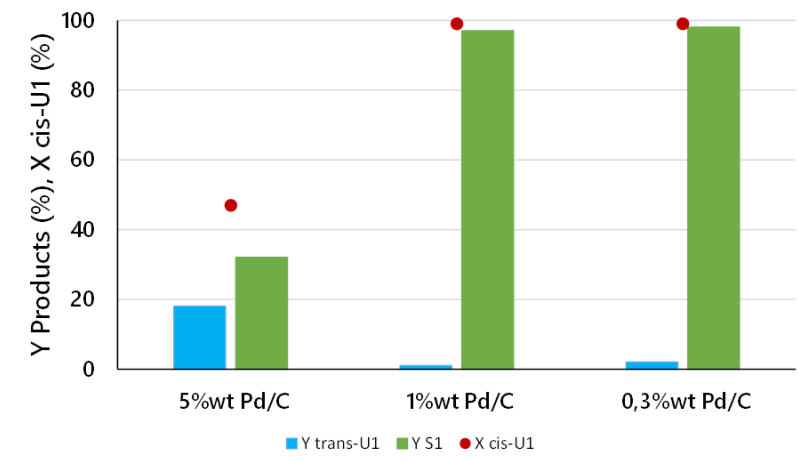

Figure 45. Conversion and yields of S1 and *trans*-U1 as function of pressure with 5%, 1% and 0.3% wt Pd/C. Reaction conditions: batch reactor, T=90°C, P H_2=4 bar, stirring rate: 750 rpm, 30 minutes of reaction, 15 mL of solution 30 g/L, 0.5% wt of catalyst.

The % w/w distribution after each reaction is summarized in Table 16.

Table16. Products distribution of the mixture after reaction with Pd/C described in Fig. 45

Fatty acid derivative	*% w/w 5% wt*	*%w/w 1% wt*	*% w/w 0.3% wt*
Cis-U1	34 ± 2	0 ± 1	0± 1
Trans-U1	18±1	3 ± 2	5± 1
S1	31 ± 2	87± 2	85± 2
Poly-U	0	0	0
Others	12 ± 2	13 ± 2	14± 1

The B.E.T analysis showed a difference in surface area: 650 m^2/g for 5% wt Pd/C, 888 m^2/g for 1% wt Pd/C and 987 m^2/g for 0.3 % wt Pd/C. A higher surface area might explain the difference in the activity of the catalyst; in fact, it might be due to better dispersion of the metal into small (nano) particles, which do not occlude the micropores of the support; an higher Pd content might lead to less efficient metal dispersion, with bigger metal particles, and a partial block of the carbon pores.

In fact, by means of TEM and SEM-EDX analysis of 5%, 1% and 0.3% wt Pd/C, the size of metal nanoparticles in the fresh catalyst was put in evidence and illustrated in fig. 46 *i) ii)* and *iii),* presenting agglomerates of nanoparticles up to 500 nm for 5% wt Pd/C (Fig 46 *iii)* evidenced by red circles), while more homogeneous and smaller Pd nanoparticles were shown for0.3 % wt and 1% wt Pd/C.

The metal agglomeration caused a decrease of Pd atoms availability for the reaction, finally leading to lower activity of the catalyst. Therefore, even if the effective amount of supported Pd was higher, it was not available for the adsorption and activation of the reactant molecules.

This confirmed that nanoparticles size and dispersion played a fundamental role for catalyst activity.

i) 0.3% wt Pd/C

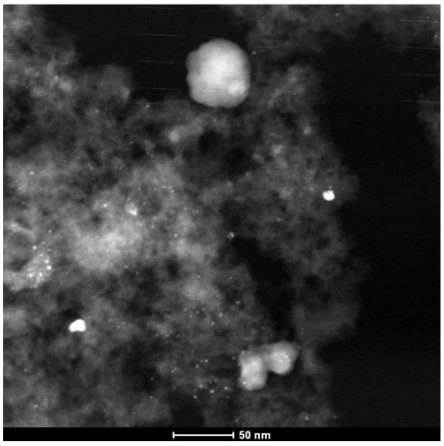

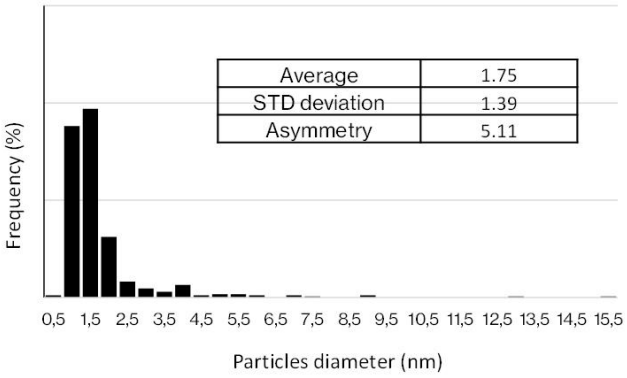

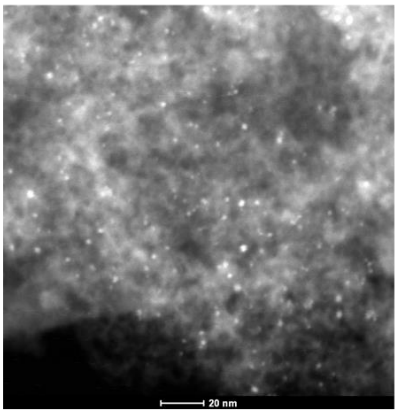

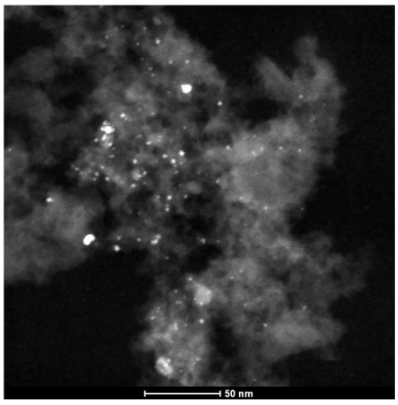

ii) 1% wt Pd/C

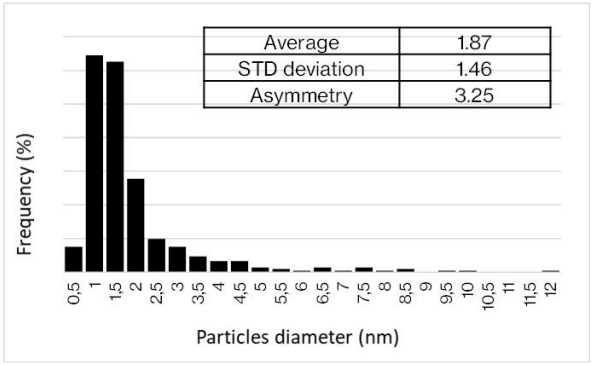

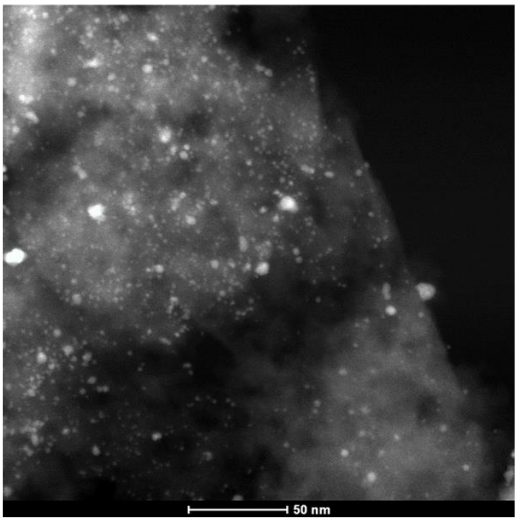

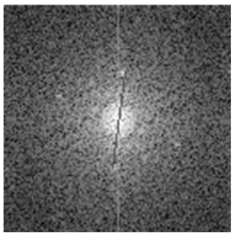

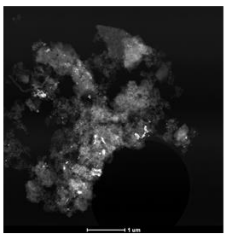

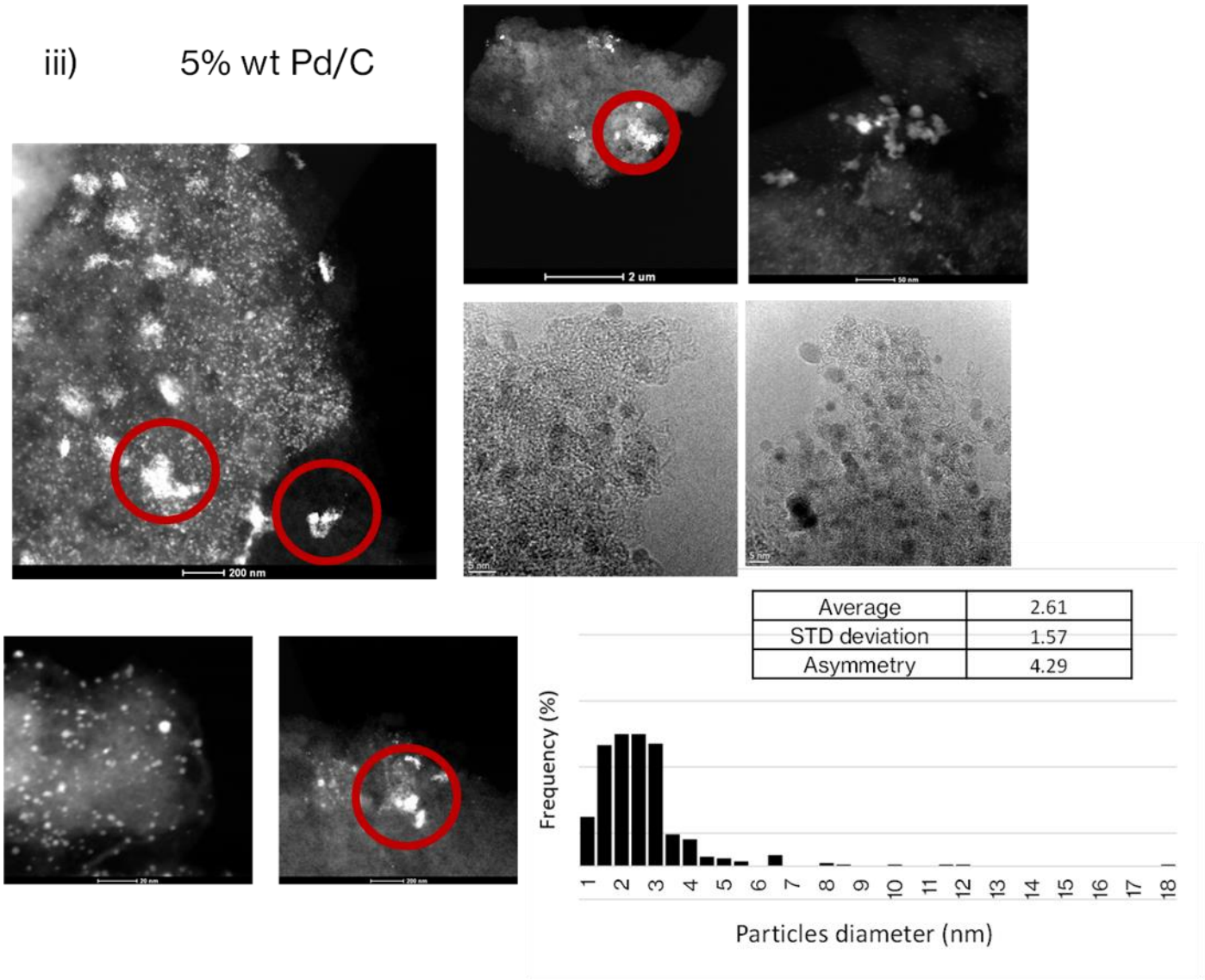

Figure 46. STEM-EDS and TEM pictures with compositional contrast of **i)** 0.3 % wt Pd/C, **ii)** 1% wt Pd/C, **iii)** 5% wt Pd/C. The pictures reveal bigger nanoparticles for 5% wt Pd/C catalyst with agglomerations up to 500 nm. Lower palladium amount revealed a more uniform NP dimension of maximum 8 nm and 10 nm for 0.3% and 1% wt Pd/C respectively.

5.3.5 Influence of the active metal: Pd, Pt, Ru, Ni-RANEY

Palladium was initially tested for its known capacity to catalyse hydrogenation reactions, however a wider look to different metals was given. All the metals were supported on carbon with different percentage of metal loading and compared with the Pd analogue.
Pt and Ru were evaluated due to their lower price compared to Pd: indeed, when considering the whole process and in view of an industrial applications, the cheapness of the catalyst can play an important role. As table 17 shows, the price of Pt and Ru is respectively 2.5 and 3.3 time lower compared to Pd.

Table 17. Price (EUR/g) for the metal employed during catalytic tests. Prices updated on 27th July 2021[129].

Metal	*Price (EUR/g)*
Pd	72.823
Pt	29.388
Ru	21.814
Ni-Raney (Ni)	17.495

Ni-Raney was employed because it is used in industry for several hydrogenation reactions. Besides the complication related to its toxicity, Ni-Raney holds a completely different structure: it is a bulk catalyst sold as a thick paste due to its extreme pyrophoricity. It is constituted of a sponge-like structure composed of Ni and Al and treated with concentrated NaOH which dissolves most of the Al present, yielding to a metallic sponge with very high active surface.
These tests allowed us to highlight significant differences of catalytic activity.
Batch reactions were executed with commercial 5% wt Pt/C and homemade 1% wt Ru/C, in standard reaction conditions using 15 mL of 30 g/L solution, T=90°C, stirring rate= 750 rpm, pressure= 4 bar of $H_2$and conducing the reaction for 4 has highlighted in Fig. 47 and 48.

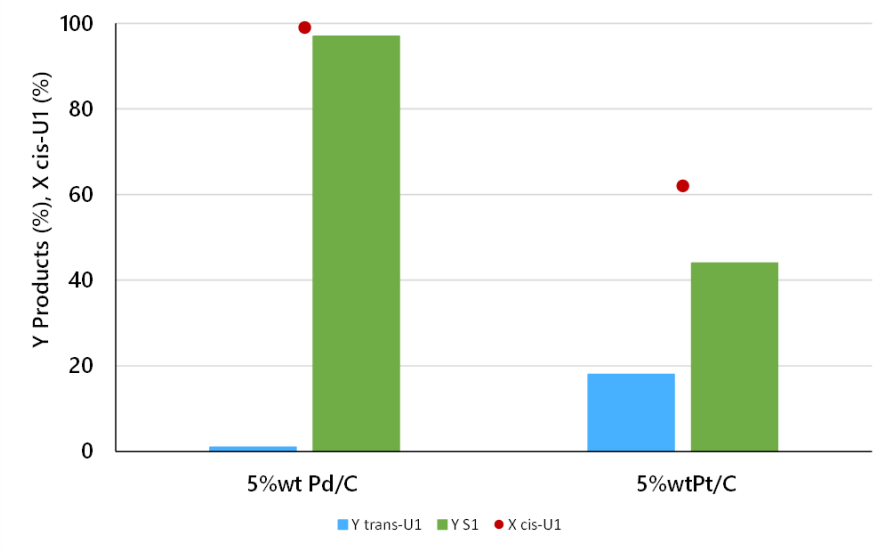

Figure 47. Conversion and yield of*trans*-U1 and S1 with 5% wtPd/C and 5% Pt/C. Reaction conditions: batch reactor, T=90°C, P H_2=4 bar, stirring rate: 750, 4h of reaction, 15 mL of solution 30 g/L, 0.5% wt of catalyst.

As figure 47 shows, Pt/C did not show promising results compared to 5% wt Pd/C. Indeed, Pt is more active for the hydrogenation of aromatic compounds[130];60% conversion of *Cis*-U1 was obtained, lower than the total conversion achieved with 5% wt Pd/C.

1% wt Ru/C offered room as a possible cheaper substitute of Pd. However, Pd was still more active than Ru, which, in fact, is generally employed for the selective hydrogenation of polycyclic aromatic compounds[131]. Almost 90% of substrate conversion was reached. The step from the *trans*-U1 to S1 was slower for Ru, still evidencing a 10% yield to*trans*-U1, which instead turned out to be negligible with Pd/C.

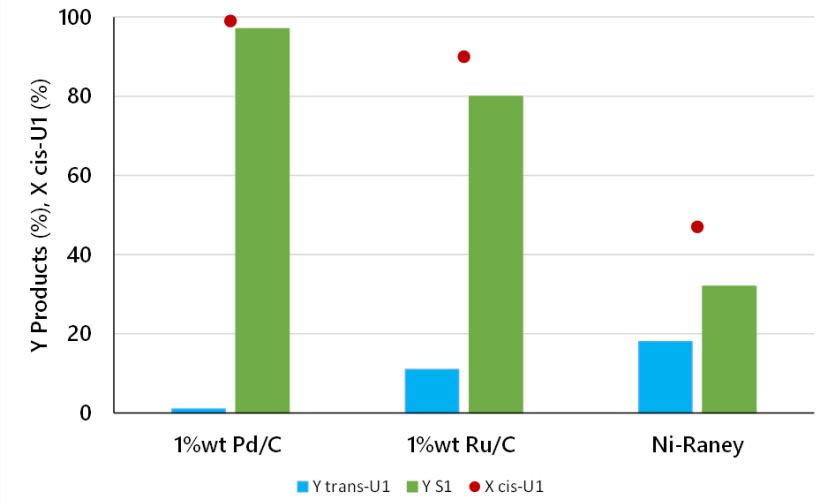

Figure 48. Conversion and yields of S1 and *trans*-U1 with Pd/C 1%, Ru/C 5% wt and Ni-Raney. Reaction conditions: batch reactor, T:90°C, P H_2=4 bar, stirring rate: 750, 30 minutes of reaction, 15 mL of solution 30 g/L, 0.5% wt of catalyst.

Ni-Raney was employed for performing two reactions: the first with the same amount as for 1% wt Pd/C catalyst (0.0245 g), which led to complete conversion and selectivity to the stearic derivative S1. However, the substantial structural difference between 1% wtPd/C and Ni-RANEY should be taken into account: the former isa supported catalyst, where the active phase is determined by the content of the metal (in this case, 1% wt), while the latter is a bulk catalyst, which means that all the mass of the loaded catalyst may potentially be active for the reaction. Therefore, another test was performed by loading the bulk Nickel catalyst, in a comparable amount with the actual grams of Pd used in the reference tests, in order to better compare the activity of the different metals.

Hence, 10 mg of Ni-Raney were loaded and reacted in standard reaction conditions.

The obtained results underlined the lower catalytic activity of the Ni catalyst, with a conversion of only 47%,compared to 99% for 1 % wt Pd/C catalyst, as shown in Fig. 48.Therefore, no further reactions were performed employing Ni-Raney, also considering the nature of the catalyst, not compatible with the *Green Chemistry principles.*

5.3.6 Influence of reaction temperature

The reaction temperature is one of the key parameters of a reaction: higher temperatures favour the kinetics of the reaction, but thermodynamic aspects should also be considered. Also, the objective of the project was to perform the reaction selectively under the mildest conditions possible, by keeping the pressure and temperature of exercise as low as possible.

Initial screening tests were executed at 90°Cwith the 0.3 % wt Pd/C catalyst. As already reported, after only 30 minutes reaction time, very promising results were reported, with a complete conversion of the substrate and a 96% yield to S1.

Therefore, the reaction temperature was decreased down to 30 °C (Figure 49).

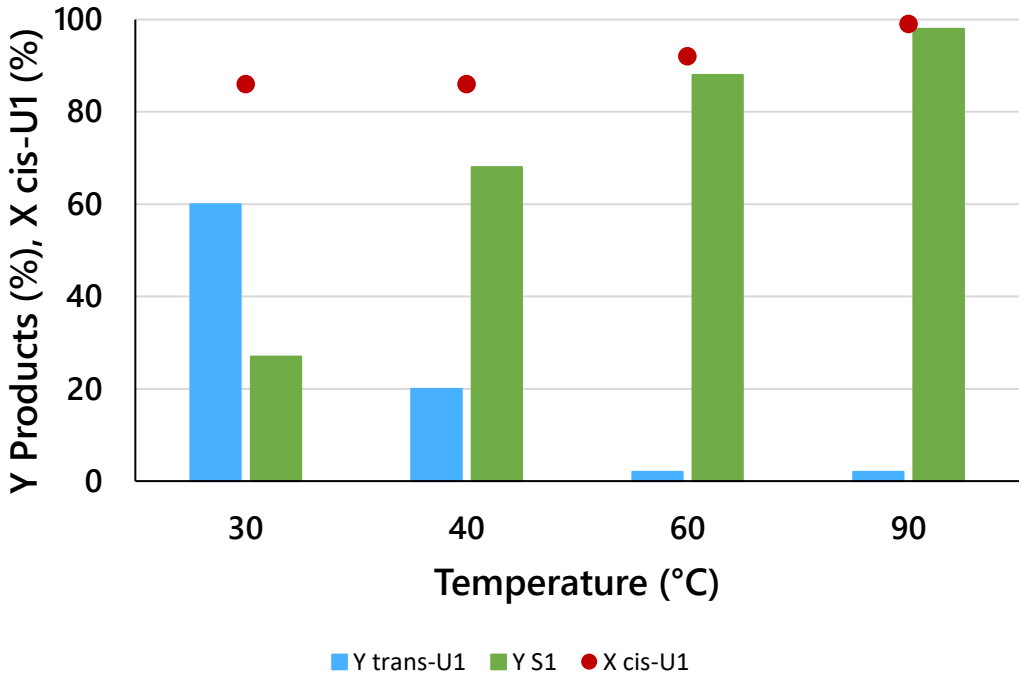

Figure 49. Conversion and yields of S1 and *trans*-U1 with 0.3% wt Pd/C as function of temperature. Reaction conditions: batch reactor, T=30-90°C, P H_2=4 bar, stirring rate: 750, 30 minutes of reaction, 15 mL of solution 30 g/L, 0.5% wt of catalyst.

Noteworthy, already after 30 min at 30°Cthe *cis*-U1 conversion was already considerable (87%), keep increasing with temperature and reaching 99% only at 90°C.

However, the more remarkable effect was on products distribution at the end of the reaction, as highlighted also in table 18 and Fig.50

Table 18. Product distribution of the mixture after reaction described in Fig. 50

Fatty acid derivative	*% w/w 30°C*	*%w/w 40°C*	*% w/w 60°C*	*% w/w 90°C*
Cis-U1	10 ± 2	9± 1	3± 1	0 ± 1
Trans-U1	25±1	17± 2	2± 1	3 ± 2
S1	47 ± 2	53± 2	76± 2	87± 2
Poly-U	0	0	0	0
Others	12 ± 2	13 ± 2	14± 1	13 ± 2

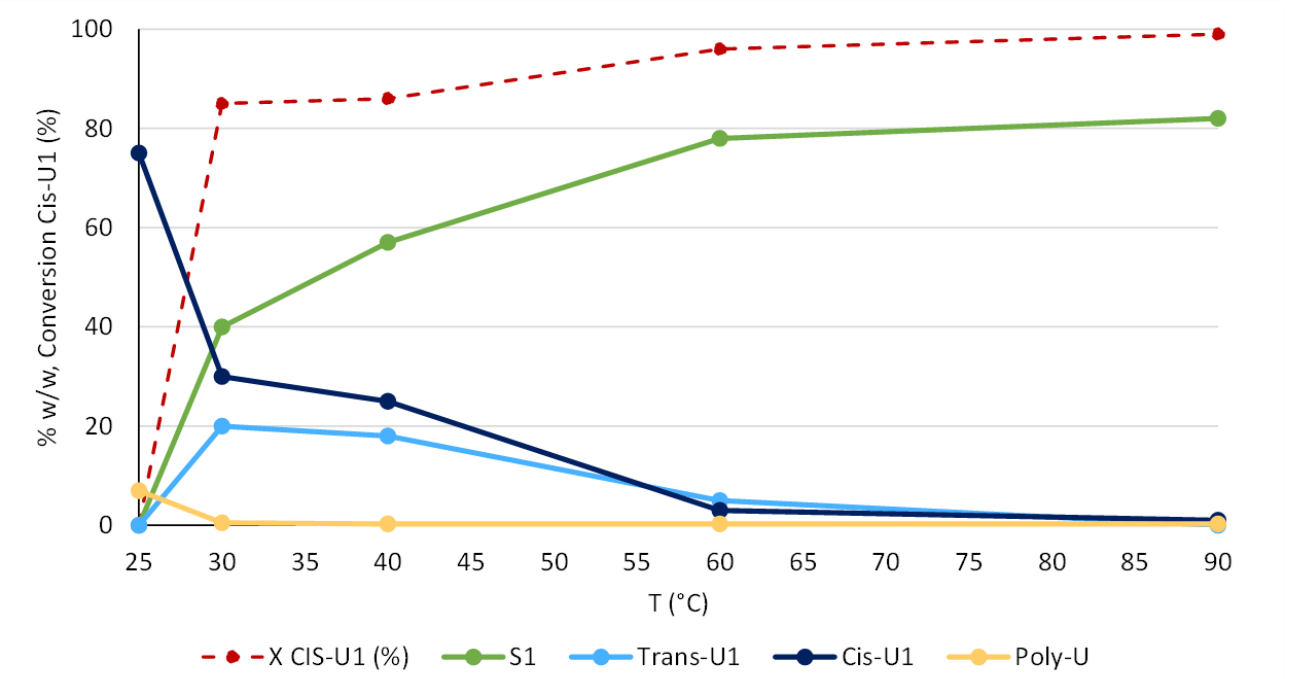

Figure 50. Trend of the products % w/w (full line) and *cis*-U1 conversion (dotted line) in function of reaction temperature (RT-90°C) for 30 min reaction time using 0.3% wt Pd/C.

Figure 50shows that at lower temperature, higher amount of the *trans* isomer was formed, reaching a maximum at 30°C. Then, its concentration started to decrease, with the corresponding increase of the Stearic derivative S1. The trend of conversion (shown in red) is

specular to the content of *cis*-U1 (in blue), the former being very high, around 85%, already at 30°C.

The Linoleic derivative (Poly-U -yellow line), was immediately consumed already at 30°C, both due to its low amount and its high tendency to bond onto the catalyst surface, because of the presence of two double bonds along the chain[80].

The content of the Elaidic derivative (*trans*-U1) and the product (S1), marked in light-blue and green respectively, showed an interesting trend: *trans*-U1 showed its highest value at 30°C,then decreased with a further increase of S1 content.

The high conversion (85%) observed at 30°C, confirmed that the conversion of the starting material occurred rapidly and in mild conditions.

However, the two reactions (isomerisation and hydrogenation represented in Fig. 44) occurred at similar rate. Increasing the temperature, the -*trans* isomer formation would be favoured[130], but even more favoured were the hydrogenation reactions from *cis*-U1 to S1 and from *trans*-U1 to S1. Therefore, an overall decrease in both *cis* and *trans* isomers were observed with following increase in S1 amount.

If no consecutive hydrogenation would occur, an increase of *trans*- species would be observed shifting from 30°C to 90°C.

5.3.7 Influence of the support

The metal plays always an important role for the catalyst performance but a crucial role may also be covered by the support.

The reasons why the support is so important are multiple, among these the most relevant are:

- Reduce the amount of the metal, which is typically the most expensive part of the catalyst.
- Stabilize the metal nanoparticles to avoid their agglomerations during the reaction which may be the cause of a rapid deactivation.
- Stabilize oxidic species in an oxidation state that is not possible to obtain for unsupported metals.
- Increase the mechanical resistance of the catalyst.
- Create multifunctional catalysts, by means of an acid or basic support.
- Confer to the whole catalyst a high active surface area.

The support could have intrinsic characteristics capable of maximizing the activity of a metal or to confer multifunctionality to the catalyst considered.

Activated carbon is an organic amorphous material. It generally comes from charcoal and is subjected to pre-treatments, which make it exploitable for catalysis purposes. In fact, among all the possible supports, it holds one of the highest surface areas (500-2000 m^2/g) and is characterized by high porosity, in particular microporosity. The latter, however, may represent a potential drawback, especially when reactants or products are sterically hindered.

The structure of carbon can be modified in order to confer the system specific functionalities. However, if not treated, it shows a slight basicity (Lewis type), due to the π-electron rich area located on the basal plane of carbon crystallites[132].

Al_2O_3represents an alternative, showing a lower surface area compared to activated carbon but presenting higher mechanical strength and inertness to several chemicals; moreover, it is characterized by a significant surface acidity[133]. Al_2O_3can undergo air treatment up to high temperature for its regeneration, while carbon presents some limitations. In fact, treatment of carbon with air can be performed until 150°C, while if it is necessary to treat the substrate at higher temperature (up to 700/800°C), an inert atmosphere must be selected.

Therefore, Pd supported on alumina and zirconia (1%wt Pd/ZrO_2, 1%wt$Pd/Al_2O_3$and 0.3 % wt Pd/Al_2O_3) were tested and compared with the carbon counterpart (1% wt Pd/C and 0.3% wt

Pd/C), in autoclave at 90°C, with a stirring speed of 750 rpm, using 4 bar of H_2, for 30 min reaction time and employing the same amount of catalyst.

Results of conversion and yields for the described catalysts are reported in figure 51 and table 19.

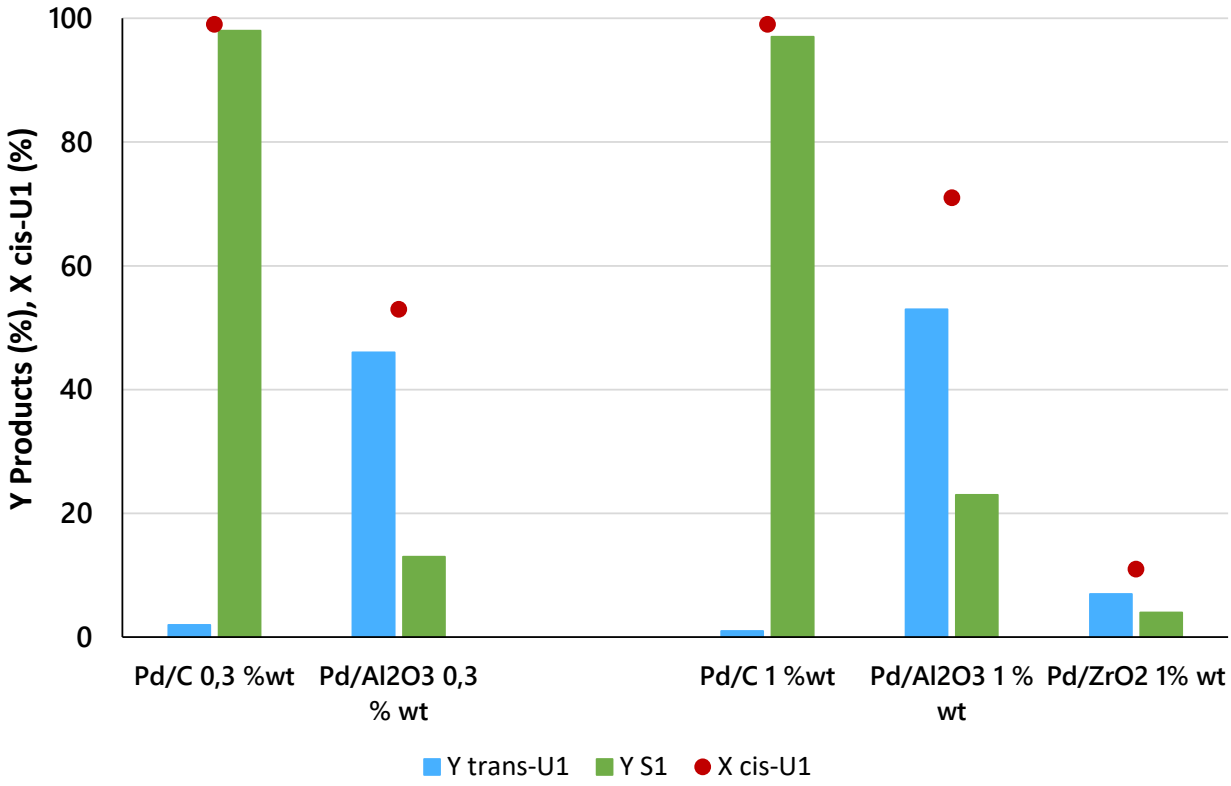

Figure 51. Conversion and yields of S1*trans*-U1 with 0.3% wt Pd/,1% Pd/C, 0.3% Pd/Al_2O_3, 1% Pd/Al_2O_3 , 1% Pd/ZrO_2.Reaction conditions: batch reactor, T:90°C, P H_2=4 bar, stirring rate: 750 rpm, 30 minutes of reaction, 15 mL of solution 30 g/L, 0.5% wt of catalyst.

Table 19. Product distribution of the mixture after reaction described in Fig. 51

	1% wt			*0.3% wt*	
Fatty acid derivative	**% w/w Pd/C**	**%w/w Pd/Al_2O_3**	**%w/w Pd/ZrO_2**	**% w/w Pd/C**	**%w/w Pd/Al_2O_3**
Cis-U1	0 ± 1	20± 2	70± 2	0± 1	33± 2
Trans-U1	3 ±1	47± 2	8± 1	5± 1	34± 2
S1	87 ± 1	20± 2	5± 1	85± 2	10± 2
Poly-U	0	0	0	0	0
Others	3-5 ± 2	3± 1	7± 1	5± 1	3± 1

Itis evident that the highest activity was shown by the Pd/C, both with 0.3% wt and 1% wt of Pd content.

In the case of the Alumina support, the following trend was shown: linoleic derivatives were immediately consumed, with no amount left after 30 min reaction time. It contributed to form Oleic (*cis*-U1) and eventually Elaidic (*trans*-U1) derivatives.

Then, *cis*-U1was converted into its -*trans* isomer Elaidic and Stearic derivative (S1).

However, the formation of the *trans*- isomer was always favoured, because despite the relevant amount of S1 formed, *trans*-U1 was the major compound detected. Therefore, it is possible to state that for Alumina the slowest step was the transformation of Elaidic or Oleic into Stearic derivative, and isomerisation was favoured.

The rate of conversion decreased in order: poly-U to *cis*-U1 >*cis*-U1 to *trans*-U1 >*cis/trans*-U1 to S1.

Mostly, unlike carbon, alumina results were directly correlated to the amount of Pd: *cis*-U1 conversion increased from ≈55% with 0.3 % wt Pd/Al_2O_3up to 70% with 1 % wtPd/Al_2O_3, as much as the selectivity to *trans*-U1 and to S1, with an increase in % w/w of S1 from 10% to 20%.

Zirconium oxide was employed to test a support showing higher Lewis acidity compared to carbon; however, low conversion of the substrate was obtained accompanied by an higher amount of the*trans*-U1.

A possible reason for the observed differences among supports is the large difference of surface-active areas: the 1% wt Pd/C holds 888 m^2/g, $Pd/Al_2O_3$201 m^2/g and $Pd/ZrO_2$120 m^2/g. Therefore, Carbon was preferred over alumina and ZrO_2, even though for experiments of thermal regeneration of spent catalysts were carried out preferably on thermally resistant supports (see Chapter 5.4.8.2).

5.3.8 Recyclability tests

5.3.8.1 Recyclabilityof 0.3% wtPd/C and 1% wtPd/C

Recoverable and recyclable are two features that have fundamental importance for heterogeneous catalysts. A catalytic process is in line with one of the *Twelve principles of the Green Chemistry*, but a catalyst must be also recoverable and recyclable. The recovery is fundamental not only for what concerns the purity of the final product, but also for generating a circular economy and reducing waste.

Recyclability is a further added value for an active catalyst, which means that the same catalyst can be reused for multiple reactions without affecting the activity or selectivity that are achieved with the fresh catalyst.

As described in the introduction (Chapter 2.5) there could be many reasons for catalyst deactivation, related either to the reaction (the conditions necessary to perform a reaction or the formation of by-products that adsorb on the active surface), to the nature of the starting material or to the modifications occurring on the active phase (e.g: sintering or agglomeration of metal nanoparticles).

The knowledge of the reasons that can eventually cause deactivation allows preventing this phenomenon and making the most out of a catalyst.

Therefore, tests were performed on the two most performing catalysts, 0.3% Pd/C and 1% wt Pd/C, as explained in the experimental section 4.7.

All the reaction parameters were kept constant and fresh solution was employed for the second and third cycle of reaction.

Fig. 52 shows a deep and fast reduction of*cis*-U1 conversion for 0.3% wt Pd/C from the first batch to the second one, which further worsened with the third cycle. Conversion decreased form 99%, to ≈55% and finally to 20% for the 1st, 2nd and 3rd cycle, respectively. Even more, it was noticed that the rate of the mono-unsaturated to S1 step had slowed down, causing an increase in *trans*-U1 amount. A comparison of the second and the third cycle revealed a switch regarding the majority of the two compounds in the final mixture: in the second cycle, the amount of *trans*-U1 after 30 min was less than the amount of S1, while in the third cycle the opposite was true. The deactivation did affect not only the conversion of *cis*-U1, but also the

final step of the reaction. Regarding Poly-U, as can be seen in Table 20, its consumption was not affected by deactivation.

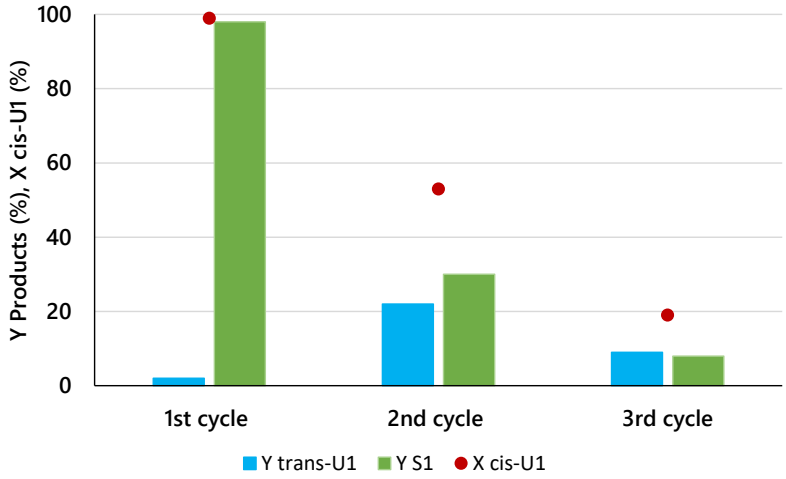

Figure 52. Conversion and yields of S1 and *trans*-U1 with 0.3% wtPd/C for recyclability tests. Reaction conditions: batch reactor, T:90°C, P H_2=4 bar, stirring rate: 750, 30 minutes of reaction, 15 mL of solution 30 g/L, 0.5% wt of catalyst.

Even if in a less drastically, the same deactivation occurred also for 1% wt Pd/C:

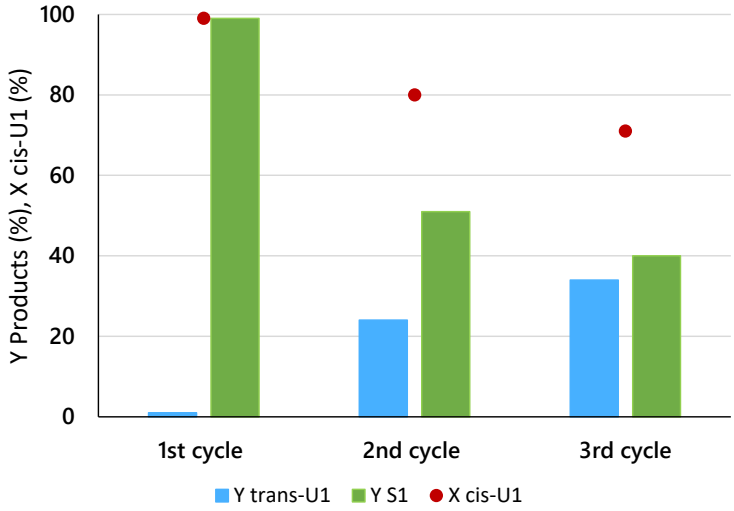

Figure 53. Conversion and yields of S1 and *trans*-U1with1% wt Pd/C for recyclability tests. Reaction conditions: batch reactor, T:90°C, P H_2=4 bar, stirring rate: 750, 30 minutes of reaction, 15 mL of solution 30 g/L, 0.5% wt of catalyst.

For this test, shown in Figure 53, conversion reached a minimum of ≈70% at the third cycle, 3.5 times greater than the value obtained with 0.3% wt Pd/C.

The higher amount of metal, when accompanied by a reduced increase of NP size, can improve the catalyst stability, keeping the conversion still at greater values. However, looking at the yields of *trans*-U1 (light-blue) and S1 (green), it is evident that the former started to be more present along the time, at the expense of S1. If after the first cycle the amount of S1 was largely

higher than *trans*-U1, the two compounds were almost equal after the third cycle: this meant that the *cis*-U1 was successfully converted but the reaction was less selective for the S1, allowing the isomerisation to occur.

Even in this case Poly-U were immediately consumed and no traces were detected after the three cycles of reaction (Table 20).

Table20. Product distribution of the mixture after reaction described in Fig. 52 and 53

	Pd/C 0.3% wt			Pd/C 1% wt		
Fatty acid derivative	**% w/w 1st cycle**	**%w/w 2ndcycle**	**% w/w 3rdcycle**	**% w/w 1st cycle**	**%w/w 2ndcycle**	**% w/w 3rdcycle**
Cis-U1	6± 1	37± 1	61 ± 1	0± 1	10± 1	17 ± 1
Trans-U1	12 ± 2	27± 2	15 ± 2	2 ± 2	20± 2	32 ± 2
S1	74± 2	15± 2	6± 2	71± 2	45± 2	40± 2
Poly-U	0	0	0	0	0	0
Others	10± 2	15 ± 2	13 ± 2	12± 2	16 ± 2	16 ± 2

The different behaviour shown by the two system could be explained by considering that with higher Pd loading the metal nanoparticles could interact more efficiently with the substrate, ensuring a more constant activity over time.

However, the decrease in catalytic performance was still present in both cases and it could be ascribed to:

- The leaching of palladium during the tests;
- The absorption of heavy molecules (reagents, products or intermediates) on the catalyst surface.

Leaching of the active metal out of the support was inspected by means of ICP-AES analysis on the post-reaction solution, by checking the signal of Pd at its characteristic absorption wavelength (λ=351.6 nm, chapter 4.3.2.2).

However, as the figure 54 displays, no Pd signal was detected, which confirms the absence of metal leaching during the reaction.

Sintering of the metal was excluded due to the mild reaction conditions used (T=90°C and P=4 bar of H_2).

Absorption of heavy molecules or impurities on the catalyst surface was considered as a

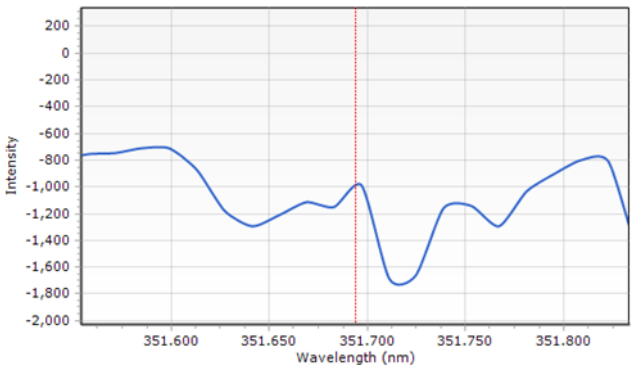

Figure 54. ICP-AES signal of post-reaction solution evidencing absence of typical pd sign at λ=351.69 nm.

secondoption: regeneration of the catalyst by air treatment could be useful to restore the initial catalytic activity, and TG analysis could evidence the loss of material.
However, carbon support was not suitable for any treatments with air at high temperature.
TGA in inert atmosphere was conducted, but no loss of material before 150°C was detected. In order to investigate the adsorption of material on the catalyst, the same tests were repeated with the 1%wt Pd/Al_2O_3 catalyst; despite the slightly lower activity, Al_2O_3 could undergo thermal treatments, allowing the regeneration by calcination with air and the characterisation by TG analysis.

5.3.8.2 Recyclability of 1%wt Pd/Al_2O_3

The same sequence of catalytic tests was repeated also for the 1%wt Pd/Al_2O_3 catalyst, with the results shown in Fig. 55.

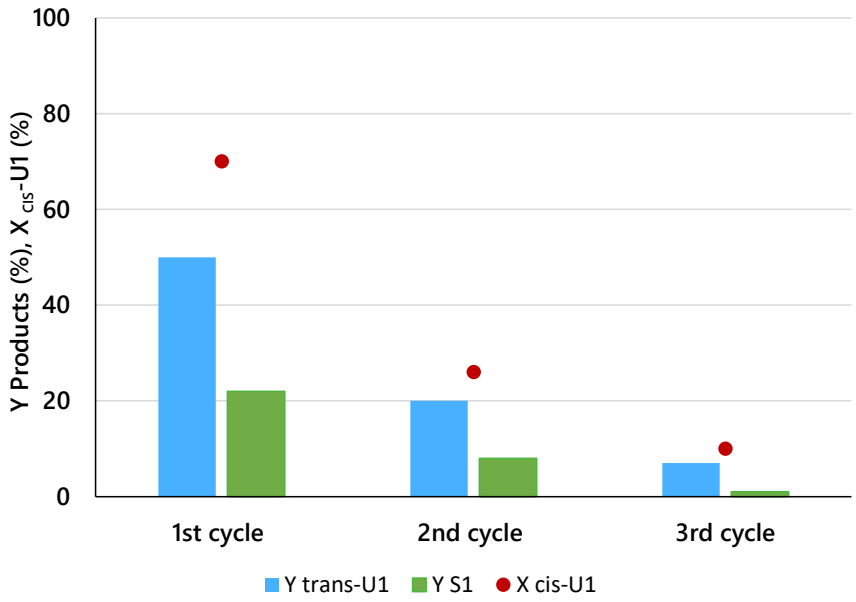

Figure 55. Conversion and yields of S1 and *trans*-U1 with 1% wtPd/Al_2O_3 for recyclability tests.Reaction conditions: batch reactor, T:90°C, P H_2=4 bar, stirring rate: 750, 30 minutes of reaction, 15 mL of solution 30 g/L, 0.5% wt of catalyst.

Fig. 55revealsthat the decrease in activity was even more relevant than for the carbon-supported catalyst. Also, as it was already shown in chapter 5.3.7, Alumina was not only less active in *cis*-U1 conversion, but also less selective towards S1, being the *trans*- isomer always the major component in every catalytic cycle.

Deactivation between the first and the second cycle was more rapid than for 1%wt Pd/C: with the alumina-supported catalyst, *cis*-U1 conversion decreased from 75% to 22%, while with the carbon-supported catalyst, the decrease of conversion was from 99% to 80% only. This could be due to the presence of acidic active sites in alumina, which are able to bind any possible basic impurities present in the mixture.

Also, with alumina as the support, no traces of Pd in the post-reaction solution were detected from ICP-AES analysis, confirming that no metal leaching had occurred.

Table 21. Product distribution of the mixture after reaction described in Fig. 55

	Pd/Al_2O_3 1% wt		
Fatty acid derivative	**% w/w 1st cycle**	**%w/w 2nd cycle**	**%w/w 3rd cycle**
Cis-U1	23± 1	56± 2	69 ± 1
Trans-U1	43 ± 2	20± 2	6 ± 2
S1	20± 2	9± 2	4± 2
Poly-U	0	0	0
Others	13± 2	15 ± 2	13 ± 2

Despite the strong deactivation shown, alumina holds the advantage of being treated with air at high temperature without structural degradation.

Therefore, the spent catalyst was separated from the solution, dried at 60°C overnight and treated in static air at 450°C for 3h.

The treated catalyst was then reused for a new catalytic test.

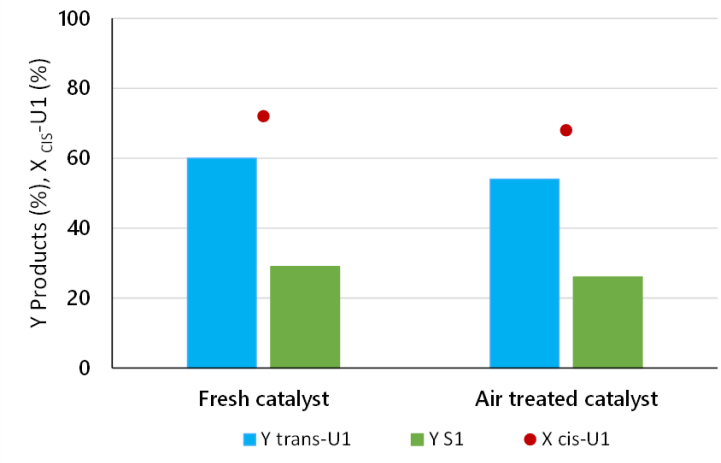

Figure 56. Conversion and yields of S1 and *trans*-U1 with 1% wtPd/Al_2O_3 for recyclability tests.Reaction conditions: batch reactor, T:90°C, P H_2=4 bar, stirring rate: 750, 30 minutes of reaction, 15 mL of solution 30 g/L, 0.5% wt of catalyst.

As Fig. 56 shows, after termal treatment the catalytic activity was restored, with similar values of conversion and yields as for the fresh catalyst

Table 22. Product distribution of the mixture after reaction described in Fig. 56

Fatty acid derivative	*% w/w fresh*	*% w/w treated*
Cis-U1	21 ± 2	24 ± 2
Trans-U1	45 ± 2	41 ± 2
S1	22 ± 2	20 ± 2
Poly-U	0	0
Others	13 ± 2	15 ± 2

TG analysis of the spent catalyst was carried out to confirm that heavy molecules were absorbed on the catalyst surface, responsible for the loss of 30%weight.

Two main highly exothermic desorption peaks could be observed (Fig. 57), evidenced by two black arrows: the first at 200°C and the second one at almost 370°C, showing the presence of organic compounds adsorbed on the catalyst.

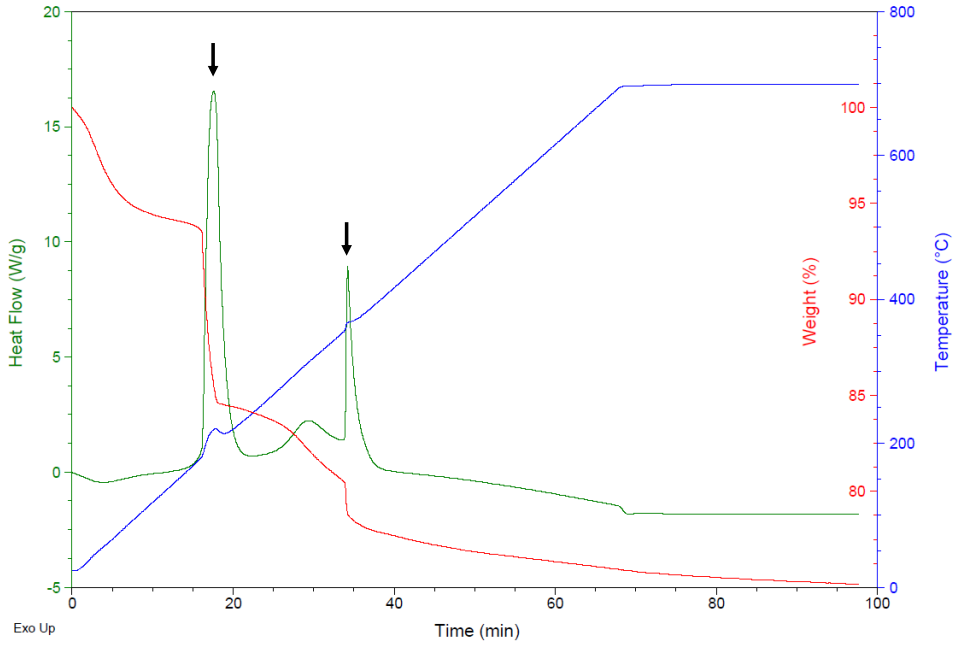

Figure 57. TG analysis of the spent catalyst Pd/Al_2O_3. On the secondary Y axis, the Temperature of the cycle is reported in blue, while the weight % in red. In proximity of two weight losses, an increase of temperature was registered ascribed to the exothermicity of the combustion.

Assuming that the compounds adsorbed were mainly unsaturated fatty acids derivatives (cis/trans-U1, poly-U or oligomers), an approximation of the amount absorbed during the

reaction was calculated, which correspond to 25% w/w, referred to the catalyst weight. This corresponds to the difference of Cis-U1 found after the 1st and 2nd cycle (Table 22).

In other words, during the second cycle, 25% of the unsaturated fatty acids derivatives could not react, because of the occupation of active sites; the compound was then released during the thermal treatment, with activity recovery.

Since no catalyst pre-reduction was carried out after the calcination treatment, we can state that the amount of hydrogen used for the reaction was enough to guarantee the in-situ reduction of the metal.

According to these results, we can state that deactivation was not caused by leaching of the active metal from the surface, but by fouling of the catalyst due to the adsorption of compounds, specifically those present in the starting material, impurities or heavier compounds, such as oligomers formed by reaction of the reactants[134,135].

5.4 Continuous-flow reaction

In order to have a more complete comparison between the two different catalytic systems, a second type of reactor configuration was used, performing the reaction in a continuous flow reactor, described in chapter 4.6.

The solution was diluted 5 times to lower the reactants concentration down to 6 g/L: this helped to prevent blockage in the line caused by an excessive concentration of the fatty acids derivatives and to avoid issues related to the alkalinity of the solution.

Each sample was collected after a defined time on stream, chosen based on the flow and the concentration (g/mL) of the solution. For example, after 30 minutes of reaction with a flow of 1.5mL/min, 45 mL of solution were collected which contained a certain amount of oleic derivative *cis*-U1 (considering zero the initial conversion and depending on the starting mixture employed -for example with 75wt%*cis*-U1).

5.4.1 Influence of the shape of the catalyst- powder and pellets

As described in chapter 5.4.1, pellets are usually preferred over powder when using a continuous flow system, due to the lower possibility of generating undesired overpressure phenomena.

Therefore, an initial comparison between catalyst powder and pellets was performed, employing two cartridges filled with powder or pellet (500 μm) of 1% Pd/C,as described in chapter 4.4.3, tested under standard reaction conditions: 90°C, 20 bar of H_2, flow: 1.5 mL/min, solution 6 g/L.

It must be underline that 20 bar of H_2 were selected because this was the lower stable pressure obtainable with the H-Cube MiniPlus®.

After collecting the outlet stream for 30 minutes, 45 ml of acidic solution was added to allow the fatty acids precipitations. The white solid obtained was filtered and after proper drying in oven, it was submitted to the standard derivatization procedure.

The results are compared in Figure 58, confirming that also in the flow system pellets were not suitable to achieve a reasonable conversion for this type of reaction.

In fact, complete conversion of the starting material was shown with the powder catalyst, whereas 9% conversion only was reached with pellets, no formation of the product and only small amount of the Elaidic derivative *trans*-U1.

From the chart showing the composition, it is shown that also the linoleic derivative, poly-U, which usually is the first compounds submitted to hydrogenation, still was present in the final reaction mixture.

Again, important diffusional limitations were likely for the catalyst shaped in pellets; powder was therefore chosen also for the continuous flow reactor.

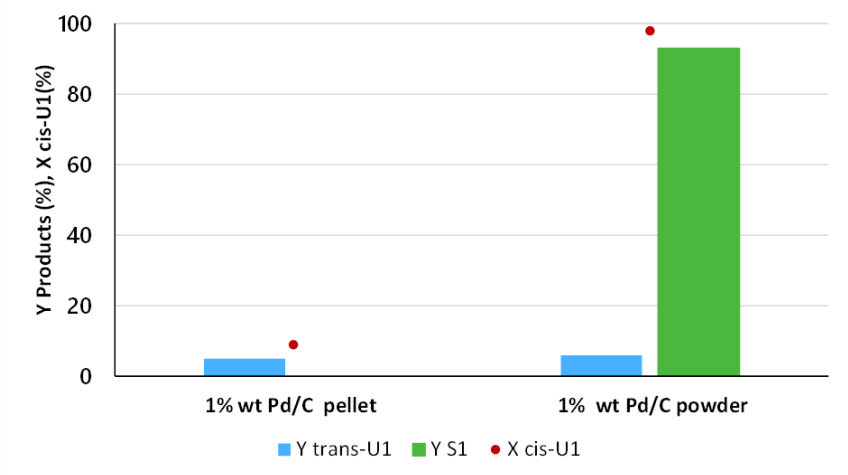

Figure 58. Conversion and yields of S1 and *trans*-U1 with 1% wt Pd/C powder and pellets. Reaction conditions: H-Cube Mini Plus continuous flow reactor, T:90°C, P H_2=20 bar, flow: 1.5 mL/min, τ=0.2 min, solution 6 g/L

Table 23. Product distribution of the mixture after reaction described in Fig. 58

Fatty acid derivative	*% w/w pellet*	*% w/w powder*
Cis-U1	68 ± 2	2 ±1
Trans-U1	8±1	10 ±2
S1	3 ±1	78 ±2
Poly-U	4 ±1	0
Others	10 ±2	10 ±1

5.4.2 Influence of the metal type

As for batch-wise tests, a screening with different carbon-supported metal catalysts was performed, comparing 5% wt Pd/C, 5% wt Ru/C, 5% wt Pt/C, 5% wt Rh/C and Ni-Raney.

A catalyst with Rh as the active component was also tested: despite its high price (it is one of the most expensive metals), it could be interesting to explore its behaviour for the catalytic hydrogenation of unsaturated fatty acids.

The conditions were set as described in chapter 4.6 and the sample was collected for 30 min reaction time.

As can be seen from figure 59, results followed the same trend as for the batch experiments: still Pdwas the most active metal, ensuring full conversion and high selectivity tothe saturated compound S1.

5% wtPt/C resulted to be the least active, with conversion of 21% only and still the presence of poly-U, as can be seen from Table 24.

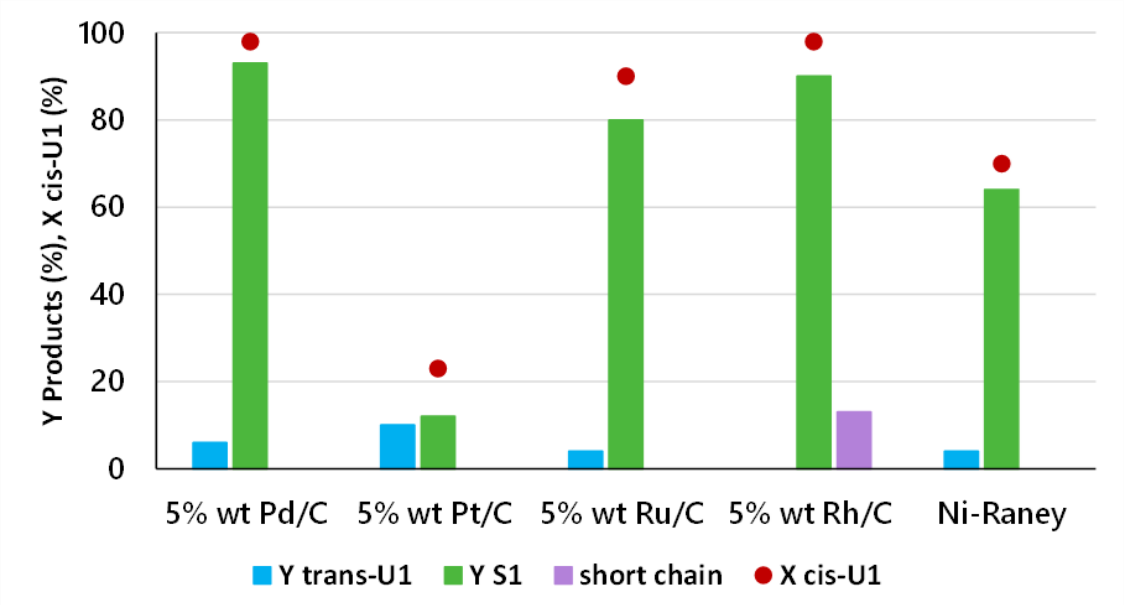

Figure 59. Conversion and yields of S1 and *trans*-U1 with 5% wt Pd/C, 5% wt Pt/C ,5% wt Ru/C, 5% wt Rh/C and Ni-Raney. Reaction conditions: H-Cube Mini Plus continuous flow reactor, T:90°C, P H_2=20 bar, flow: 1.5 mL/min, τ=0.2 min, solution 6 g/L

Also Ni-Raney, which is a catalyst that typically had been widely used for hydrogenation reactions, was not as active as the metal-supported catalysts, showing 70% conversion and 63%yield toS1.

Table 24. Product distribution of the mixture after reaction described in Fig. 59

Fatty acid derivative	*Pd/C 5% wt*	*Pt/C 5% wt*	*Ru/C 5% wt*	*Rh/C 5% wt*	*Ni-Raney*
Cis-U1	1 ± 1	57± 1	7±1	1±1	25±2
Trans-U1	10± 2	5± 2	5±1	0	7±1
S1	78± 2	12± 2	74±1	77±1	50±1
Poly-U	0	7± 1	0	0	0
Others	10±1	13±1	10±1	10±1	10±1
Short chain *	--	--	--	15±2	--

Better results were achieved with Ru and Rh. However, Rh catalysed the formation of short chain molecules, detected by GC-MS analysis, such as pelargonic acid, undecenoic acid, suberic acid, octanoic acid and lauric acid; they were not present as major by-products, but the sum of their overall content summed up to the 15wt %. This may be due to either the higher intrinsic activity of the catalyst for hydrogenolysis, or to the higher dispersion of the metal nanoparticles, which made it very active for all reactions, including the isomerization and subsequent cleavage of the double bond.

Finally, Ruthenium showed good activity for the cis-U1 conversion, showing results similar to Palladium, but the reaction led to favour the formation of the trans- isomer rather than S1. This highlights the similarity between the two metals.

The screening of the catalysts allowed us to conclude that still Pd was the most performing metal, but interestingly Ru revealed an improved performances compared to what shown in chapter 5.4.5.

5.4.3 Influence of the metal loading and support

5% wt Pd/C, 1% wt Pd/C and 0.3% wt Pd/C catalysts were tested to evaluate the possibility to decrease the amount of the noble metal.

Fig. 60 shows that, as already demonstrated for the batch reactions, a decrease in the metal content of the metal did not cause a similar decrease of activity.

In fact, 0.3% wt Pd/C showed the best catalytic performance despite the lowest amount of metal, leading not only to complete conversion of *cis*-U1 but also the highest formation of S1 rather than*trans*-U1.

In fact, with higher metal loading (5% wt and 1% wt), despite the same conversion of cis-U1 and poly-U, a higher concentration of the intermediate was shown, hence a lower S1 selectivity.

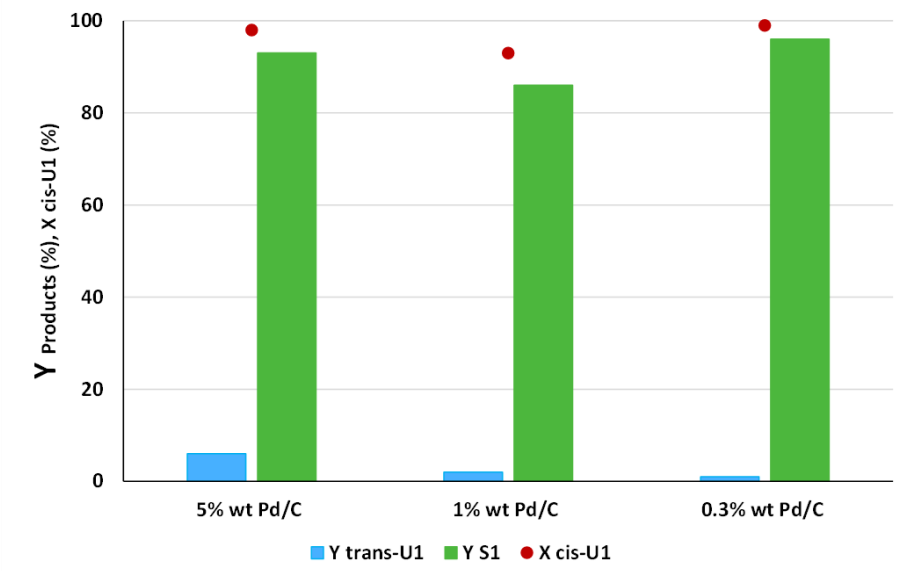

Figure 60. Conversion and yields of S1 and trans-U with 5% wt Pd/C, 1% wt Pd/C and 0.3% wt Pd/C. Reaction conditions: H-Cube Mini Plus continuous flow reactor, T:90°C, P H_2=20 bar, flow: 1.5 mL/min, τ=0.2 min, solution 6 g/L

Table 25. Product distribution of the mixture after reaction described in Fig. 60

Fatty acid derivative	*% w/w 5% wt*	*%w/w 1% wt*	*%w/w 0.3% wt*
Cis-U1	2± 1	7± 1	0± 1
Trans-U1	10± 2	5± 1	5± 1
S1	78± 2	71± 1	80±2
Poly-U	0±1	0± 1	0± 1
Others	12± 1	14± 1	13± 1

Al_2O_3 was evaluated as an alternative support, in a 1% wt Pd/ Al_2O_3 catalyst.

Results (Fig.61) show that the Al_2O_3 catalyst led to good conversion of the starting material, but not comparable to the results provided by the carbon supported catalyst.

In fact, after 30 min reaction at 1.5 mL/min, 60% conversion only was obtained, compared to the 92% of Pd/C.

Moreover, comparing the rate of *trans*-U1 conversion to S1, we can estimate the amount of intermediate if conversion with 1% wt Pd/Al_2O_3 was 92% (as much as with the 1% wt Pd/C catalyst). Considering the rate of conversion of cis-U1 and the rate of consumption of *trans*-U1to be linear over time, the amount of the latter should be equal to 17% w/w and the amount of S1 to 75% w/w (calculated with the proportion based on the data obtained).

This meant that with Al_2O_3, not only the rate of *cis*-U1 conversion but also the step from the unsaturated to the final product were slowed down, the step *cis*-U1 to-*trans*-U1being favoured over the *cis*/*trans*-U1-to-S1 step.

On the contrary, for the C-based catalyst, an immediate formation of the saturated molecule was observed, with a faster rate for the hydrogenation step.

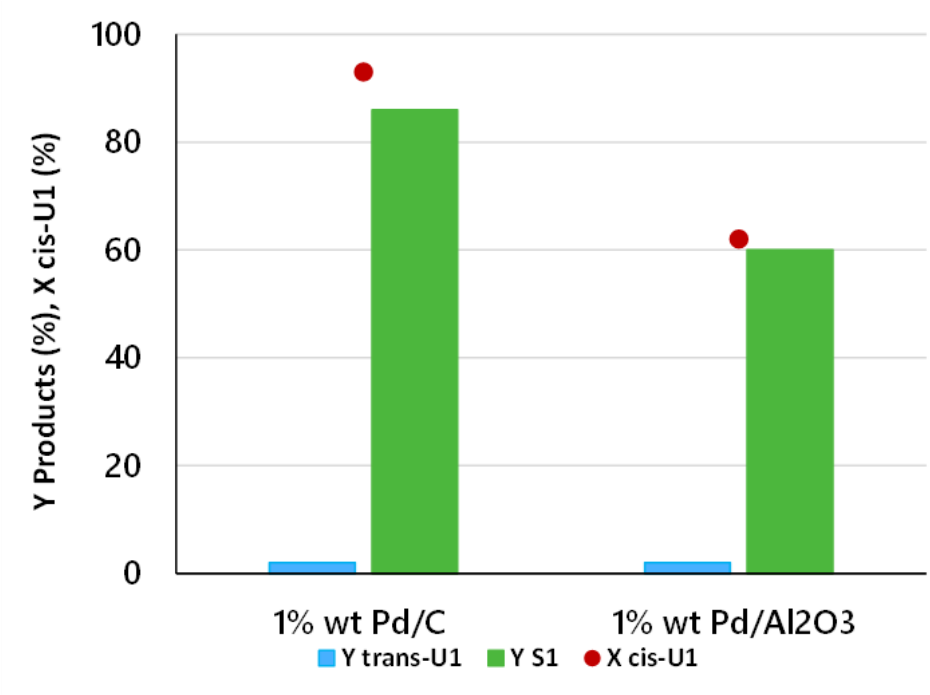

Figure 61. Conversion and yields of S1 and *trans*-U1 with Pd/C 1% wt, Pd/Al_2O_3 1%wt. Reaction conditions: H-Cube Mini Plus continuous flow reactor, T:90°C, P H_2=20 bar, flow: 1.5 mL/min, τ=0.2 min, solution 6 g/L

Table 26. Product distribution of the mixture after reaction described in Fig. 61

Fatty acid derivative	**% w/w Pd/C 1% wt**	**%w/w Pd/ Al_2O_3 1% wt**
Cis-U1	7 ±1	24 ±1
Trans-U1	8 ±1	11 ±1
S1	71 ±2	47 ±1
Poly-U	0 ±1	0±1
Others	15 ±1	13±1

5.4.4 Deactivation – initial tests

Deactivation was evaluated by carrying out the reaction for longer time (3-5 hours), collecting the outlet stream of the reaction every 30 minutes, and proceeding with the analysis.

Deactivation tests were initially performed with the standard solution containing 75% wt of monounsaturated oleic derivative (*cis*-U1) and 7% of linoleic derivative, using the0.3% wt Pd/C.

The contact time (τ) was 0.2 min with a flow of 1.5 mL/min; the post-reaction solution was collected every 30 minutes, precipitated, derivatized with BF_3 and quantified via GC analysis.

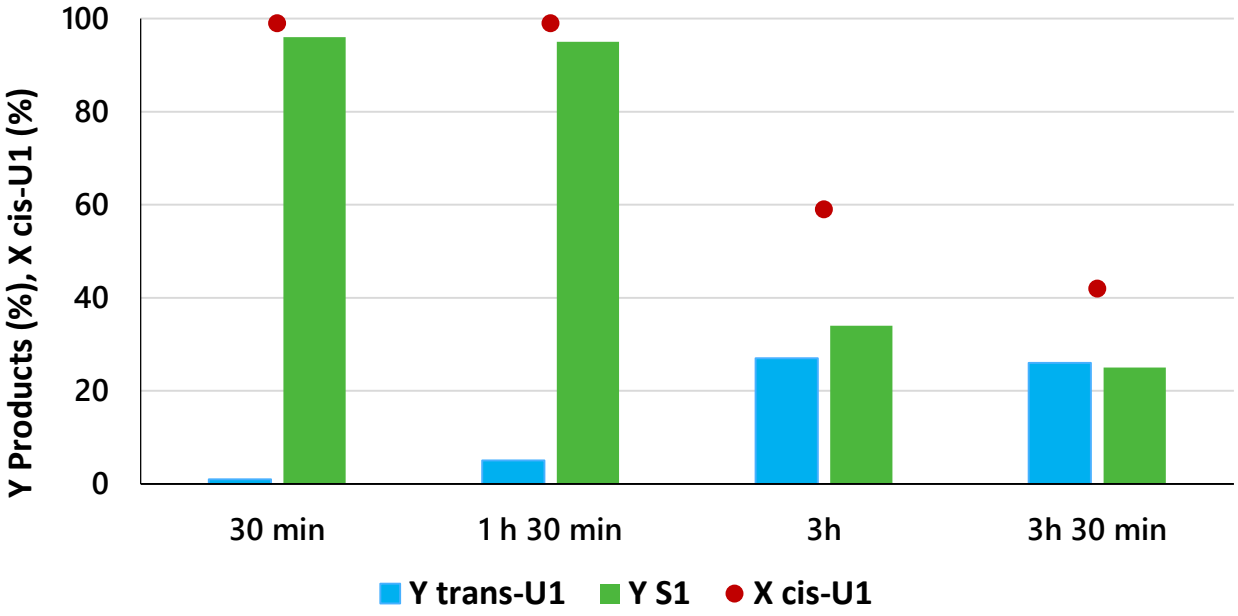

Figure 62. Conversion and yields of S1 and *trans*-U1 with 0.3% wt Pd/C for testing the deactivation in flow system. Reaction conditions: H-Cube Mini Plus continuous flow reactor, T:90°C, P H_2=20 bar, flow: 1.5 mL/min, τ=0.2 min, solution 6 g/L

From the Fig. 62it can be noticed that catalyst deactivation started to be more relevant between 1h 30 minutes and 3 hours: at 1h 30 minutes the formation of major amounts of the *trans*-isomer suggested a deactivation for the *cis/trans-U1* →*S1*step with accumulation of the *trans* isomer, while complete consumption of the starting material was still guaranteed. Visible effect of deactivation was evidenced at 3 hours of reaction time: conversion started to decrease from almost 100% down to 60%, accompanied by a decline in selectivity of S1.

Even more, after 3h 30 minutes, a further slowdown of the hydrogenation rate was observed, causing the formation of a higher amount of*trans*-U1 and less S1.

Each post reaction sample was analysed by means of ICP-AES to check if metal leaching occurred but any signals of Pd were detected from the spectra, excluding Pd leaching as the cause of deactivation.

Absorption of molecules like reagents or oligomers formed by side-reactions were believed to be the reason for deactivation, therefore further tests were executed to study the effect of reaction parameters on deactivation.

Table 27. Product distribution of the mixture after reaction described in Fig. 62

Fatty acid derivatived	***% w/w 30 min***	***%w/w 1h 30***	***%w/w 3h***	***%w/w 3h 30***
Cis-U1	0± 1	1± 1	30± 1	44± 2
Trans-U1	5± 1	3± 1	21± 1	29± 2
S1	80±2	79± 1	20±2	16± 2
Poly-U	0± 1	0± 1	2± 1	3± 1
Others	13± 1	14± 1	15± 1	12± 1

5.4.4.1 Influence of H_2 pressure

We assumed that deactivation was caused by adsorption of molecules on the surface of the catalyst, such as be either reagents or oligomers formed between two fatty acids derivatives. Tests with 40 bar of hydrogen were then performed: if the previous hypothesis were correct, by increasing H_2 pressure the oligomerization process should be discouraged, because the double bond should be more prone to react with hydrogen rather than begin oligomerization reactions, leading to a decrease in deactivation and improvement of catalyst's life.
Observing the graph in figure 63 it is possible to notice that a shift to higher hydrogen pressure led to an improvement of catalyst's longevity: the*cis*-U1 conversion did not suffer from a rapid decline after 1h 30 minutes of reaction, but only a slight amount of the -*trans* isomer was formed. Activity was still high after 2h 30 minutes and 3 hours, reaching 90% and 83% of conversion respectively, whereas after 4 hours the deactivation began to be more relevant with a decline in conversion down to ≅ 60% and ≅40%. Selectively to S1 changed accordingly to conversion decrease.

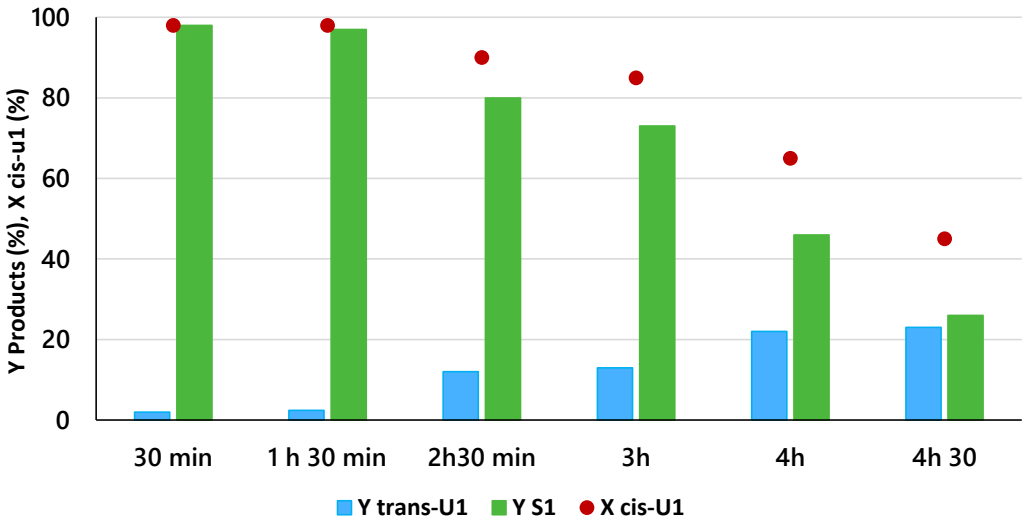

Figure 63. Conversion and yields of S1 and *trans*-U1 with Pd/C 0.3% wt for testing the deactivation in flow system after 4.30 hours of reaction increasing H_2 pressure. Reaction conditions: H-Cube Mini Plus continuous flow reactor, T:90°C, P H_2=40 bar, flow: 1.5 mL/min, τ=0.2 min, solution 6 g/L.

For a better comparison of deactivation, the conversion at 20 and 40 bars were plotted in the same graph (Fig. 64): it is evident how the conversion decreased less rapidly at 40 bar hydrogen pressure (full line)than at 20 bar (dotted line).

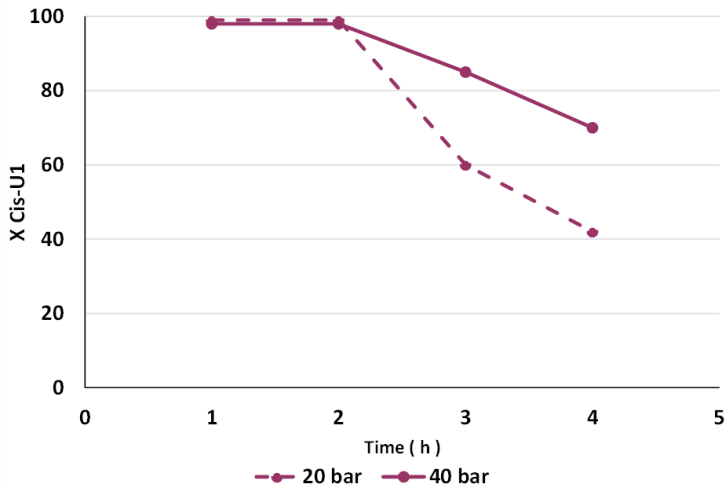

Figure 64. Comparison of conversion trend for the reaction of Fig. 62 and Fig. 63 changing the pressure of H_2. The full line represents the system with higher pressure which shows slower deactivation while dotted line represents the system at lower pressure.

The graph in Fig. 65reports the products distribution as a function of time at 20 bar H_2 (dotted line) and at 40 bar hydrogen pressure (full line).

The difference in the behaviour was evident observing the decline in S1 % after 2 h 30 minutes at 20 bar, while at 40 bar the decrease of yield occurred more smoothly.

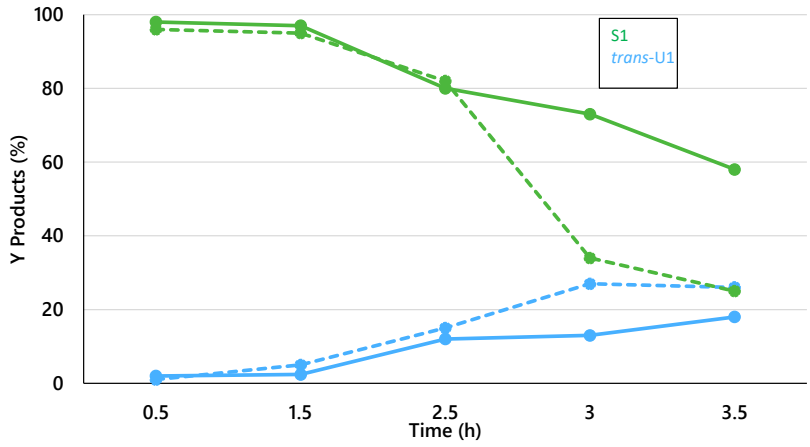

Figure 65. Comparison of Yields trend for the reaction of Fig. 62 and Fig. 63 changing the pressure of H_2.

The **full line** represent the system with higher hydrogen pressure (**40 bar**) which shows slower decrease in S1 yields, while **dotted line** represents the system at lower hydrogen pressure (**20 bar**) which had faster decrease in S1 yield.

Table 28. Product distribution of the mixture after reaction described in Fig. 63

Fatty acid derivative	*% w/w 30 min*	*%w/w 1h 30*	*%w/w 2h30*	*%w/w 3 h*	*%w/w 4 h*	*%w/w 4h30*
Cis-U1	0± 1	1± 1	8± 1	11± 1	26± 2	41± 2
Trans-U1	5± 1	3± 1	18± 1	10± 1	16± 2	17± 2
S1	80±2	79± 1	66±2	58± 1	34± 2	20± 1
Poly-U	0± 1	0± 1	2± 1	1± 1	1± 1	2 ± 1
Others	13± 1	14± 1	10± 1	13± 1	16± 1	12 ± 1

However, deactivation was impossible to avoid: the S1amountobtained after 3 hours at 20 bar (38%) was shown after 4 hours if using 40 bar; Pd leaching was, again, excluded after ICP-AES analysis.

However, working with higher hydrogen pressure allowed understanding that deactivation was originated by two concomitant causes:

- Formation of oligomers as by-products.
- Adsorption of reagents/ impurities present in the starting material.

For the first point, an increase in hydrogen pressure diminished the side-reaction rate, contributing to an increase in catalyst lifetime. However, the contribution of adsorption by the solution was not tuneable by increasing H_2 pressure leading, together with a probable lower but non-null oligomerization phenomena, to deactivation of the catalyst.

5.4.4.2 Influence of contact time

The contact time τ is a crucial parameter for flow-reactions: the higher the value of τ, the longer is the residence of the starting material onto the catalyst. On the other hand, reducing the τ lead to a decrease of the residence time of the reactants on the catalyst's surface, with consequent possible decrease of conversion and unwanted consecutive reactions.

Therefore, this parameter was lowered and evaluated with the aim to counteract the deactivation phenomena previously observed.

As described before, τ was calculated considering the volume of the catalyst and the volumetric flow of the solution. In order to obtain a lower contact time, it is possible to either decrease the volume of the catalyst or increase the flow rate.

To keep the behaviour of the solution flowing inside the cartridge constant, the first option was excluded, to avoid the formation of unpredicted preferential paths within the cartridge. Therefore, the flow of the starting material was increased to a value equal to 2.5 ml/min ensuring a τ = 0.1 min (against 0.2 min when using 1.5 ml/min); the reaction was run for 3 hours.

For a reliable comparison between the two reactions carried out at different τ values, results obtained at the same number of starting material moles processed should be considered.

The moles processed after 3 hours with a flow of 1.5 mL/min correspond to the moles processed after 1 h and 50 minutes with the flow of 2.5 mL/min.

Figure 66 reports*cis*-U1 conversion as function of time: full blue line for experiments carried out at low contact time τ (flow: 2.5 mL/min), dotted yellow line for those at higher contact time (flow: 1.5 mL/min).

Red vertical lines indicate the conversion achieved for an equal amount of moles processed, and the two points marked with a star are the points comparable.

It is possible to notice that the two reactions showed the same trend of conversion over time, with clear signs of deactivation.

If we now compare the conversion shown at the same value of moles processed (the two points marked with the red star), it is evident that for the higher contact time (yellow dotted line) the conversion was much lower (60%) compared to that one shown at lower contact time (light-blue full line), which is equal to 82%.

This means that possible slower consecutive reactions, such as oligomerization, were disadvantaged.

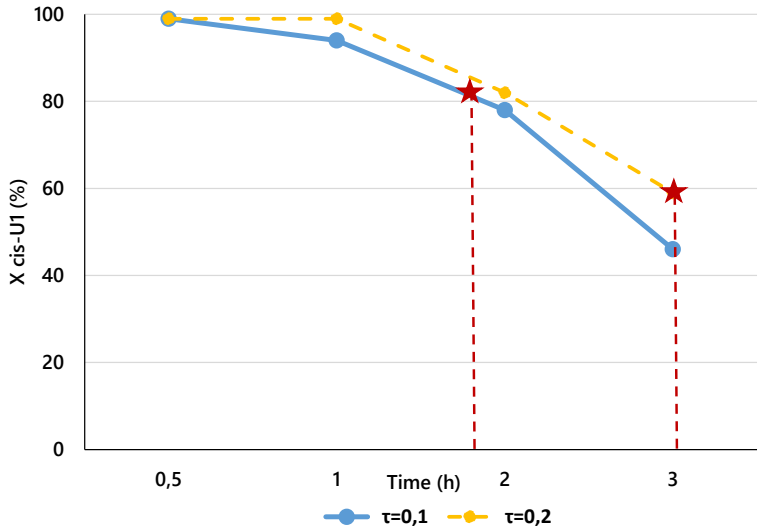

Figure 66. Comparison of conversion for the reaction carried out at different contact time. The full line represents the reaction with higher flow rate, hence low contact time (0.1 min), while dotted line represents the situation at lower flow rate and higher contact time (0.2 min). The stars represent the point of comparison between the two systems, corresponding to the same amount of moles processed.

Moreover, the products distribution followed the same trend in function of time (S1 in green and *trans*-U1 in light-blue).

Again, yields achieved after 3 hours at low flow rate must be compared with yields shown at less than2 hours for high flow rate; still the amount of S1 was higher in this latter case.

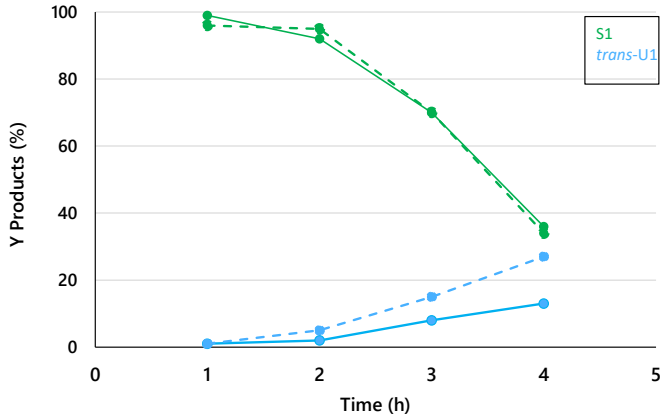

Figure 67. Comparison of Yields for the reaction carried outat different contact time. The full line represents the case with higher flow rate and lower contact time (0.1 min), while dotted line represents the case at lower flow rate and higher contact time (0.2 min). The trend of yields is similar in the two cases, however, comparing the moles processed, the higher the contact time, the faster the decrease of S1 yield.

With this test it was possible to evince that an increase of flow rate did not worsen the starting material conversion but allowed to obtain a more stable system over time. This meant that the *cis*-U1 conversion occurred faster than possible oligomerisation reactions, which instead required longer residence time on the catalyst to occur. The number of absorptions of impurities present in the reaction mixture, as well as the number of absorptions of poly-unsaturated compounds, was reduced thank to higher flow rate, but poisoning of the catalyst was unavoidable, causing, even if less remarkable, decrease in catalyst's performances.

Table 29. Products distribution of the mixture after reaction described in Fig. 66

Fatty acid derivative	***% w/w 30 min***	***% w/w 1h 30***	***% w/w 3 h***
Cis-U1	0 ± 1	5 ± 1	40± 2
Trans-U1	6 ± 1	7± 1	17± 1
S1	82 ± 2	73 ± 2	28± 1
Poly-U	0 ± 1	0± 1	0± 1
Others	12 ± 1	15± 1	10± 1

5.4.4.3 Influence of the solution composition

Considering that the deactivation of the catalyst may in part be attributable to the adsorption of molecules (reactants and impurities) on the catalyst surface, a study on the nature of the interaction between reactants and active sites could be useful to better understand the deactivation phenomena.

Four solutions, A, B, C, D, which differ in the concentration of impurities, were tested with the 0.3 % wt Pd/C catalyst and compared with the "*reference*" solution named F13516_10.

After proper characterization, a difference in the mixture composition was revealed, especially for the linoleate derivatives Poly U, as shown in table 30.

Table 30. Concentration (g/L)of fatty acids derivatives, composition (expressed as % w/w) and impurities concentration (mg/L) for standard solution F13516_10, and for solutions A, B, C and D used to study the influence of mixture composition on deactivation.

Sol.	*Conc. (g/L)*	*Cis-U1 (%)*	*Poly-U (%)*	*Others(%)*	*Impurities (mg/L)*
F13516_10	30	79 ± 2	4 ± 1	17 ± 2	0.48
A	19	88 ± 2	<1 ± 1	10± 1	0.2
B	25.2	82 ± 2	10± 1	10± 1	1.76
C	24.1	92 ± 2	2± 1	7± 1	4.4
D	25.8	79± 2	10± 1	10± 1	1.4

Before starting the reaction in the continuous flow system, each solution was diluted as described before. However, due to differences in fatty acids derivatives concentration (see column Conc. (g/L)) and composition, the dilution factor was different for each solution in order to have a constant concentration of unsaturated fatty acid derivatives (Oleic and Linoleic derivatives), equal to 16.5 mM.

Therefore, solution A was diluted 3.3 times; solution B 4.6 time; solution C 5 times and finally solution D was diluted 4.9 times. However, the Cis-U1/Poly-U ratio was unaffected.

Results were also compared with a reference solution (F13516_10) almost equal to the solution typically used for tests discussed so far, named *"Standard solution"*: the two solutions differed for small amount in Cis-U1, which did not cause relevant differences in catalytic tests, as shown in figure 68.

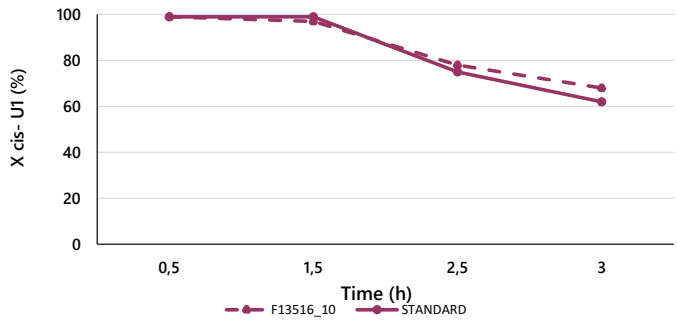

Figure 68. Conversion in function of time for the reaction carried out using the new F13516_10 solution and the standard solution. These results evidenced the reproducibility of the data for the two similar solutions.

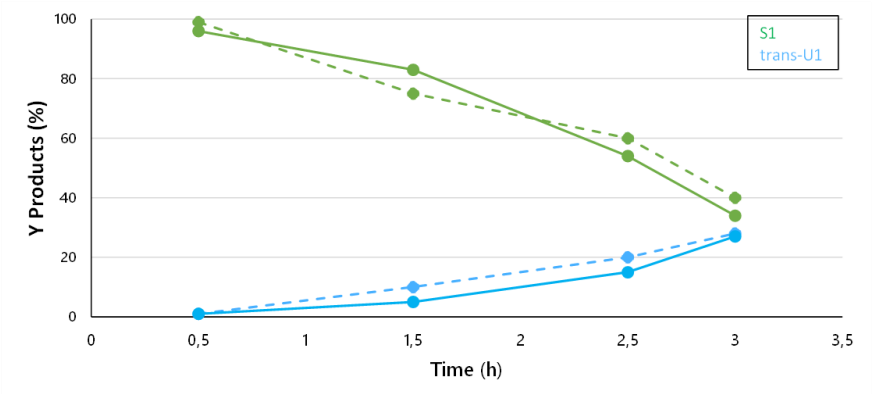

Figure 69. Comparison between yields of S1 and trans-U1 over time using the standard solution (full line) and the reference solution F13516_10 (dotted line)

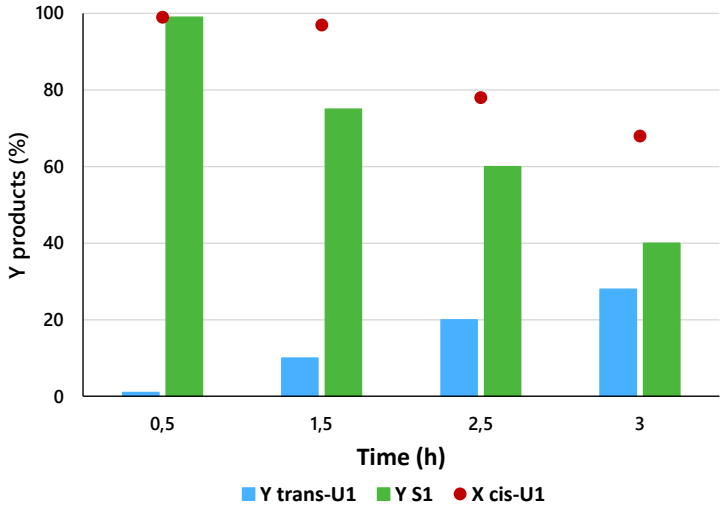

Figure 70. Conversion and yields toS1and trans-U1 with the 0.3% wt Pd/C catalyst, for testing the deactivation with the solution F13516_10. Reaction conditions: H-Cube Mini Plus continuous flow reactor, T:90°C, P H2=20 bar, flow: 1.5 mL/min, τ=0.2 min, solution 6 g/L.

5.4.4.3.1 Solution "A"

The first solution tested was the so-called "A", which had the lowest amount of linoleic derivatives concentration and impurities at all, with a decrease of the latter equal to 2.4 times compared to the reference F13516_10 solution.

From Figure 71 it was evident how the catalyst 0.3% wt Pd/C showed astable performance for3 hours, without any deactivation sign, maintaining complete conversion and constant full selectivity toS1 for 3 hours of reaction time. Only slight traces of *trans*-U1 were detected.

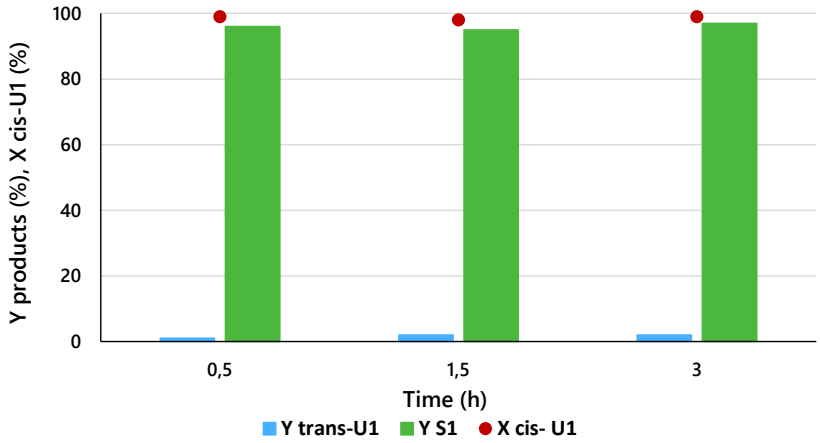

Figure 71. Conversion and yields of S1 trans-U1 with 0.3% wt Pd/C for testing the deactivation with solution A (composition described in Table 30). Reaction conditions: H-Cube Mini Plus continuous flow reactor, T:90°C, P H_2=20 bar, flow: 1.5 mL/min, τ=0.1 min, solution 6 g/L.

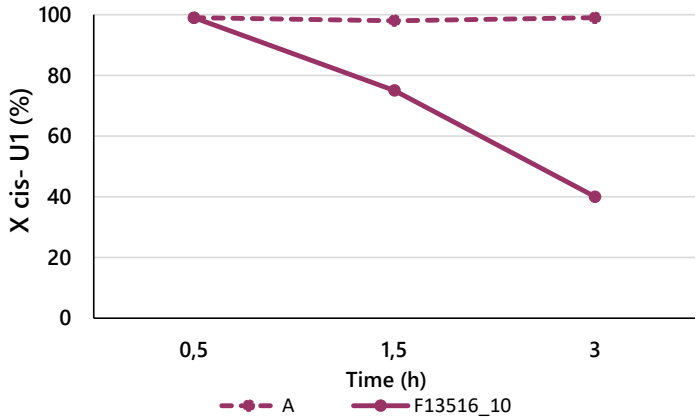

Figure 72. Conversion in function of time for the reaction using the reference solution F13516_0 and the solution A (composition present in Table 30) with the catalyst 0.3% wt Pd/C.

Solution "A" presented low concentration ofboth linoleic derivative and impurities; therefore, it was not possible to attribute the deactivation to any of the two classes of compounds.

5.4.4.3.2 Solutions "B" and "D"

The solutions "B" and "D" presented a greater content of linoleic derivatives (Poly-U = 10% wt, from Table 30) and impurities compared to the reference solution.

Both of them showed a remarkable deactivation: conversion decreased very rapidly compared to solution "A" and the reference solution F13516_10. The similar behaviour of"B" and "D" solutions was evident from their catalytic behaviour, which resulted to differ fora few points only, witha slightly higher deactivation rate for solution "B" than "D".

However, considering the overall trend and the error associated to the measures, the deactivation on the catalyst, with the two aformentioned solutions, can be considered equal, with major negative effect on catalyst's longevity compared to solution "A" and the reference, as evidenced in Fig. 73.

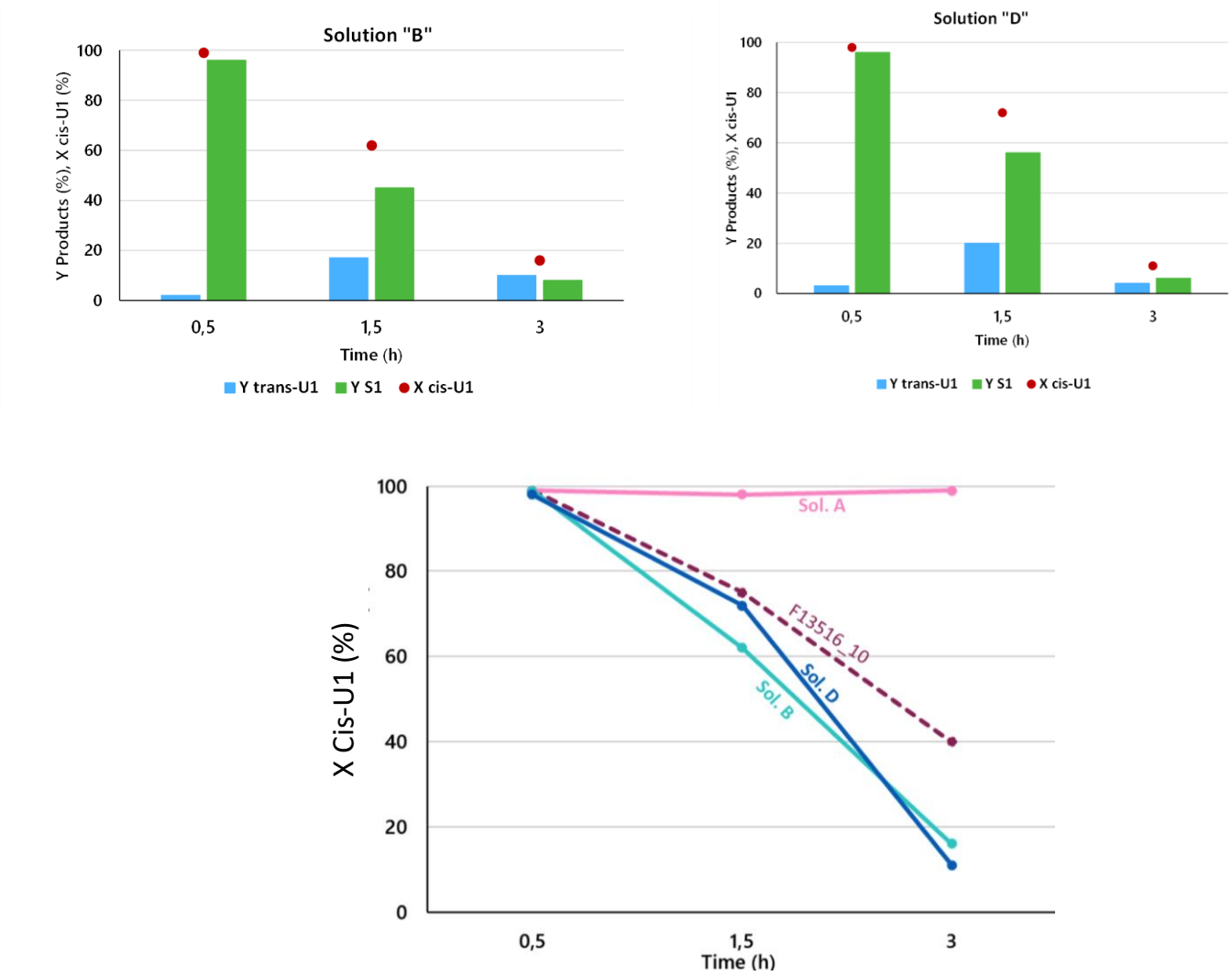

Figure 73. Top: Conversion and yields of S1 and *trans*-U1 with the 0.3% wt Pd/C catalyst, for testing the deactivation with solution "B" (left) and "D" (right). Reaction conditions: H-Cube Mini Plus continuous flow reactor, T:90°C, P H_2=20 bar, flow: 1.5 mL/min, τ=0.2 min. The composition of the solutions B and D were similar (for more details consult Table 30) and this similarity did correspond to a similar catalyst performance.

Bottom: comparison of the Conversion in function of time for solution "A" (pink), F13516_10 (purple), solution "D" (blue) and solution "B" (light blue) over time using 0.3% wt Pd/C.

5.4.4.3.3 Solution "C"

Lastly, solution "C", with a concentration of linoleic derivatives similar to solution "A"butthe highest amount of impurities, was tested and results after 3 hours of reaction are reported in figure 74.

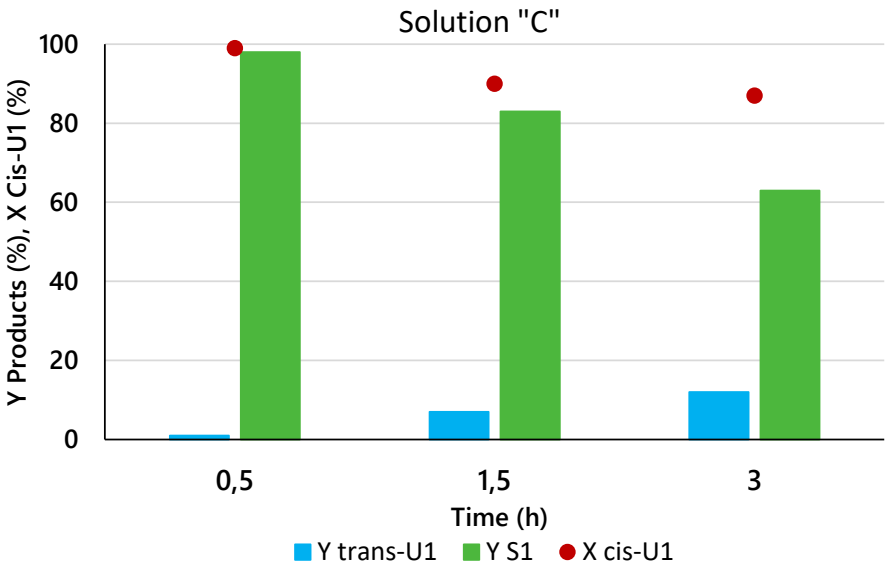

Figure 74. Conversion and yields of S1 and *trans*-U1 with 0.3% wt Pd/C for testing the deactivation with solution C (exact composition is reported in Table 30). Reaction conditions: H-Cube Mini Plus continuous flow reactor, T:90°C, P H_2=20 bar, flow: 1.5 mL/min, τ=0.2 min.

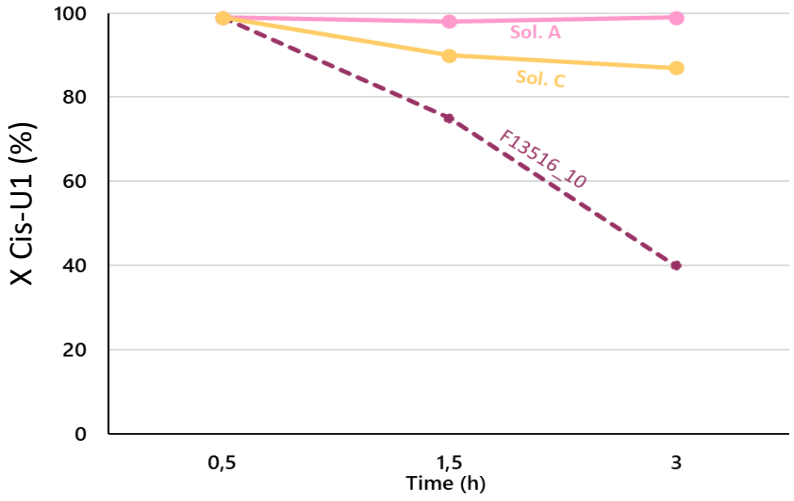

Figure 75 Comparison of *Cis*-U1 conversion using 0.3% wt Pd/C with solutions"A","C" and the reference solution F13516_10.

In terms of deactivation rate, with solution "C" it was located between the F13516_10 reference and solution "A", which was the only one showing negligible deactivation. Solution "C" presented a composition poor in linoleic acid derivative (Poly-U= 2% wt) but with the highest amount of impurities (≅ 4 mg/L).

By plotting the conversion in function of time for the different solutions (F13516_10 ,"A", "B", "C", "D"- Figure 76) it is possible to notice that the decrease of *Cis*-U1 conversion was not so correlated to the concentration of impurities in the solution but rather to the linoleic acid derivative (Poly-U) content in the mixture. In fact, deactivation occurred more rapidly in samples where Poly-U concentration was higher ("B","D"); on the other hand, decreasing the content of the di-unsaturated derivative, the catalyst maintained its activity for 3 hours (solution "A") or deactivated more slowly (solution "C").

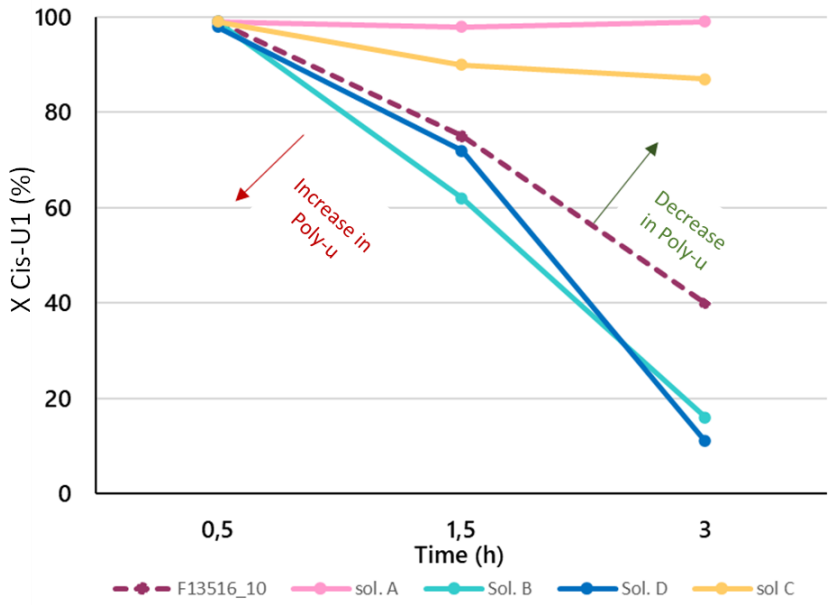

Figure 76. Comparison of conversion in function of time with the solutions having different composition, as listed in Table 30.

As can be noticed, by increasing the amount of linoleic derivative (Poly-U) in the feeding solution the conversion decreased more rapidly, while for solutions poorer in Poly-U (solution "A" and "C") the activity of the catalyst resulted to be more stable and a smaller deactivation was detected.

To resume:

- The concentration of impurities decreased in order: “C”>“B”, “D”>F13516_10 >“A”;
- Linoleic derivatives % decreased in order: “B”, “D”>F13516_10 >“C”>“A” .
- Deactivation rate occurred in order: “B”, “D”>F13516_10 >“C”> “A”;

Based on these results, it is possible to conclude that deactivation was not to be attributed to the impurities but rather to the amount of linoleic acid derivative present in the starting material, due to its propensity to bind onto the catalyst’s active sites, and eventually promoting oligomerization reactions.

5.4.4.3.3. Solution with high amount of Impurities

Further experiments were then performed in order to evaluate the effect of both compounds on deactivation rate.

Three solutions were tested: one was mainly composed of linoleic acid derivatives, with a very low content of impurities, the other two were poorer in linoleic acid derivative but with higher concentration of Impurities, up to14 and 9 mg/L.

Table 31. Composition of the solutions tested to investigate the influence on deactivation rate.

Sol.	*Cis-U1 (%)*	*Poly-U (%)*	*Others(%)*	*Impurities (mg/L)*
F13516_10	79 ± 2	4 ± 1	17 ± 2	0.48
S0_6	86± 2	6± 1	9± 1	13.6
S5_1+2	84± 2	10± 1	9± 1	8.5

Solutions S0_6 and S5_1+2 were first diluted as described before in order to obtain the concentration of unsaturated fatty acids derivatives equal as for tests previously done.

With these tests we could understand how relevant differences in impurities concentration could interfere on catalytic activity; in fact, the "S0_6" solution had a concentration of impurities 28 times higher than the reference F13516_10, while the "S5_1+2" 18 times greater.

Because of technical problems for the H-Cube Mini Plus®, the reaction using the solution "S0_6" could be run for 1hour and 30 minutes only.

However, it is possible to compare this result with the results at 1.5h for the reference solution and the S5_1+2.

Figure 77 and 78 report conversion of *cis*-U1and Yield towards trans-U1 and S1 for the two different solutions.

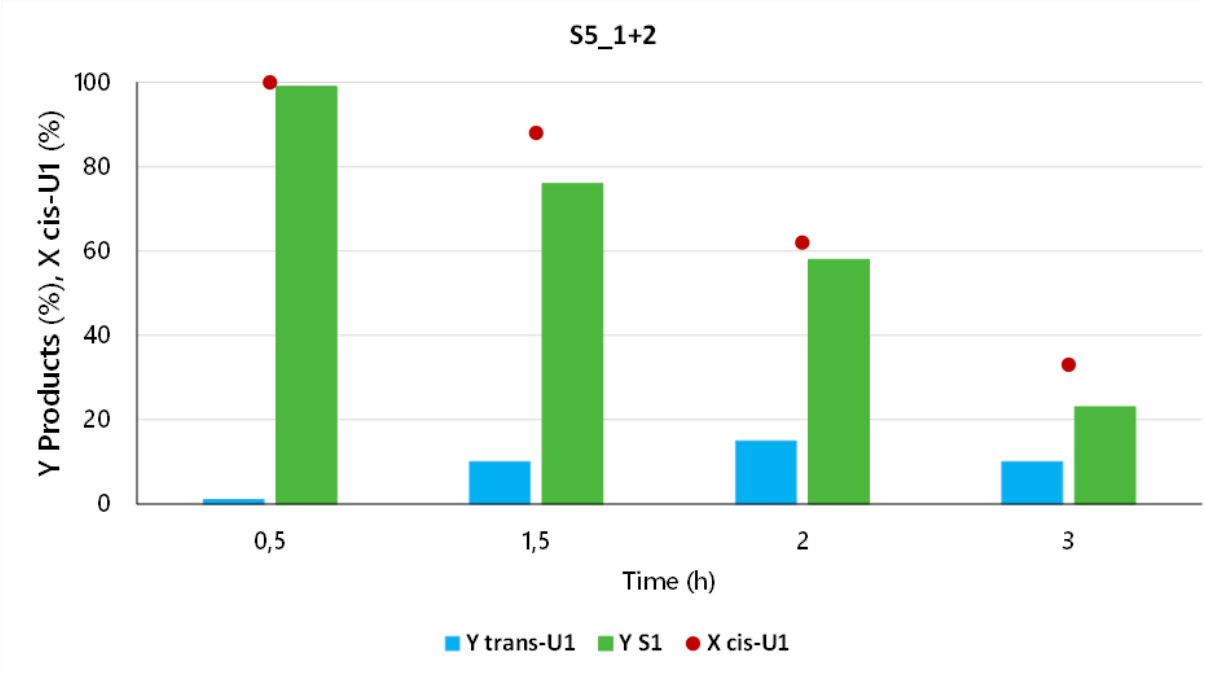

Figure 77. Conversion of cis-U1 and Yields to S1 and*trans*-U1shown by feeding the solution S5_1+2 (composition listed in table31) with 0.3% wt Pd/C. Reaction conditions: H-Cube Mini Plus continuous flow reactor, T:90°C, P H_2=20 bar, flow: 1.5 mL/min, τ=0.2 min.

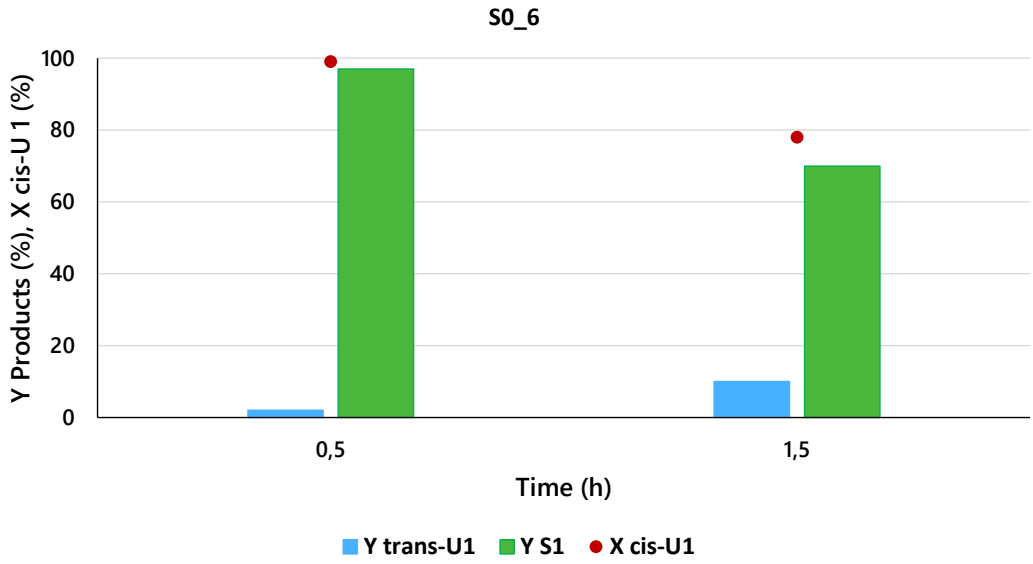

Figure 78 Conversion of cis-U1 and Yields to S1 and *trans*-U1 shown by feeding the solution S0_6 (composition listed in table 31)with 0.3% wt Pd/C. Reaction conditions: H-Cube Mini Plus continuous flow reactor, T:90°C, P H_2=20 bar, flow: 1.5 mL/min, τ=0.2 min.

Comapring the conversion over time (Fig. 79), it can be assumed that there is no a relevant difference on the deactivationeffect among the three solutions, despite the unequal amount of impurities.

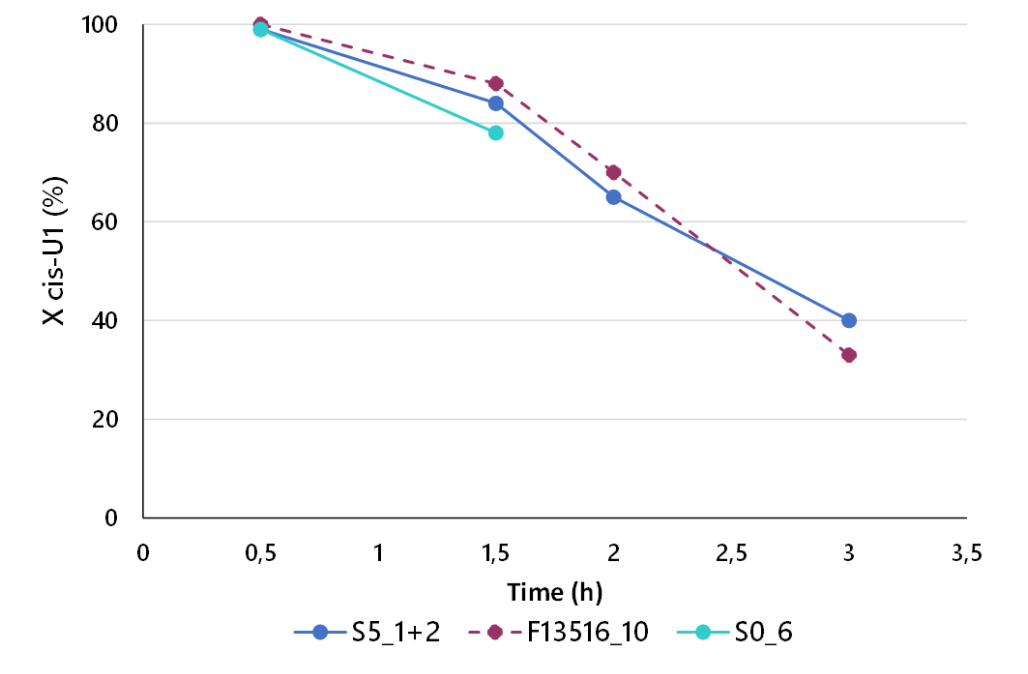

Figure 79. Comparison of conversion of oleic derivativeCis-U1 in function of time between solutions rich in impurities and the reference F13516_10

In view of the above results, it was possible to conclude that:

- The nature and composition of the starting material played a central role for the deactivation phenomena.
- The factors that possible influenced the catalyst behaviour and its stability were the percentage of linoleic derivatives (Poly-U) present in the mixture and the concentration of impurities.
- Solution "A" with the minimum value of both impurities and Poly-U did not cause any deactivation on the catalyst, ensuring unchanged complete*Cis*-U1 conversion and S1 selectivity after 3 hours of reaction.
- Whether for lower or higher concentration of impurities the deactivation was strictly correlated to the amount of linoleic acid derivative. The higher the amount of the di-unsaturated fatty acid derivative in the mixture, the more relevant the deactivation. In fact, when the impurities were increased keeping constant Poly-U concentration, no evidences of deactivation variation were observed.

- The influence of the amount of Poly-U on deactivation was therefore more pronounced than the impurities' concentrations.
- It was assumed that the Poly-U compounds, being more capable to strongly adsorb on the catalyst surface, could allow oligomerization reaction with subsequent fouling of the active surface.

5.5 Comparison of deactivation between batch and continuous flow reactor

Deactivation occurred for both continuous and discontinuous systems and in both cases palladium leaching was excluded as a cause for the loss of activity.

Comparing the two results in Figure 80, it was evident that the catalyst used in the batch system was more prone to deactivation.

However, it must keep in mind that for the continuous reaction the solution fed had to be diluted; a common factor that can be used to compare the deactivation of these two systems was the number of moles of starting material processed, after normalisation of the data based on the amount of catalyst employed.

Considering the different concentration of the solution in one batch with 15 ml of 30 g/L of starting material, an equivalent number of moles were processed during 40 minutes of continuous flow reaction. Therefore 1 hour and 20 minutes of flow reaction correspond to two batches.

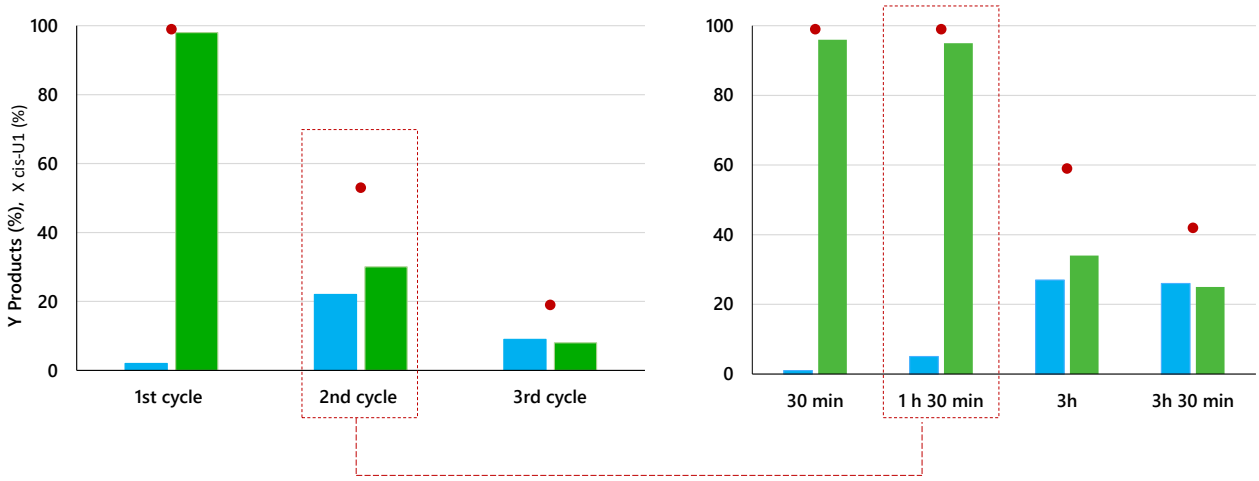

Figure 80. Comparison between the deactivation of 0.3% wtPd/C in the batch system and in the continuous flow system. Squares in red line evidence two conditions with equal amount of processed moles**. Batch conditions**: solution 30 g/L, T= 90°C, P H_2 =4 bar, stirring rate= 750 rpm, cat. 0.5% wt. **Continuous flow:** solution 6g/L, T=90°C, P H_2= 20 bar, flow rate: 1.5 mL/min.

Comparing the results obtained with the second cycle in batch reaction with those obtained after 1h and 30 minutes of continuous flow reaction, it is evident how in the former case the deactivation rate was more pronounced.

In fact, even if equal moles of starting material were processed, the longer residence time and contact of reactants with the catalyst in the batch reactor for 30 minutes either facilitated the

adsorption of the molecules on the catalyst surface or favoured the formation of heavy by-products.

On the other hand, the short residence time of the solution over the catalyst ensured in the flow system discouraged the long adsorption of reagents and decreased the oligomerization of reactants so prolonging catalyst lifetime.

6.Conclusions

The three years of PhD project described in this thesis were devoted to investigate a robust catalytic system for the selective hydrogenation of a real mixture of carboxylic fatty acids derivatives, mainly composed of unsaturated molecules.

The first period was dedicated to the optimization of the analytical system, which required different steps, including derivatization with BF_3 in methanol, to obtain the fatty acids methyl esters, necessary to allow an appropriate analysis of the mixture via GC.

The attention was then pointed out to batch reactions for an initial screening of the most suitable catalyst and the optimization of the reaction conditions.

Different noble metals, including Pd, Ru, Rh and Pt were tested in combination to a variety of supports, such as active carbon, γ-alumina and zirconium oxide.

Pd/C resulted the most active and selective catalyst towards the saturated fatty acid derivative, even more than Ni-Raney, which is still used in many industrial hydrogenation processes.

The reaction parameters were optimized resulting in temperature=90°C, 4 bar of H_2 and 750 rpm as stirring rate. It was demonstrated that with lower mixing rate the system worked under diffusional regime, which resulted disadvantageous because of reduction of reagents concentration to the catalyst's active sites. On the other hand, elevated stirring speed led to an excessive swirling with subsequent spread of the catalyst on the reactor's wall and its ineffective utilization.

Surprisingly complete conversion of the *cis*-U1 was achieved after only 30 minutes employing 0.3%wt Pd/C, with almost full selectivity towards S1: this catalyst resulted even more active than 5% Pd/C, thanks to the uniformity of NPs dimension and absence of agglomerates. Also, considering that the catalyst was air-exposed and none pre-treatments were executed before the reaction, we could observe that the reaction conditions were sufficient to successfully activate the metal NPs by in-situ reduction.

After optimization of the batch reactions, a second approach was adopted, performing the reaction in a continuous-flow system, the H-Cube Mini Plus®, capable to produce H_2 in situ by electrolysis of water. The same screening tests for reactions parameters evaluation were executed, as well as tests with different metal-supported catalysts. Again, 0.3% wt Pd/C gave the best results, with full conversion of the starting material and complete selectivity towards S1 with a contact time of only 0.2 minutes.

Despite these Pd-supported catalyst resulted in excellent behaviour, it was observed a rapid decline in activity with their reutilization for multiple reactions, being a second or third cycle for the batch reactions or long time-on-stream for the continuous flow ones. Therefore, investigations on the cause of deactivation were executed, adopting different techniques such as ICP-AES and TG analysis. The first analysis allowed to exclude metal leaching in the solution, while TGA evidenced the presence of adsorbed material on the catalyst's surface, after observing a loss in %weight of the heated post reaction catalyst. This evidence was proven by restoration of catalyst's activity after thermal treatment of 1% wt Pd/Al_2O_3.

These compounds were assumed to be oligomers formed after absorption of molecules already present in the starting material.

The deactivation cause was in depth studied in the continuous system by increasing the H_2 pressure and lowering the contact time of the starting material, with beneficial effects for catalyst's longevity in both cases. More importantly, it was found that deactivation was directly associable to the composition of the starting material employed. Indeed, two variables were considered: the amount of impurities and the %w/w of poly-unsaturated fatty acids. While a variation of the purity of the starting material did not influence the trend of deactivation, the amount of polyunsaturated compounds played a central role for the catalyst's stability, being directly responsible for a reduction in the catalyst's performance.

These results make us concluded that poly-unsaturated compounds probably had a higher tendency to bind on the catalyst's active surface forming by-products via oligomerization, which, being anchored on the catalyst surface, lead to deactivation and worsen the catalyst's performances.

To conclude, during these years, the following achievements were reached:

- Hydrogenation reaction was successfully performed both in a batch and continuous flow system, employed simple, commercial and toxic-free catalysts, with possibility to reduce the metal NPs in-situ.
- Work in mild reaction conditions maintaining high standard of starting material conversion and selectivity towards the saturated product.
- Investigate and understand the reason that caused deactivation on the catalyst.

The results obtained during this research open new possibilities for the evaluation of these catalytic systems for further studies and interesting industrial applications.

7.References

(1) Collins, T. J. Review of the Twenty-Three Year Evolution of the First University Course in Green Chemistry: Teaching Future Leaders How to Create Sustainable Societies. *J. Clean. Prod.***2017**, *140*, 93–110.

(2) Jessop, P. G.; Trakhtenberg, S.; Warner, J. The Twelve Principles of Green Chemistry. *ACS Symp. Ser.***2009**, *1000*, 401–436.

(3) Anastas, P.; Eghbali, N. Green Chemistry: Principles and Practice. *Chem. Soc. Rev.***2010**, *39* (1), 301–312.

(4) Beach, E. S.; Cui, Z.; Anastas, P. T. Green Chemistry: A Design Framework for Sustainability. *Energy Environ. Sci.***2009**, *2* (10), 1038–1049.

(5) Sheldon, R. A. Fundamentals of Green Chemistry: Efficiency in Reaction Design. *Chem. Soc. Rev.***2012**, *41* (4), 1437–1451.

(6) Tkemaladze, G. S.; Makhashvili, K. A. Climate Changes and Photosynthesis. *Ann. Agrar. Sci.***2016**, *14* (2), 119–126.

(7) Agbor, V. B.; Cicek, N.; Sparling, R.; Berlin, A.; Levin, D. B. Biomass Pretreatment: Fundamentals toward Application. *Biotechnol. Adv.***2011**, *29* (6), 675–685.

(8) Renewable Resources and Renewable Energy: A Global Challenge, Second Edition - Google Libri.

(9) Peters, M.; Von Der Assen, N. It Is Better to Prevent Waste than to Treat or Clean up Waste after It Is Formed - Or: What Benjamin Franklin Has to Do with “Green Chemistry.” *Green Chem.***2016**, *18* (5), 1172–1174

(10) Koel, M.; Kaljurand, M. Application of the Principles of Green Chemistry in Analytical Chemistry. *Pure Appl. Chem.***2006**, *78* (11), 1993–2002.

(11) Anastas, P. T. Green Chemistry as Applied to Solvents. *ACS Symp. Ser.***2002**, *819* (3), 1–9.

(12) Sheldon, R. A. Green Solvents for Sustainable Organic Synthesis: State of the Art. *Green Chem.***2005**, *7* (5), 267–278.

(13) Horváth, I. T. Solvents from Nature. *Green Chem.***2008**, *10* (10), 1024–1028.

(14) Stijepovic, M. Z.; Linke, P. Optimal Waste Heat Recovery and Reuse in Industrial Zones. *Energy***2011**, *36* (7), 4019–4031.

(15) Sheldon, R. A. Green Chemistry and Resource Efficiency: Towards a Green Economy. *Green Chem.***2016**, *18* (11), 3180–3183.

(16) Amidon, T. E.; Wood, C. D.; Shupe, A. M.; Wang, Y.; Graves, M.; Liu, S. Biorefinery:

Conversion of Woody Biomass to Chemicals, Energy and Materials. *J. Biobased Mater. Bioenergy***2008**, *2* (2), 100–120.

(17) Bakshi, B. R.; Balasubramanian, S.; Banerji, S. K. *B Ioenergy and B Iofuel From*; 2010.

(18) Anastas, P. T.; Bartlett, L. B.; Kirchhoff, M. M.; Williamson, T. C. The Role of Catalysis in the Design, Development, and Implementation of Green Chemistry. *Catal. Today***2000**, *55* (1–2), 11–22.

(19) Trost, B. M. The Atom Economy - A Search for Synthetic Efficiency. *Science (80-.).***1991**, *254* (5037), 1471–1477.

(20) Cavani Fabrizio, Albonetti Stefania, Basile Francesco, G. A. *Chemicals and Fuels from Bio-Based Buolding Blocks*.

(21) Faaij, A.; Moreira, J.; Berndes, G.; Dhamija, P.; Dong, H.; Gabrielle, B.; Eng, A. G.; Cerutti, O. M.; Mcintyre, T.; Minowa, T.; et al. *Chapter 2 2*; 2011.

(22) Erickson, L. E.; Brase, G. Paris Agreement on Climate Change. *Reducing Greenh. Gas Emiss. Improv. Air Qual.***2019**, 11–22.

(23) Kaushika, N. D.; Reddy, K. S.; Kaushik, K. Sustainable Energy and the Environment: Gasification.Pdf A Clean Technology Approach. *Sustain. Energy Environ. A Clean Technol. Approach***2016**, 1–242.

(24) McKendry, P. Energy Production from Biomass (Part 3): Gasification Technologies. *Bioresour. Technol.***2002**, *83* (1), 55–63.

(25) Jacobsson, S.; Johnson, A. The Diffusion of Renewable Energy Technology: An Analytical Framework and Key Issues for Research. *Energy Policy***2000**, *28* (9), 625–640.

(26) McKendry, P. Energy Production from Biomass (Part 1): Overview of Biomass. *Bioresour. Technol.***2002**, *83* (1), 37–46.

(27) Tursi, A. A Review on Biomass: Importance, Chemistry, Classification, and Conversion. *Biofuel Res. J.***2019**, *6* (2), 962–979.

(28) Global Bioenergy Statistics. WBA Global Bioenergy Statistics 2018. *World Bioenergy Assoc.***2018**, 43.

(29) Habert, G.; Bouzidi, Y.; Chen, C.; Jullien, A. Development of a Depletion Indicator for Natural Resources Used in Concrete. *Resour. Conserv. Recycl.***2010**, *54* (6), 364–376.

(30) Blass, S. D.; Hermann, R. J.; Persson, N. E.; Bhan, A.; Schmidt, L. D. Conversion of Glycerol to Light Olefins and Gasoline Precursors. *Appl. Catal. A Gen.***2014**, *475*, 10–15.

(31) Vassoi, A.; Tabanelli, T.; Sacchetti, A.; Di Gioia, F.; Capuzzi, L.; Cavani, F. The Oxidative Cleavage of 9,10-Dihydroxystearic Triglyceride with Oxygen and Cu Oxide-Based

Heterogeneous Catalysts. *ChemSusChem***2021**, *14* (11), 2375–2382.

(32) Petersen Raymer, A. K. A Comparison of Avoided Greenhouse Gas Emissions When Using Different Kinds of Wood Energy. *Biomass and Bioenergy***2006**, *30* (7), 605–617.

(33) Carpentieri, M.; Corti, A.; Lombardi, L. Life Cycle Assessment (LCA) of an Integrated Biomass Gasification Combined Cycle (IBGCC) with CO2 Removal. *Energy Convers. Manag.***2005**, *46* (11–12), 1790–1808.

(34) Gustavsson, L.; Börjesson, P.; Johansson, B.; Svenningsson, P. Reducing CO2 Emissions by Substituting Biomass for Fossil Fuels. *Energy***1995**, *20* (11), 1097–1113.

(35) Lauri, P.; Havlík, P.; Kindermann, G.; Forsell, N.; Böttcher, H.; Obersteiner, M. Woody Biomass Energy Potential in 2050. *Energy Policy***2014**, *66*, 19–31.

(36) Commission, E. https://ec.europa.eu/clima/policies/eu-climate-action/law_en.

(37) Star-COLIBRI. Joint European Biorefinery Vision for 2030: Strategic Targets for 2020 - Collaboration Initiative on Biorefineries. **2011**, 54.

(38) uropean Commission (2019) Biofuels in the European Union - a vision for 2030 and beyond, 14 03 2006. Access Aug 2019.

(39) Metzger, J. O. Fats and Oils as Renewable Feedstock for Chemistry. *Eur. J. Lipid Sci. Technol.***2009**, *111* (9), 865–876.

(40) Biermann, U.; Bornscheuer, U.; Meier, M. A. R.; Metzger, J. O.; Schäfer, H. J. Oils and Fats as Renewable Raw Materials in Chemistry. *Angew. Chemie - Int. Ed.***2011**, *50* (17), 3854–3871

(41) Behr, A.; Seidensticker, T. *Chemistry of Renewables*; 2020.

(42) *Report of the World Summit on Sustainable Development, Johannesburg, South Africa, 26 August-4 September 2002*.

(43) Zhang, M.; Yu, Y. Dehydration of Ethanol to Ethylene. *Ind. Eng. Chem. Res.***2013**, *52* (28), 9505–9514.

(44) Braskem. https://www.braskem.com.br/.

(45) Singhvi, M.; Gokhale, D. Biomass to Biodegradable Polymer (PLA). *RSC Adv.***2013**, *3* (33), 13558–13568.

(46) Works, N. https://www.natureworksllc.com/.

(47) DuPont. https://duponttateandlyle.com/.

(48) Song, H.; Lee, S. Y. Production of Succinic Acid by Bacterial Fermentation. *Enzyme Microb. Technol.***2006**, *39* (3), 352–361.

(49) Balat, M. Production of Biodiesel from Vegetable Oils: A Survey. *Energy Sources, Part A*

*Recover. Util. Environ. Eff.***2007**.

(50) Ramadhas, A. S.; Jayaraj, S.; Muraleedharan, C. Biodiesel Production from High FFA Rubber Seed Oil. *Fuel***2005**, *84* (4), 335–340.

(51) Demirbas, A. Biodiesel from Vegetable Oils with MgO Catalytic Transesterification in Supercritical Methanol. *Energy Sources, Part A Recover. Util. Environ. Eff.***2008**, *30* (17), 1645–1651.

(52) Pyl, S. P.; Schietekat, C. M.; Reyniers, M. F.; Abhari, R.; Marin, G. B.; Van Geem, K. M. Biomass to Olefins: Cracking of Renewable Naphtha. *Chem. Eng. J.***2011**, *176–177*, 178–187.

(53) https://www.novamont.com/.

(54) Acid, P. L.; Wood, P.; Knitter, M.; Wo, A.; Dobrzy, M.; Laura, M.; Lorenzo, D. -Lactic Acid) / Pine Wood Bio-Based Composites 1, * ,. **2020**, 1–22.

(55) Biorefineries - Industrial Processes and Products, 2 Vols Bound Together. *Focus Catal.***2010**, *2010* (11), 8.

(56) Bartholomew, C. H. Mechanisms of Catalyst Deactivation. *Appl. Catal. A Gen.***2001**, *212* (1–2), 17–60.

(57) Vassilev, S. V.; Baxter, D.; Andersen, L. K.; Vassileva, C. G. An Overview of the Chemical Composition of Biomass. *Fuel***2010**, *89* (5), 913–933..

(58) Kamm, B; Gruber, P R; Kamm, M. *Biorefineries - Industrial Processes and Products. Status Quo and Future Directions. Vol. 2*; 2006.

(59) Shimizu, K. I.; Satsuma, A. Toward a Rational Control of Solid Acid Catalysis for Green Synthesis and Biomass Conversion. *Energy Environ. Sci.***2011**, *4* (9), 3140–3153.

(60) Anneken D. J., Both S., Christoph R., Fieg G., Steinberbner U., W. A. Fatty Acids. *Ulmann's-Encyclopedia of Industrial Chemistry*; 2012.

(61) Kerenkan, A. E.; Béland, F.; Do, T. Catalysis Science & Technology. **2016**, 971–987.

(62) https://www.statista.com/statistics/267271/worldwide-oilseed-production-since-2008/.

(63) Sheldon, R. A. Green and Sustainable Manufacture of Chemicals from Biomass: State of the Art. *Green Chem.***2014**, *16* (3), 950–963.

(64) DeWilde, J. F.; Czopinski, C. J.; Bhan, A. Ethanol Dehydration and Dehydrogenation on γ-Al2O3: Mechanism of Acetaldehyde Formation. *ACS Catal.***2014**, *4* (12), 4425–4433.

(65) Herrick, A. B.; Jungermann, E. Manufacture of Soap from Fatty Acids. *J. Am. Oil Chem. Soc.***1963**, *40* (11), 615–618.

(66) Harwood, H. J. REACTIONS OF THE HYDROCARBON CHAIN OF FATTY ACIDS **1981**.

(67) Lie Ken Jie, M. S. F.; Pasha, M. K. Fatty Acids, Fatty Acid Analogues and Their Derivatives. *Nat. Prod. Rep.***1998**, *15* (6), 607–629.

(68) Knothe, G. Structure Indices in FA Chemistry. How Relevant Is the Iodine Value? *JAOCS, J. Am. Oil Chem. Soc.***2002**, *79* (9), 847–854.

(69) Baron Hübl, k. k. österr. H. Eine Allgemein Anwendbare Methode Zur Untersuchung Der Fette. *Dingler's Polytech. J.***1884**, *253*, 281–295.

(70) Maranghi, S.; Brondi, C. *Life Cycle Assessment in the Chemical Product Chain: Challenges, Methodological Approaches and Applications*; 2020.

(71) Althoff, J.; Biesheuvel, K.; De Kok, A.; Pelt, H.; Ruitenbeek, M.; Spork, G.; Tange, J.; Wevers, R. Economic Feasibility of the Sugar Beet-to-Ethylene Value Chain. *ChemSusChem***2013**, *6* (9), 1625–1630.

(72) Minoux, D., Nesterenko, N., Vermeiren, W., and Sander Van, D. WO 2009098268A1, 2009.

(73) Cartwright, S. US20070117724A1, 2006.

(74) Ahmad, M. Y.; Basir, N. I.; Abdullah, A. Z. A Review on One-Pot Synthesis of Acrylic Acid from Glycerol on Bi-Functional Catalysts. *J. Ind. Eng. Chem.***2021**, *93*, 216–227.

(75) Lin, Y. C. Catalytic Valorization of Glycerol to Hydrogen and Syngas. *Int. J. Hydrogen Energy***2013**, *38* (6), 2678–2700.

(76) Dry, M. E. The Fischer-Tropsch Process: 1950-2000. *Catal. Today***2002**, *71* (3–4), 227–241.

(77) I. Horiuti, M. P. EXCHANGE REACTIONS OF HYDROGEN ON METALLIC CATALYSTS. *Trans. Farady Soc.***1934**.

(78) Piqueras, C. M.; Costilla, I. O.; Belelli, P. G.; Castellani, N. J.; Damiani, D. E. Pd-ΓAl2O3 Applied to Triglycerides Hydrogenation with Supercritical Propane. Experimental and Theoretical Catalysts Characterization. *Appl. Catal. A Gen.***2008**, *347* (1), 1–10.

(79) K.Gupta, M. *Practical Guide to Vegetable Oil Processing*; Elsevier, A. P. B., Ed.; 2017.

(80) Mäki-Arvela, P.; Kuusisto, J.; Sevilla, E. M.; Simakova, I.; Mikkola, J. P.; Myllyoja, J.; Salmi, T.; Murzin, D. Y. Catalytic Hydrogenation of Linoleic Acid to Stearic Acid over Different Pd- and Ru-Supported Catalysts. *Appl. Catal. A Gen.***2008**, *345* (2), 201–212.

(81) Bernas, A.; Myllyoja, J.; Salmi, T.; Murzin, D. Y. Kinetics of Linoleic Acid Hydrogenation on Pd/C Catalyst. *Appl. Catal. A Gen.***2009**, *353* (2), 166–180.

(82) Rothenberg, G. Catalysis-Concept and Green Applications. *978-3-527-31824-7.***2017**.

(83) Allen, R. R.; Foods, A. C. Hydrogenation. **1979**, *275* (1978).

(84) Knothe, G. Wilhelm Normann.

(85) Makaryan, B. V. I. S. and I. A. Palladium Catalyst for the Production of Pure Margarine. *Platin. Met. Rev.***1999**, *43* (2), 74–82.

(86) Farvid, M. S.; Chen, W. Y. Adolescent Diet and Breast Cancer Risk. *Curr. Nutr. Rep.***2016**, *5* (1), 29–33

(87) Oomen, C. M.; Ocké, M. C.; Feskens, E. J. M.; Van Erp-Baart, M. A. J.; Kok, F. J.; Kromhout, D. Association between Trans Fatty Acid Intake and 10-Year Risk of Coronary Heart Disease in the Zutphen Elderly Study: A Prospective Population-Based Study. *Lancet***2001**, *357* (9258), 746–751.

(88) Commission, E. Trans Fat in Food.

(89) Moss, J. Labeling of Trans Fatty Acid Content in Food, Regulations and Limits-The FDA View. *Atheroscler. Suppl.***2006**, *7* (2), 57–59.

(90) Lauro, M. F. Metallic Soaps. *Oil Fat Ind.***1928**, *5* (11), 329–332.

(91) Veldsink, J. W.; Bouma, M. J.; Schöön, N. H.; Beenackers, A. A. C. M. Heterogeneous Hydrogenation of Vegetable Oils: A Literature Review. *Catal. Rev. - Sci. Eng.***2008**, *39* (3), 253–318.

(92) Allen, R. R.; Foods, A. C. R.R. ALLEN, W.L. Clayton Research Center, Anderson Clayton Foods, 3333 N. Central Expressway, Richardson, TX 75080 Presented by Anthony H. Chen. **1979**, *275* (1978).

(93) Mikhail Alexandrovich Ginzburg, Kair Akhmetovich Zhubanov, F. K. K. N. F. V. Method of Producing Commercial Stearic Acid, 1987.

(94) Lieber, E.; Morritz, F. L. The Uses of Raney Nickel. *Adv. Catal.***1953**, *5* (C), 417–455.

(95) Kitayama, Y.; Muraoka, M.; Takahashi, M.; Kodama, T.; Itoh, H.; Takahashi, E.; Okamura, M. Catalytic Hydrogenation of Linoleic Acid on Nickel, Copper, and Palladium. *JAOCS, J. Am. Oil Chem. Soc.***1996**, *73* (10), 1311–1316.

(96) Chen, L.; Li, G.; Zhang, M.; Wang, D.; Li, S.; Zhang, C.; Li, X.; Chung, K. H. Preparation of Reduced Ni-Nb-O Composite Hydrogenation Catalysts for Highly Selective Conversion of Free Fatty Acids to n-Alkanes. *Fuel***2020**, *282* (July), 118842.

(97) Iida, H.; Takahashi, K.; Yanagisawa, A.; Hashimoto, H.; Igarashi, A. Reduction of Trans Fatty Acids in Hydrogenated Soybean Oil Using Ni/TiO2 Catalysts. *Food Chem.***2021**, *340* (April 2020), 127927.

(98) Sarno, M.; Iuliano, M.; Viscusi, G.; Zarli, A.; Ciambelli, P. A Nickel/Palladium/Ruthenium-Graphene Based Nanocatalyst for Selective Catalytic Hydrogenation of Vegetable Oils.

*Ind. Crops Prod.***2021**, *170* (July).

(99) Belkacemi, K.; Boulmerka, A.; Arul, J.; Hamoudi, S. Hydrogenation of Vegetable Oils with Minimum Trans and Saturated Fatty Acid Formation Over a New Generation of Pd-Catalyst. *Top. Catal.***2006**, *37* (2–4), 113–120.

(100) Legor. Legor Quotazione metalli.

(101) Plourde, M.; Belkacemi, K.; Arul, J. Hydrogenation of Sunflower Oil with Novel Pd Catalysts Supported on Structured Silica. *Ind. Eng. Chem. Res.***2004**, *43* (10), 2382–2390.

(102) Cizmeci, M.; Musavi, A.; Tekin, A.; Kayahan, M. Comparison of Two Palladium Catalysts on Different Supports during Hydrogenation. *JAOCS, J. Am. Oil Chem. Soc.***2006**, *83* (12), 1063–1068

(103) Thunyaratchatanon, C.; Luengnaruemitchai, A.; Chollacoop, N.; Chen, S. Y.; Yoshimura, Y. Catalytic Hydrogenation of Soybean Oil-Derived Fatty Acid Methyl Esters over Pd Supported on Zr-SBA-15 with Various Zr Loading Levels for Enhanced Oxidative Stability. *Fuel Process. Technol.***2018**, *179* (August), 422–435.

(104) C.H. Bartholomew, J. B. B. *Catalyst Deactivation*; 1991.

(105) M. R. Heck, R.J. Farruto, S. T. G. *Catalytic Air Pllution Control*; 2009.

(106) Hegedus, L. L.; McCabe, R. W. *Catalyst Poisoning*; Elsevier Scientific Publishing Company, 1980; Vol. 6.

(107) Bartholomew, C. H. Catalyst Deactivation. *Stud. Surf. Sci. Catal.***1987**, *34*.

(108) J. M. Thomas, W. J. T. *Principle and Practice of Heterogeneous Catalysis*; 1997.

(109) Trimm, D. L. The Regeneration or Disposal of Deactivated Heterogeneous Catalysts. *Appl. Catal. A Gen.***2001**, *212* (1–2), 153–160.

(110) Alstrup, R.-N. High Temperature H2S Chemisorption on Nickel Catalyst. *Langmuir***1981**, No. 10, 303–314.

(111) Menon, P. G. Coke on Catalyst-Harmful,Harmless, Invisible and Beneficial Types. *J-Moelcular Catal.***1990**, *59* (2), 207–220.

(112) B. C. Gates, J.R. Katzer, G. C. S. *Chemistry of Catalytic Process*; 1979.

(113) Naccache, C. *Deactivation and Poisoning of Catalyst*; wise, Ed.; 1985.

(114) McCulloch, D. C. No Title. *Appl. Ind. Catal.***1983**, 103–110.

(115) Kirk Stephenson, W., Lemke, Harald K., Bannayan, M. A. Fouling Mechanisms and Effect of Process Conditions on Deposit Formation in H-Oil Equipment. **1996**.

(116) Trimm, D. Catalyst Design for Reduced Coke. **1983**, 263–290.

(117) Rostrup-Nielsen, J. R. Activity of Nickel Catalysts for Steam Reforming of Hydrocarbons.

*J. Catal.***1973**, *31* (2), 173–199.

(118) Summers, J. C.; Hegedus, L. L. Modes of Catalyst Deactivation in Stoichiometric Automobile Exhaust. *Ind. Eng. Chem. Prod. Res. Dev.***1979**, *18* (4), 318–324.

(119) J. Anderson, M. E. D. No Title. *Catal. Sci. Technol.* 159.

(120) HuberGuymon, C. Hydrothermal Stability of CO/SiO2 Fischer-Tropsch Synthesis Catalysts. *Stud. Surf. Sci. Catal.***2001**.

(121) G.K. Chuah , S. Jaenicke, S.A. Cheong, K. S. C. The Influence of Preparation Conditions on the Surface Area of Zirconia. *Appl. Catal. A***1996**, *145*, 267–284.

(122) Rossetti, I.; Forni, L. Effect of Ru Loading and of Ru Precursor in Ru / C Catalysts for Ammonia Synthesis. **2005**, *282*, 315–320.

(123) Rossetti, I.; Mangiarini, F.; Forni, L. Promoters State and Catalyst Activation during Ammonia Synthesis over Ru / C. **2007**, *323*, 219–225.

(124) Karl Blau (Editor), J. M. H. (Editor). *Handbook of Derivatives for Chromatography, 2nd Edition*; 1993.

(125) Zhao, F.; Ikushima, Y.; Arai, M. Hydrogenation of 2-Butyne-1 , 4-Diol in Supercritical Carbon Dioxide Promoted by Stainless Steel Reactor Wall. **2004**, *95*, 439–443.

(126) Dijkstra, A. J. Review Article Kinetics and Mechanism of the Hydrogenation Process – the State of the Art. **2012**, 985–998.

(127) Dijkstra, A. J. Revisiting the Formation of Trans Isomers during Partial Hydrogenation of Triacylglycerol Oils. **2006**, *108*, 249–264.

(128) Hashimoto, K.; Muroyama, K.; Nagata, S. Kinetics of the Hydrogenation of Fatty Oils. 1–5.

(129) Legor-quotazione-metalli https://www.legor.com/it/quotazione-metalli.

(130) Rylander, P. *Catalytic Hydrogenation over Platinum Metals*; 2012.

(131) Emma Bresó-Femenia ab, B. C. *a and S. C. *b. Selective Catalytic Hydrogenation of Polycyclic Aromatic Hydrocarbons Promoted by Ruthenium Nanoparticles†. *Catal. Sci. Technol.***2015**, *5*, 2741–2751.

(132) Shafeeyan, M. S.; Mohd, W.; Wan, A.; Houshmand, A.; Shamiri, A. Journal of Analytical and Applied Pyrolysis A Review on Surface Modification of Activated Carbon for Carbon Dioxide Adsorption. *J. Anal. Appl. Pyrolysis***2010**, *89* (2), 143–151.

(133) Escribano, V. S.; Garbarino, G.; Finocchio, E.; Busca, G. γ-Alumina and Amorphous Silica – Alumina : Structural Features , Acid Sites and the Role of Adsorbed Water. *Top. Catal.***2017**, *60* (19), 1554–1564.

(134) Bonetti, R.; Parker, W. O. Insights into Polymerization of Vegetable Oil : Oligomerization

of Oleic Acid. **2019**, No. August, 1181–1184.

(135) Ngo, H.; Latona, R.; Sarker, M. I.; Yee, W.; Hums, M.; Moreau, R. A. Industrial Crops & Products A Process to Convert Sun Fl Ower Oil into a Value Added Branched Chain Oil with Unique Properties ⋆. *Ind. Crop. Prod.***2019**, *139* (May), 111457.

8. Acknowledgments

I am now concluding, with considerable emotion, this thesis and looking back it is impossible to do not realize that bad moments maybe were not so bad because I was never walking alone, but I always had special people next to me.

Who is this I should thank?

First, the professor **Fabrizio Cavani** and **Tommaso**: without them this journey would have never begin. Thank you for making this experience reality, allowing me to participate and contribute to many congresses around Europe, to always find a solution to many problems, to be open to listen to my requests. I wish I could have more occasions for asking your opinion and listen to your stimulating suggests.

Thanks to **Luigi Capuzzi** and **Maria Grazia Capraro** from Novamont S.p.A: collaborating with them made me even more proud of my work. Thank you for making me an active collaborator in this project and for the constant exchange of opinions and ideas about the evolution of the research.

Thanks to the big family of **"Catalytic Globetrotter**": an extraordinary group which took me in and accepted my ideas since the first day. These three years have been full of joy, laugh, experience together, discussion and sometimes disasters. They will remain unforgettable.

Triple L...how could I don't cite you? My mates of mountains-exploration, to make "Sundays less boring" but also amazing collaborators and tremendous "manifoldi". Thank you, our moments are precious, without you everything would have been different.

Thanks to **Nicola**: you have always been patience with people, but I think with me your level touches the maximum. Thanks for always having a heartwarming hug, a support world or just for urging to give the best I could. You are my "safe place" where all the problems disappear.

Thanks to the **Marianne**: since the first years of university, they don't only bear my "chemistry pills", but they also support me, believing in my choices and shaking my fears off. Our bond is special, there is no way to break it.

And finally, but not less important, thanks to my **parents, Andrea and Raffaella**, my **sister Chicca**, my aunt **Angela** and uncles **Stefano** and **Alberto**, my special cousins **Chiara, Davide** and **Daniele** and my **Nonna Vanda**: no one like them was able to make me feel right and no wrong, to be capable of my work in discouragement moments and to cheer always for me.